IAEA TECDOC SERIES

Evaluation of Conditions for Hydrogen Induced Degradation of Zirconium Alloys during Fuel Operation and Storage

Final Report of a Coordinated Research Project 2011–2015

IAEA
International Atomic Energy Agency

EVALUATION OF CONDITIONS FOR HYDROGEN INDUCED DEGRADATION OF ZIRCONIUM ALLOYS DURING FUEL OPERATION AND STORAGE

The following States are Members of the International Atomic Energy Agency:

AFGHANISTAN
ALBANIA
ALGERIA
ANGOLA
ANTIGUA AND BARBUDA
ARGENTINA
ARMENIA
AUSTRALIA
AUSTRIA
AZERBAIJAN
BAHAMAS
BAHRAIN
BANGLADESH
BARBADOS
BELARUS
BELGIUM
BELIZE
BENIN
BOLIVIA, PLURINATIONAL
   STATE OF
BOSNIA AND HERZEGOVINA
BOTSWANA
BRAZIL
BRUNEI DARUSSALAM
BULGARIA
BURKINA FASO
BURUNDI
CAMBODIA
CAMEROON
CANADA
CENTRAL AFRICAN
   REPUBLIC
CHAD
CHILE
CHINA
COLOMBIA
CONGO
COSTA RICA
CÔTE D'IVOIRE
CROATIA
CUBA
CYPRUS
CZECH REPUBLIC
DEMOCRATIC REPUBLIC
   OF THE CONGO
DENMARK
DJIBOUTI
DOMINICA
DOMINICAN REPUBLIC
ECUADOR
EGYPT
EL SALVADOR
ERITREA
ESTONIA
ETHIOPIA
FIJI
FINLAND
FRANCE
GABON

GEORGIA
GERMANY
GHANA
GREECE
GUATEMALA
GUYANA
HAITI
HOLY SEE
HONDURAS
HUNGARY
ICELAND
INDIA
INDONESIA
IRAN, ISLAMIC REPUBLIC OF
IRAQ
IRELAND
ISRAEL
ITALY
JAMAICA
JAPAN
JORDAN
KAZAKHSTAN
KENYA
KOREA, REPUBLIC OF
KUWAIT
KYRGYZSTAN
LAO PEOPLE'S DEMOCRATIC
   REPUBLIC
LATVIA
LEBANON
LESOTHO
LIBERIA
LIBYA
LIECHTENSTEIN
LITHUANIA
LUXEMBOURG
MADAGASCAR
MALAWI
MALAYSIA
MALI
MALTA
MARSHALL ISLANDS
MAURITANIA
MAURITIUS
MEXICO
MONACO
MONGOLIA
MONTENEGRO
MOROCCO
MOZAMBIQUE
MYANMAR
NAMIBIA
NEPAL
NETHERLANDS
NEW ZEALAND
NICARAGUA
NIGER
NIGERIA
NORWAY

OMAN
PAKISTAN
PALAU
PANAMA
PAPUA NEW GUINEA
PARAGUAY
PERU
PHILIPPINES
POLAND
PORTUGAL
QATAR
REPUBLIC OF MOLDOVA
ROMANIA
RUSSIAN FEDERATION
RWANDA
SAN MARINO
SAUDI ARABIA
SENEGAL
SERBIA
SEYCHELLES
SIERRA LEONE
SINGAPORE
SLOVAKIA
SLOVENIA
SOUTH AFRICA
SPAIN
SRI LANKA
SUDAN
SWAZILAND
SWEDEN
SWITZERLAND
SYRIAN ARAB REPUBLIC
TAJIKISTAN
THAILAND
THE FORMER YUGOSLAV
   REPUBLIC OF MACEDONIA
TOGO
TRINIDAD AND TOBAGO
TUNISIA
TURKEY
UGANDA
UKRAINE
UNITED ARAB EMIRATES
UNITED KINGDOM OF
   GREAT BRITAIN AND
   NORTHERN IRELAND
UNITED REPUBLIC
   OF TANZANIA
UNITED STATES OF AMERICA
URUGUAY
UZBEKISTAN
VANUATU
VENEZUELA, BOLIVARIAN
   REPUBLIC OF
VIET NAM
YEMEN
ZAMBIA
ZIMBABWE

The Agency's Statute was approved on 23 October 1956 by the Conference on the Statute of the IAEA held at United Nations Headquarters, New York; it entered into force on 29 July 1957. The Headquarters of the Agency are situated in Vienna. Its principal objective is "to accelerate and enlarge the contribution of atomic energy to peace, health and prosperity throughout the world".

IAEA-TECDOC-1781

EVALUATION OF CONDITIONS FOR HYDROGEN INDUCED DEGRADATION OF ZIRCONIUM ALLOYS DURING FUEL OPERATION AND STORAGE

FINAL REPORT OF A COORDINATED RESEARCH PROJECT 2011–2015

INTERNATIONAL ATOMIC ENERGY AGENCY
VIENNA, 2015

COPYRIGHT NOTICE

FOREWORD

This publication reports on the work carried out in 2011–2015 in the coordinated research project (CRP) on the evaluation of conditions for hydrogen induced degradation of zirconium alloys during fuel operation and storage. The CRP was carried out to evaluate the threshold condition for delayed hydride cracking (K_{IH}) in pressurized water reactors and zircaloy-4 and E635M fuel claddings, with application to in-pile operation and spent fuel storage. The project consisted of adding hydrogen to samples of cladding and measuring K_{IH} by one of four methods.

The CRP was the third in the series, of which the results of the first two were published in IAEA-TECDOC-1410 and IAEA-TECDOC-1649, in 2004 and 2010, respectively. This publication includes all of the research work performed in the framework of the CRP, including details of the experimental procedures that led to a set of data for tested materials. The research was conducted by representatives from 13 laboratories from all over the world. In addition to the basic goal to transfer the technology of the testing techniques from experienced laboratories to those unfamiliar with the methods, the CRP was set up to develop experimental procedures to produce consistent sets of data, both within a single laboratory and among different laboratories. The material condition and temperature history were prescribed, and laboratories chose one or two of four methods of loading that were recommended in an attempt to develop standard sets of experimental protocols so that consistent results could be obtained. Experimental discrepancies were minimized through careful attention to details of microstructure, temperature history and stress state in the samples, with the main variation being the mode of loading.

The IAEA wishes to thank all the participants in the CRP for their contributions to this publication, in particular to Studsvik Nuclear and Cameco for donating the zircaloy-4 test materials. The IAEA is especially grateful to the Paul Scherrer Institute (Switzerland) and Nippon Nuclear Fuel Development (Japan) for organizing the second and third research coordination meetings at their institutes, and C.E. Coleman (Canada) for organizing the consultancy at Chalk River, Canada, and providing technical advice and programme coordination throughout the project and drafting the final report. The IAEA officer responsible for this publication was V. Inozemtsev of the Division of Nuclear Fuel Cycle and Waste Technology.

CONTENTS

SUMMARY

Zirconium alloys are susceptible to embrittlement by hydrogen when hydrides are precipitated. The two main forms of embrittlement are: short-term loss of toughness and a stable, time-dependent crack growth mechanism. Hydrogen diffuses up the stress gradient at a flaw stressed in tension and, if the solubility limit is exceeded, hydrides nucleate and grow slowly. When the hydrides reach a critical condition, probably related to size, they fracture, the crack extends and the process is repeated. This mechanism is called delayed hydride cracking (DHC). It is of technological importance to the nuclear industry because several components have failed by this mechanism. Examples include:

- Zr-2.5Nb fuel cladding cracked before irradiation during storage at room temperature. High residual stresses from welding were an important factor in these fractures.
- Similar stresses were also responsible for cracking in Zr-2.5Nb pressure tubes. The source of these stresses was either the process used to join the pressure tube to the ends of its fuel channel or from tube straightening.
- Several examples show that fuel cladding made from Zircaloy is also not immune from DHC. In some Zircaloy nuclear fuel cladding used in Boiling Water Reactors (BWR), hydride cracking was strongly implicated in long splits that allowed substantial leakage of fission products.
- A DHC-type of mechanism has been identified as being responsible for radial cracking starting at the outside surface of BWR fuel cladding when power ramped after a high burn-up.
- Cracks in the axial direction, about 20 mm long and close to the end-plugs of CANDU fuel have been detected. Several partial radial cracks had also started from the inside surface.

The two technologically relevant quantities for DHC are the critical stress intensity factor, K_I, for crack initiation, called K_{IH}, and the rate of crack propagation, called V. The latter was the subject of the first two parts of this IAEA Coordinated Research Project (CRP), one on Zr-2.5Nb pressure tube material, issued as IAEA-TECDOC-1410 in 2004 and the other on Zircaloy-4 fuel cladding, issued as IAEA-TECDOC-1649 in 2010.

Retention of the capacity to withstand the hoop stress imposed by filler and fission gasses during dry fuel storage is important for structural integrity of the fuel. DHC is one possible fracture mechanism during storage, especially since the temperature history is ideal for such cracking. Thus it is important to evaluate the DHC property that controls its initiation, K_{IH}, so that the possibility of cracking can be assessed. Therefore as an extension of this CRP, K_{IH} has been measured in Zircaloy-4 fuel cladding at several temperatures.

The loading method is the same as that used successfully on fuel cladding, as described in IAEA-TECDOC-1649. It is based on the Pin-Loading Tension (PLT) technique developed at Studsvik. The specimen contains two axial cracks that are grown by DHC with load values being varied to aid in the evaluation of K_{IH}. Four loading sequences were used:
- *Multiple specimen method*: measuring crack growth rate, V, in several specimens subjected to different values of K_I and finding the value at which V = 0.
- *Constant displacement method*: starting at a moderate value of K_I and fixing the displacement until the load decays to a constant value for up to 24 h, which represents K_{IH}.

These first two methods are based on ASTM E1681 - Standard Test Method for Determining Threshold Stress Intensity Factor for Environment-Assisted Cracking of Metallic Materials.

- *Uploading method*: starting at a low value of K_I and raising the load after 24 h if no cracking was observed or until cracking starts, thus representing K_{IH}.
- *Unloading method*: starting at a moderate value of K_I and lowering the load in small steps until cracking has stopped for up to 24 h. This value of K_I represents K_{IH}.

The IAEA set up this extension to the CRP with the objective of evaluating the various methods for measuring K_{IH} and transferring "know-how" on laboratory practices to the member states who were unfamiliar with this aspect of DHC testing of fuel cladding using the PLT method. The first objective of the project was to evaluate the various methods and establish a uniform and consistent practice for each laboratory so that a meaningful inter-laboratory comparison of the results could be made. A detailed evaluation showed that the technology transfer was partially successful. Testing on a single batch representing PWR fuel cladding containing 120 ppm hydrogen showed that most laboratories obtained values of K_{IH}, at 250 ºC but with a wide distribution around 5.4 MPa√m.

The second objective of the project was to examine the effects of microstructure on K_{IH} by testing CANDU cladding and to evaluate the temperature dependence of K_{IH} for each material. The results showed that:

- K_{IH} appeared to be independent of crack length and difference in length of the two cracks in each specimen.
- K_{IH} had little temperature dependence between 225 and 285°C but increased rapidly at higher temperatures.
- The increase in K_{IH} coincided with a sudden drop in crack growth rate with temperatures around 300°C. These two results imply that above a certain temperature, Zircaloy-4 fuel cladding becomes immune from DHC.
- K_{IH} was slightly higher and the upper temperature where it increased was lower in CANDU cladding than in PWR cladding. This difference was attributed to the lower strength of the CANDU cladding.

The fractographic feature called striations were observed in a few tests on cladding made from VVER alloy E635M, but were absent in all but one example of Zircaloy-4. Microfractography revealed cleaved hydride platelets.

These result fit within the general framework of DHC in zirconium alloys. During the project all four methods for measuring K_{IH} were used with success and provided similar values. The multiple specimen method was the easiest to implement but required much material. The constant displacement and up-loading method were found to be straightforward. The unloading method was the trickiest to implement because it relied on feedback for load control from crack extension; once the difficulties were overcome, valid values were obtained. The results were reported in three papers at international conferences, WRFPM-2014 and WRFPM-2015 and the summary paper has been accepted for the ASTM Zirconium Symposium to be held in 2016.

The results provide a useful base for analysis of the behaviour of fuel cladding during dry storage. They imply that in the early part of fuel storage, where the temperature is up to 400°C, DHC will be absent. At temperatures where DHC is possible, any flaw would have to be larger than the wall thickness of the cladding and should have been detected before dry storage.

Continuation of this type of testing on irradiated material and the heat-affected zone in CANDU fuel is recommended. Experiments at the EC Joint Research Centre – Institute for

Transuranium Elements (JRC-ITU) are planned on irradiated fuel and will use these results as a guide for experimental conditions.

1. INTRODUCTION

Zirconium has a low capture cross-section for thermal neutrons and is therefore chosen as the main base metal for alloys used as fuel cladding and structural components in water-cooled nuclear power reactors. These alloys maintain good mechanical properties both during and after irradiation with fast neutrons. Although zirconium alloys resist corrosion in water, one of the products of any corrosion is hydrogen that can lead to the formation of hydrides. Hydrides are brittle, and as with other hydride-forming metals, zirconium alloys are susceptible to embrittlement when hydrides are formed [1]. The embrittlement takes two forms: short-term loss of toughness and a stable, time-dependent crack growth mechanism called Delayed Hydride Cracking (DHC).

This form of time dependent cracking was discovered during the storage at room temperature of Zr-2.5Nb fuel cladding before irradiation [2]. High residual tensile stresses from welding were a dominating factor in these failures. Large residual tensile hoop stresses were also responsible for cracking in Zr-2.5Nb pressure tubes. The source of these stresses was either the process used to join the pressure tube to the ends of its fuel channel [3] or from tube straightening [4]. DHC was the mechanism for propagation of cracks formed at hydride blisters in Zircaloy-2 pressure tubes [5]; here a large temperature gradient contributed to the accumulation of hydrides at the crack tip.

Hydride cracking was strongly implicated in long splits that allowed substantial leakage of fission products from some Zircaloy nuclear fuel cladding used in boiling-water reactors (BWR), [6, 7, 8]. With fuel expansion during fuel rearrangement, the hydrided cladding was stressed in tension, which led to crack initiation. The cracks grew through-wall, propagated axially, and could be over 1 m long. Brittle regions in "chevrons" characterized the fractures, with the crack being longer on the outside surface than the inside surface of the cladding [9]. The lower bounds of the crack velocities were in the range 4×10^{-8} to 6.6×10^{-7} m/s based on assuming constant growth rates in the time between first detection of the defect and removal of the fuel. The mechanism of cracking appeared to be a form of DHC [10], perhaps exacerbated by a continuous additional supply of hydrogen from the steam inside the fuel element [11, 12]. A DHC-type of mechanism has been identified as being responsible for radial cracking starting at the outside surface of BWR fuel cladding when power ramped after a high burnup [13].

DHC consists of four stages:

- If a zirconium alloy component containing a flaw and hydrogen is loaded in tension, hydrogen in solution diffuses up the stress gradient to the tip of the stress raiser and increases the local hydrogen concentration.
- A hydride nucleates if the accumulated concentration of hydrogen exceeds the solubility limit. The hydride grows as more hydrogen arrives at the flaw tip.
- The hydride fractures if the tensile stress is large enough and if the hydride reaches a critical condition, probably related to size.
- The crack extends when the process is repeated.

Stages 1 to 3 take time and represent an incubation time before cracking starts. Stage 3 implies a threshold condition must be exceeded before cracking is observed. In fracture mechanics, the stress intensity factor, K_I, is proportional to the product of the tensile stress, σ, and square root of the crack length, $\sqrt{a}$. The threshold value for DHC is called K_{IH} (threshold stress intensity factor). At values of K_I greater than K_{IH}, the rate of cracking is controlled by the rate of hydrogen accumulation and is almost independent of K_I, Fig. 1.
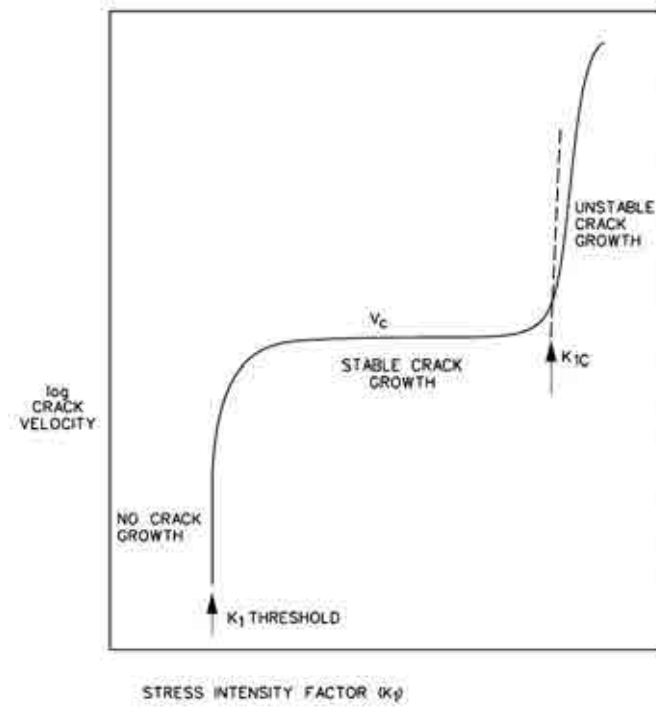
FIG. 1. Schematic diagram of crack history showing threshold for DHC, K_{IH}, region of stable crack growth followed by rupture [1].

The rate of hydrogen accumulation is mostly determined by the solubility limit, C_H, and the diffusivity, D_H, of hydrogen in solution in the zirconium. Although the temperature dependence of cracking would be expected to be controlled by C_H and D_H, it is complicated and is described in the schematic diagram depicted in Fig. 2 [14].
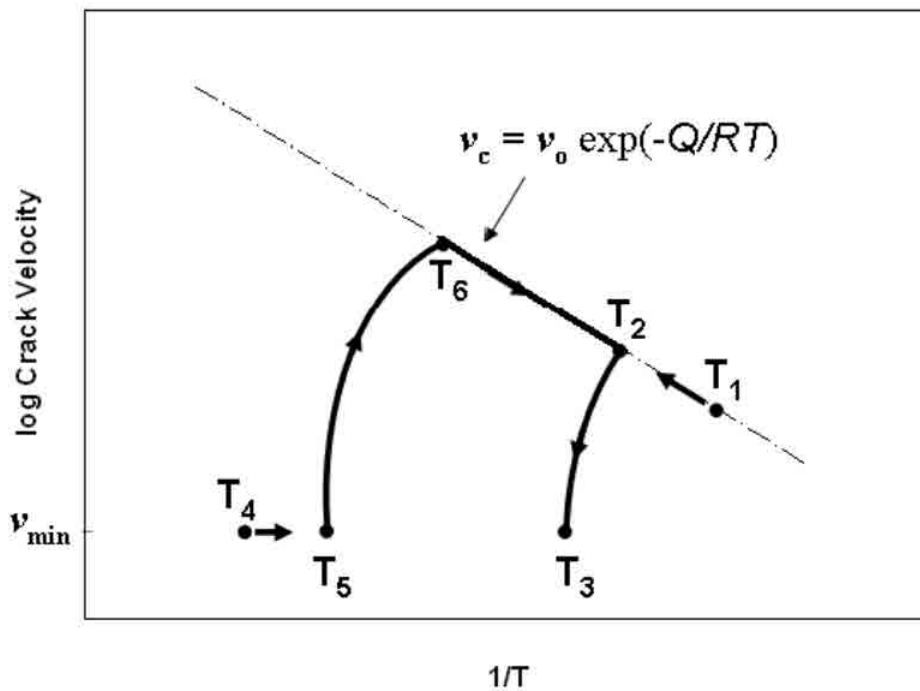
FIG. 2. Schematic diagram of temperature dependence of DHC in zirconium alloys [14]. The conditions for testing are aimed at cooling from T_4, with all the hydrogen in solution, and cooling below T_6.

If the temperature is attained by heating from T_1, initially V increases with temperature but as the temperature is increased, V starts to decline at T_2 and cracking eventually stops at T_3. On cooling from a high temperature, especially where all the hydrogen is in solution, T_4, a temperature is reached where cracking will reinitiate, T_5, and reach a maximum value at T_6. At temperatures below T_6, V has an apparent exponential behaviour and follows:

$$V = A \cdot exp(-Q/RT) \qquad\qquad (1)$$

where

Q is often called the activation energy for DHC in kJ/mol;
R is the Gas Constant (8.314 J/mol.K), and
T is the temperature in K, and
A is a constant.

This temperature behaviour must be taken into account when evaluating failures and reactor operation as well as when considering testing procedures; often a test temperature is attained by cooling to maximise DHC growth rate. A sharp decline in DHC is observed at high test temperatures, T_U, despite the temperature being attained by cooling and sufficient hydrogen being present to form hydrides. In Cold-Worked Stress-Relieved (CWSR) Zircaloy the decline starts below 300°C [15] while in Cold-Worked (CW) Zr-2.5Nb pressure tubes, T_U is about 310 ºC [16].

These descriptions indicate four limits for DHC in zirconium alloys:

- The hydrogen concentration must be high enough and the temperature low enough for hydrides to form.
- The combination of tensile stress and flaw dimensions must be sufficient to exceed K_{IH}.
- Above about 180°C, the temperature must be attained by cooling, otherwise cracking is difficult.
- Flaws will not propagate by DHC at temperatures around 300°C, even when other conditions conducive to DHC are present.

The two technologically important quantities for DHC are the conditions for crack initiation, represented by K_{IH}, and the rate of crack propagation. The latter was the subject of the first part of this IAEA Coordinated Research Project (CRP). The details of the results of testing on Zr-2.5Nb pressure tube material and a state of the art review were issued for CRP-I in an IAEA TECDOC [17] and summarised in a referred paper [18]. As an extension, CRP-II, the rate of DHC was measured in Zircaloy fuel cladding and the results were reported in an IAEA TECDOC [15] and summarised in a referred paper [19]. The current project, CRP-III, is part of an IAEA programme on "Hydrogen and Hydride-Induced Degradation of the Mechanical and Physical Properties of Zirconium based Alloys" with the specific task to investigate the temperature dependence of conditions for crack initiation, K_{IH}. Knowledge of K_{IH} is important because it can be used to evaluate the health of components and their resistance to failure. This information is required as part of the assessment of spent fuel during storage where the temperature history of continuous cooling is perfect for DHC following the temperature sequence 4 to 5 to 6 to 1 in Figure 2. Based on information from Zr-2.5Nb pressure tube material [20], the expected behaviour of Zircaloy-4 fuel cladding should be similar to Fig. 3, where the sharp decline in DHC growth rate at T_U is matched with an equivalent rise in K_{IH} at high test temperatures.
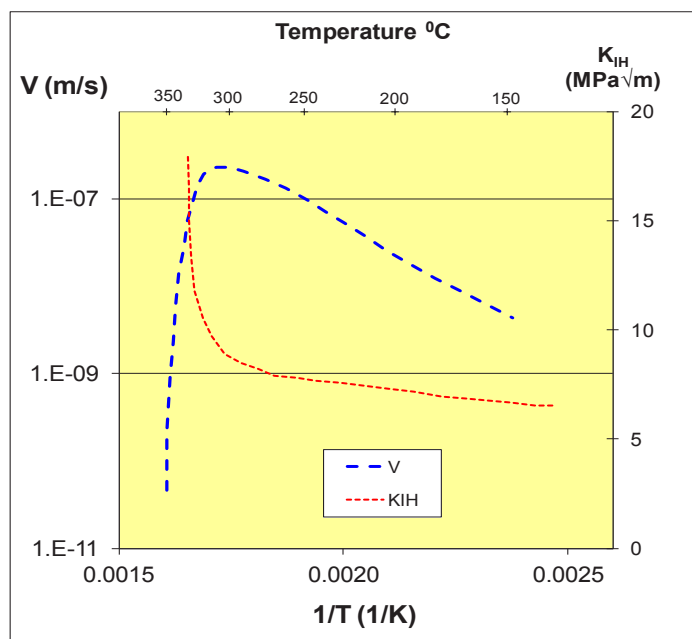
FIG. 3. Temperature dependence of DHC growth rate, V, and K_{IH} in Zr-2.5Nb showing drop in V and concomitant large increase in K_{IH} at high test temperature defining T_U, based on data in [20].

Although several methods are available to test fuel cladding for DHC, the rate of axial crack propagation was successfully measured using the Pin-Loading Tension (PLT) technique [21]. This method was originally developed at Studsvik for fracture toughness evaluation of thin walled tubing [22, 23] and was chosen for the CRP programme because:

- its loading is similar to that in a compact toughness specimen used in CRP-I;
- in a comparison of test methods for fracture toughness of Zircaloy-4 fuel cladding, the PLT technique provided the lowest values of $J_{0.2}$ and dJ/da indicating that this technique provides good constraint and limits plasticity at the crack tip [24];
- the technique was thought to be amenable to technology transfer, especially since the method was developed by an established member of the CRP.

The IAEA set up this CRP on "The Evaluation of Conditions for Hydrogen-Induced Degradation of Zirconium Alloys during Fuel Operation and Storage" with the objective of establishing a uniform and consistent laboratory practice to determine the limit of stress intensity factor for DHC, K_{IH}, in the axial direction of fuel cladding to be followed internationally so that a meaningful interlaboratory comparison of the results could be made. The test materials were two versions of Zircaloy-4 representing PWRs and CANDUs. A few tests were also performed at VNIINM (Russian Federation) in their programme on the experimental alloy E635M and these results are included for comparison with the IAEA programme on Zircaloy-4 [25, 26]. This collection of results constitutes a guiding data base for JRC-ITU to perform experiments on cladding materials from spent fuel rods. The long term programme will study the structural integrity of cladding from spent fuel rods to assure their safety during transport, handling and dry storage.

The participating in the CRP countries, institutes and names of Chief Scientific Investigators are listed in Table 1. Overall scientific lead and advisory support during the project were provided by Mr. C.E. Coleman of CNL, Canada.

TABLE 1. PARTICIPATING COUNTRIES, INSTITUTES, NAMES OF CHIEF SCIENTIFIC INVESTIGATORS AND THEIR REACTOR TYPES OF INTEREST

Country	Institute[1]	Chief Scientific Investigators	Reactor type
Argentina	CNEA	Mizrahi, R.	CANDU, PHWR
Brazil	IPEN	Ramanathan, L.	PWR
Canada	CNL/AECL	He, Z.	CANDU
India	BARC	Chakravartty, J.K.	PHWR
Japan	NFD	Sakamoto, K.	PWR, BWR
*Republic of Korea	KAERI	Kim, Y.S.	CANDU, PWR
Lithuania	LEI	Makarevicius, V.	RBMK
Pakistan	PINSTECH	Ali, K.L.	CANDU
Romania	RATEN ICN	Roth, M.	CANDU
Russia	VNIINM	Markelov, V.A.	RBMK, VVER
Sweden	STUDSVIK	Alvarez-Holston, A.M.	BWR, PWR, surveillance on RBMK
Switzerland	PSI	Vallence, S.	PWR, BWR
Ukraine	NSC KIPT	Chernyaeva, T.	RBMK, VVER
European Union	JRC-ITU	Papaioannou, D.	PWR, BWR, RBMK

*Dropped out of the CRP after the 2nd RCM

In this report, Section 2 describes the materials, specimen preparation and test methods, the test results are displayed in Section 3 and discussed in Section 4, while in Section 5 conclusions and recommendations are made.

---

[1] The names of the participating Institutes and their usual abbreviation are given in the list of contributors, page 64. For simplicity, in the text participants are referred to by their country.

2. EXPERIMENTAL PROGRAMME

2.1. ORGANIZATION OF TESTING PROGRAMME

The programme was set up using the previous CRPs as a guide. For the experiments, Studsvik (Sweden) supplied a section of PWR fuel cladding and CNL/AECL supplied a section of CANDU fuel cladding for each country to prepare test specimens. Each laboratory tested several specimens at a single temperature, 250ºC, to establish techniques and solve any experimental problems. The remaining material was tested at other temperatures prescribed by a test matrix with the aim of finding the limiting upper temperature for DHC. VNIINM (Russian Federation) also tested a few specimens of the alloy E635M. All the specimens contained between 120 and 180 ppm hydrogen so the peak temperature before testing was not too high to guarantee most of the hydrogen was in solution before cooling to the test temperature.

Groups of four or five laboratories tested specimens at one other temperature. In principle each group would attempt three valid tests on each material at the following temperatures:

Group 1 - 227°C: Sweden, Argentina, Brazil, Japan;

Group 2 - 282°C: Romania, Canada, India, Pakistan, Switzerland;

Group 3 - 267°C: Russia, Lithuania; Ukraine, Korea.

Several laboratories also performed tests at higher temperatures in an attempt to evaluate T_U.

Several situations developed during the project that impeded the completion of the programme of testing in the allotted time. Most countries did not test CANDU material. Testing for K_{IH} is more complicated than measuring crack growth rate and several laboratories had much difficulty in obtaining reliable results. Part of the problem was caused by infrastructure deficiencies. Other laboratories had less than wholehearted support from their management while in others, experienced participants were no longer available for the CRP or were new to this type of testing. Korea had to drop out of Group 3, and Argentina, Japan and Ukraine obtained no valid results for crack behaviour.

2.2. MATERIALS

The test materials were standard PWR Zircaloy-4 from Sandvik, lot 407130 and standard CANDU Zircaloy-4 supplied by Cameco, lot 106499. VNIINM investigated own material- E635M alloy. The main elements in the chemical composition are given in Table 2.

TABLE 2. CHEMICAL COMPOSITION OF TEST MATERIALS

Materials			
	PWR Sandvik Lot 407130	CANDU Cameco Lot 106499	E635M VNIINM Ref. [25]
Element			
Nb (wt.%)	-	-	0.8
Sn (wt.%)	1.31	1.27	0.8
Fe (wt.%)	0.21	0.21	0.32
Cr (wt.%)	0.11	0.11	<0.01
O (ppm)	1355	1180	0.08
Si (ppm)	95	93	<40
C (ppm)	145	140	40
N (ppm)	29	36	<20
H (ppm)	5	4	7

During fabrication the final pilgering imposed 78 to 90% cold-work, based on area reduction on a cylindrical mandrel, and the final heat-treatment was 480ºC for 3.5 h for PWR, 500°C for 8 h for CANDU and 400°C for 24 h for E635M. The tube dimensions are listed in Table 3.

TABLE 3. DIMENSIONS OF TEST MATERIALS

Materials			
Dimensions	PWR Sandvik Lot 407130	CANDU Cameco Lot 106499	E635M VNIINM Ref. [26]
Outside diameter, mm	9.5	13.1	9.5
Wall thickness, mm	0.57	0.39	0.57

The starting microstructures were examined by light and transmission electron microscopy. For the PWR material, the microstructure consisted of elongated grains, with between 5 and 10% recrystallized grains, Fig. 4(a) and Zr-(FeCr)$_2$ second phase particles, Fig. 4(b).
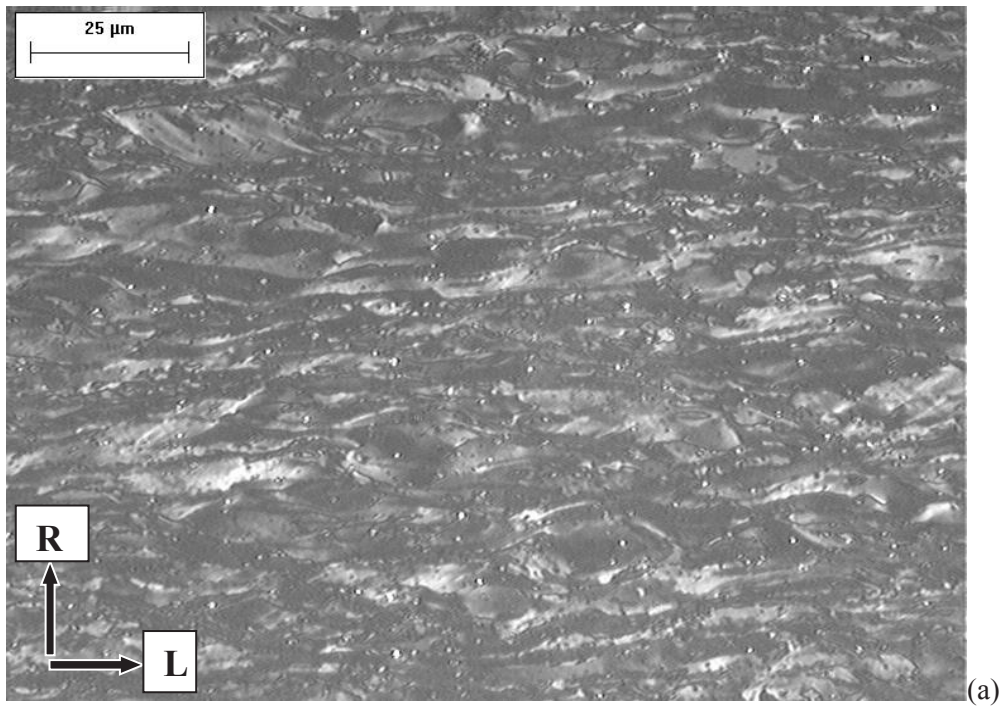
FIG. 4 (a). Representative microstructure of Zircaloy-4 from PWR cladding in the cold-worked and stress-relieved condition revealed by light microscopy; longitudinal section.
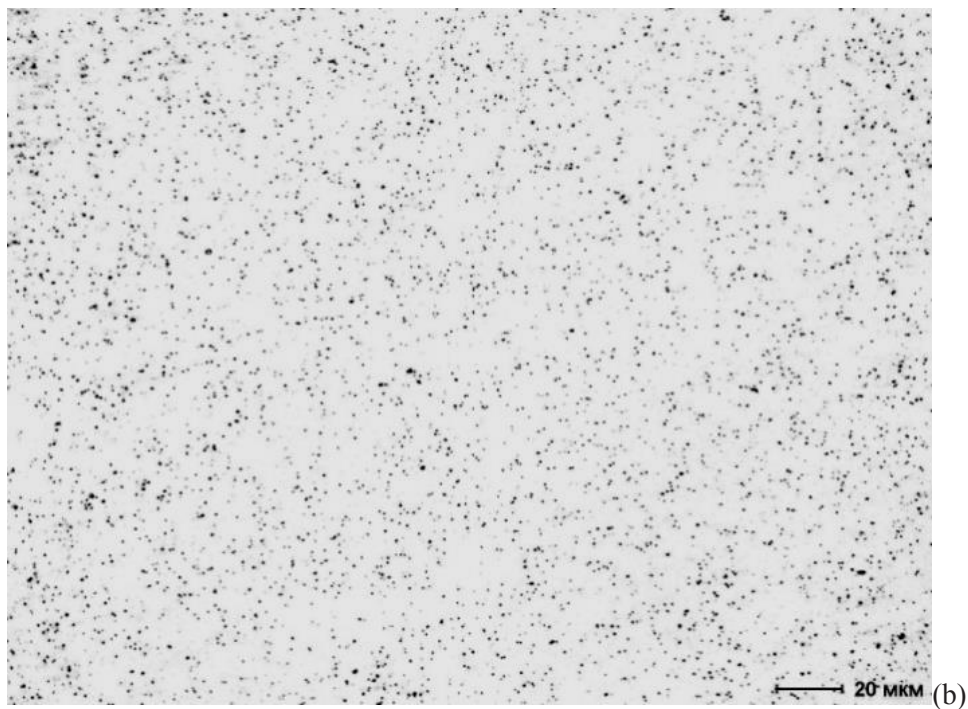
FIG. 4 (b). Representative microstructure of Zircaloy-4 from PWR cladding in the cold-worked and stress-relieved condition revealed by light microscopy showing Fe-Cr intermetallic particles.

The dislocation structure and start of recrystallization are depicted in Figs 5(a) and b)).
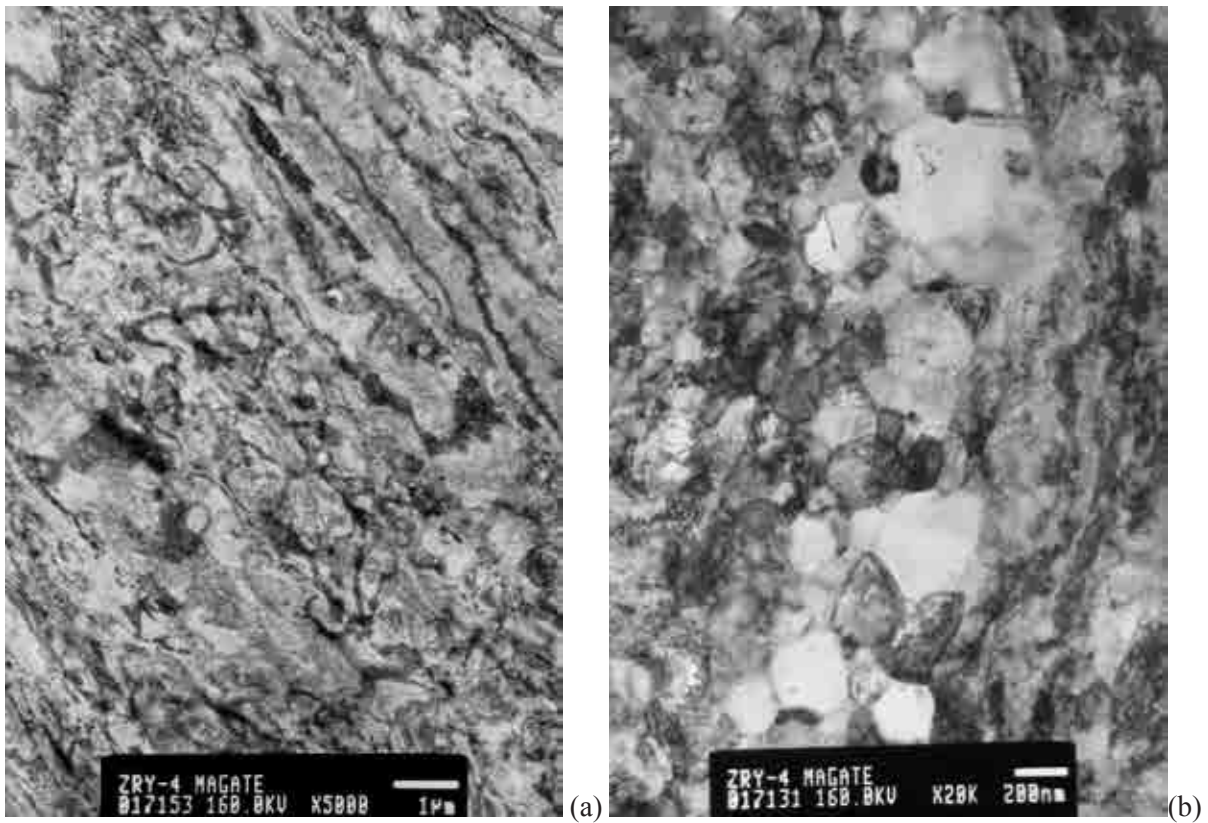
FIG. 5. (a,b). Microstructure of Zircaloy-4 from PWR cladding in the cold-worked and stress-relieved condition revealed by transmission electron microscopy, showing large density of dislocations and incipient recrystallization.

The microstructure of the CANDU material consisted of elongated grains in the axial direction, Fig. 6, but almost equiaxed grains on the transverse-radial plane, with a mean grain diameter of about 4 μm, Fig. 7(a). The small recrystallized grains and about 30% remnants of cold-work, indicated by the small areas of dislocations, are illustrated in Fig. 7(b). The inverse pole figures for each material and a (0002) direct pole figure for CANDU cladding are summarised in Fig. 8.
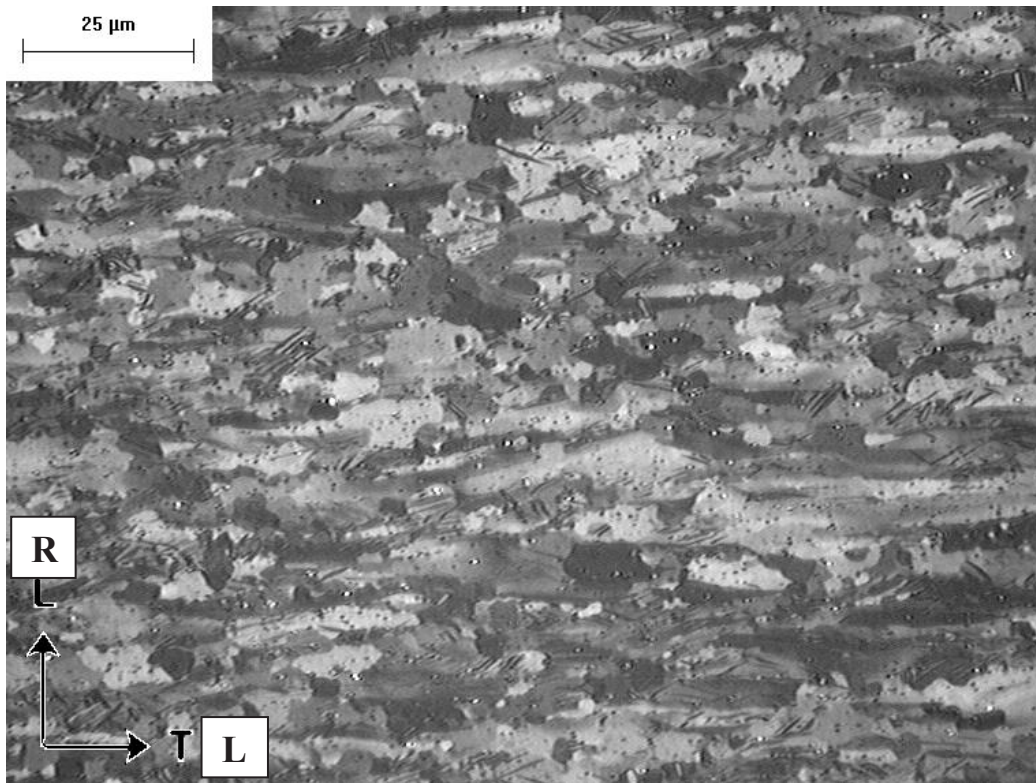
FIG. 6. Representative microstructure of Zircaloy-4 from CANDU cladding in the cold-worked and stress-relieved condition revealed by light microscopy; longitudinal section.
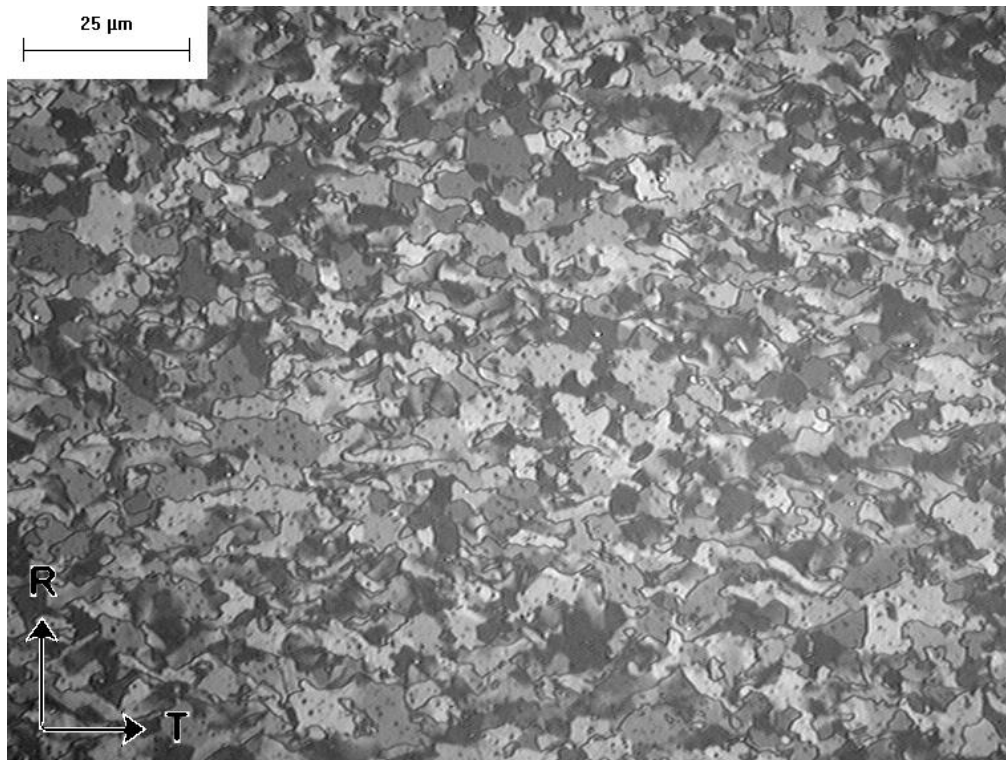

FIG. 7(a). Representative microstructure of Zircaloy-4 from CANDU cladding in the cold-worked and stress-relieved condition revealed by light microscopy; transverse section.

FIG. 7(b). Microstructure of Zircaloy-4 from CANDU cladding in the cold-worked and stress-relieved condition revealed by transmission electron microscopy, showing recrystallized grains and remnants of cold-work.
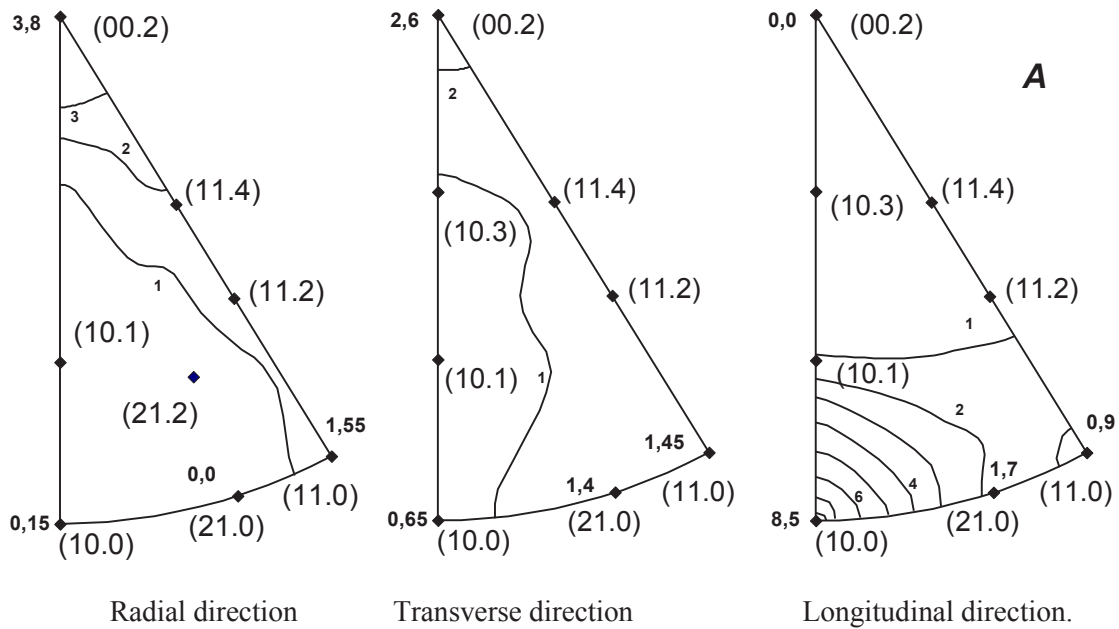
FIG. 8(a). Inverse pole figures for PWR Zircaloy-4 material, Lot 407130.

Radial direction   Transverse direction   Longitudinal direction.
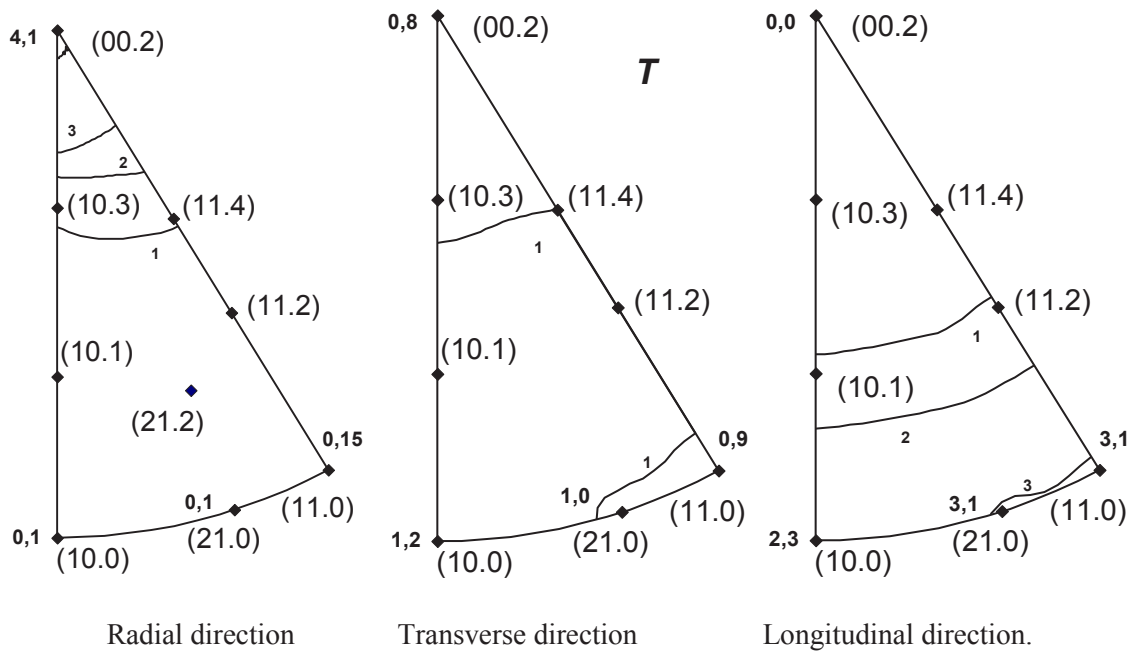
FIG. 8(b). Inverse pole figures for CANDU Zircaloy-4 material, Lot 106499.

XRD# BK8A Zircaloy-4 Fuel Sheath
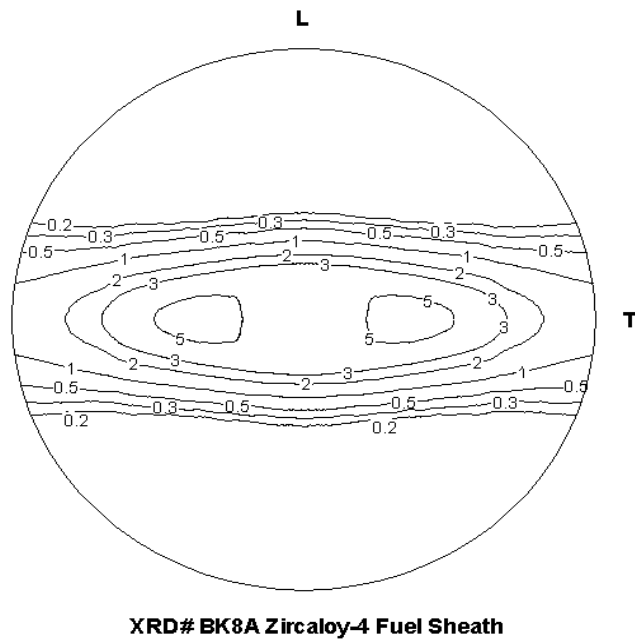
FIG. 8(c). Direct pole figure of basal planes in CANDU Zircaloy-4 cladding, Lot 106499. L is longitudinal direction and T is transverse direction.

The basal plane normals were concentrated about 30º from the radial direction in the radial-transverse plane; the texture factors, F, in the three principal directions, radial, R, transverse, T, and longitudinal, L, are summarised in Table 4. The tensile properties of the tubes are provided in Table 5.

TABLE 4. TEXTURE FACTORS FOR BASAL PLANES IN TEST MATERIALS. ([#]INVERSE POLE FIGURE; [*] DIRECT POLE FIGURE)

| Texture factors	PWR Sandvik Lot 407130 CWSR	PWR TECDOC 1649 CWSR	CANDU Cameco Lot 106499	CANDU TECDOC 1649	E635M Ref. [25]
F_R	0.57[#]	0.64	0.66[#], 0.66[*]	0.65	0.59
F_T	0.37	0.30	0.28, 0.282	0.30	0.35
F_L	0.05	0.05	0.08, 0.058	0.05	0.05

TABLE 5. TENSILE PROPERTIES OF TEST MATERIALS IN TRANSVERSE DIRECTION USING RING TENSILE TESTS. NUMBERS IN BRACKETS REPRESENT NUMBER OF SPECIMENS TESTED

Material	Test Temperature (ºC)	0.2% Yield Stress (MPa)	UltimateTensile Stress (MPa)
PWR Sandvik Lot 407130 CWSR 480°C for 3.5 h	20	713	750
	250	408	457
	250	408	452
	250	422	440
	250	436	488
	283	432	432
	283	443	443
	380	382	394
CANDU Cameco Lot 106499 500°C for 8 h	20	524	572 (3)
	220		397 (4)
	250	256	324 (7)
	330		334 (4)
	350	250	304 (3)
E635M 400°C for 24 h. Ref. [26]	20		711 (3)
	250		490 (3)
	380		426 (3)

Compared with the strengths reported previously in IAEA-TECDOC-1649, the values for the PWR cladding are about 50 MPa lower and those for the CANDU cladding are about 40 MPa lower, Fig. 9. The current PWR cladding is about 100MPa stronger than the CANDU cladding, as expected from the degree of recovery and recrystallization. Due to the specially selected for this CRP regime of thermal treatment of E635M alloy, the strengths of the E635M and PWR cladding are similar.
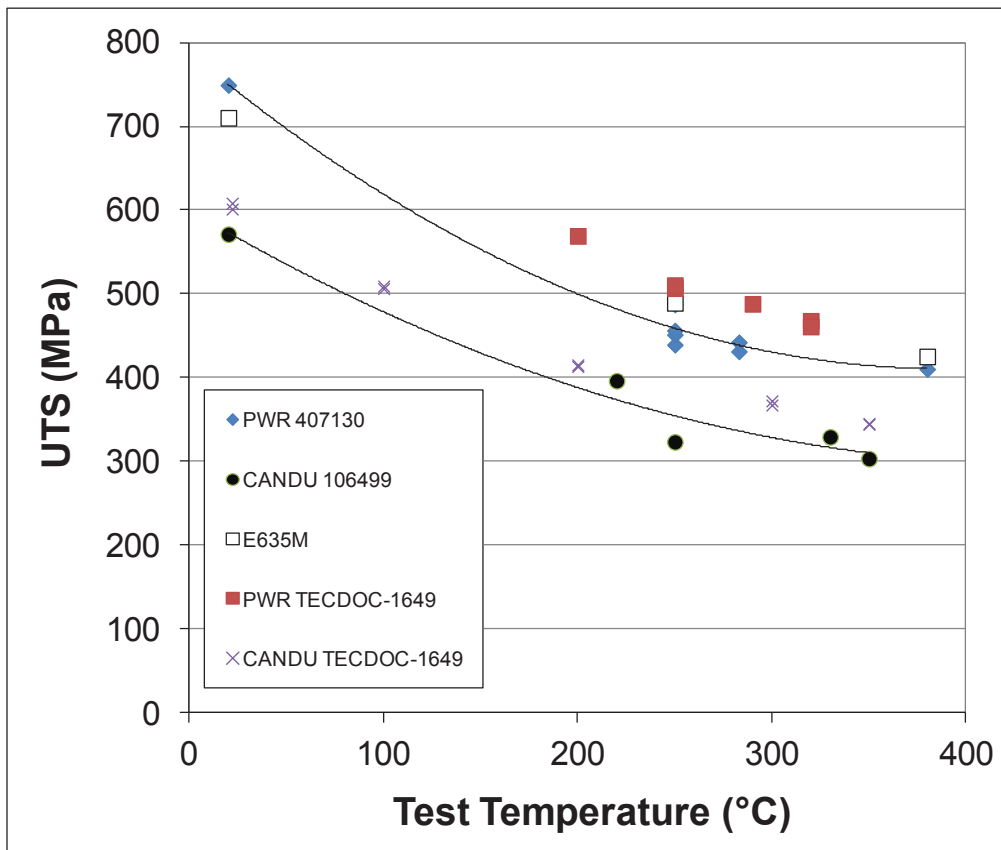
FIG. 9. Temperature dependence of transverse UTS of Zircaloy-4 fuel cladding.

2.3. SPECIMEN AND FIXTURE PREPARATION

The basic procedure for testing is given in [27, 28].

Hydrogen was added to between 120 and 180 ppm by one of two methods:

1) After cleaning, a layer of hydride was deposited on the surfaces electrolytically using 0.1 molar H_2SO_4, a temperature of 65 ± 5 ℃ and a current density of 1 kA/m^2. Diffusing the hydrogen in to the metal by annealing at 350 to 380 °C for 24 h added a homogeneous hydrogen concentration of about 120 to 180 ppm.

2) Some specimens were placed in a vacuum or argon, and hydrogen was added gaseously at between 340 and 380℃.

The resulting hydrides had plate normals in the radial direction, Fig. 10.
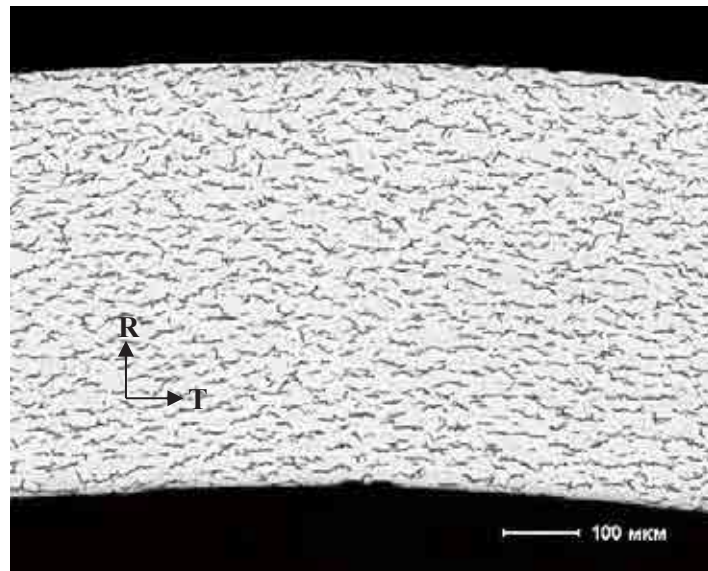
a)
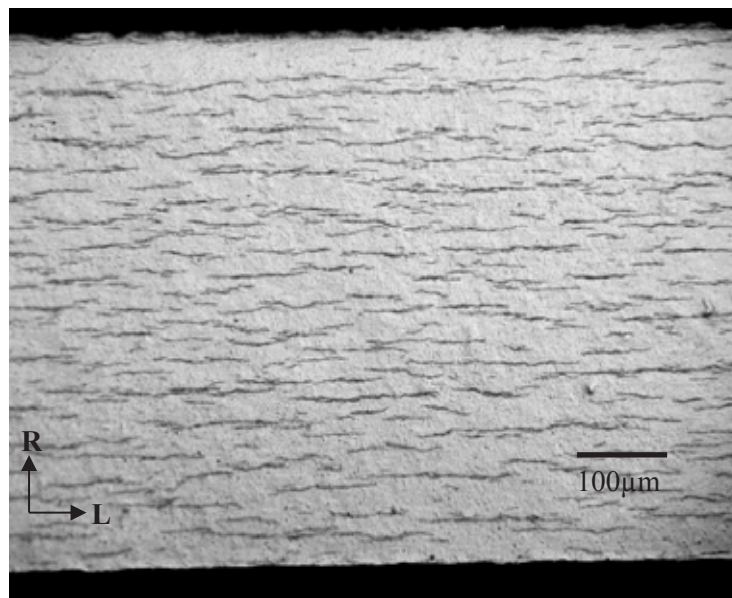
b)

FIG. 10. Representative distribution of hydrides on (a) transverse-radial plane, and (b) longitudinal-radial plane in PWR cladding.

The hydrogen concentration was usually confirmed by analysis, using an inert gas fusion technique. Some laboratories estimated the hydrogen concentration from the initial hydride thickness and time of annealing (Method 1) or from weight change and metallography (Method 2).

The test specimen is shown in Fig. 11. The 13 mm long specimen (c_A) contained diametrally opposite axial notches at both edges with those at one end being sharpened by fatigue at room temperature for a starting length of a_A; the notch at the other end provided an effective specimen length of b_A. The notch that was fatigued to a crack was 0.15 mm wide while the rear notch was 0.5 mm wide. The fatigue pre-cracking was done at 1 to 5 Hz with starting maximum loads of 200 to 300 N cycled down to 50 N. The maximum load was gradually reduced to 90 to 100 N as the crack progressed. The final load was chosen to be

lower than the starting load for the DHC test, typically 160 N, so the plastic zone at the crack tip from fatigue did not interfere with DHC. Between 8000 and 50 000 cycles were required to produce a suitable starting crack, about 1.5 mm in length. The crack length was measured either visually on the surface or using potential drop. In two countries the starter crack could not be made by fatigue and DHC was started from DHC performed at a low temperature (Pakistan) or from as sharp a notch as possible (Brazil). The scatter in results from these latter specimens was larger than in those that were started from a fatigue crack.
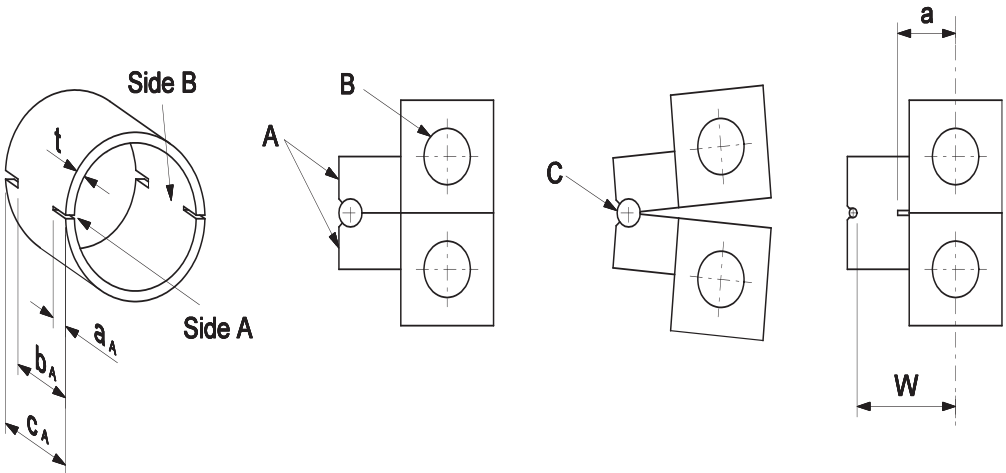
FIG. 11. Schematic diagram of test specimen and Pin-Loading Tension fixture.

The Pin-Loading Tension fixture is shown schematically in Fig. 11 and in a photograph in Fig. 12. Some fixtures were made from Nimonic 90 but successful testing has been achieved using fixtures made from carbon steel. The fixture consisted of two halves, which, when placed together, form a cylindrical holder, A. The diameter of the holder allowed it to be inserted into the specimen while maintaining a small gap. The fixture halves were loaded in tension through pins at B and rotated about a pin C at the ends of the cylindrical holder providing similarity to the loading of a compact toughness specimen, but on two cracks. Care was taken to line up the pre-cracked notches with the join of the two halves of the fixture.
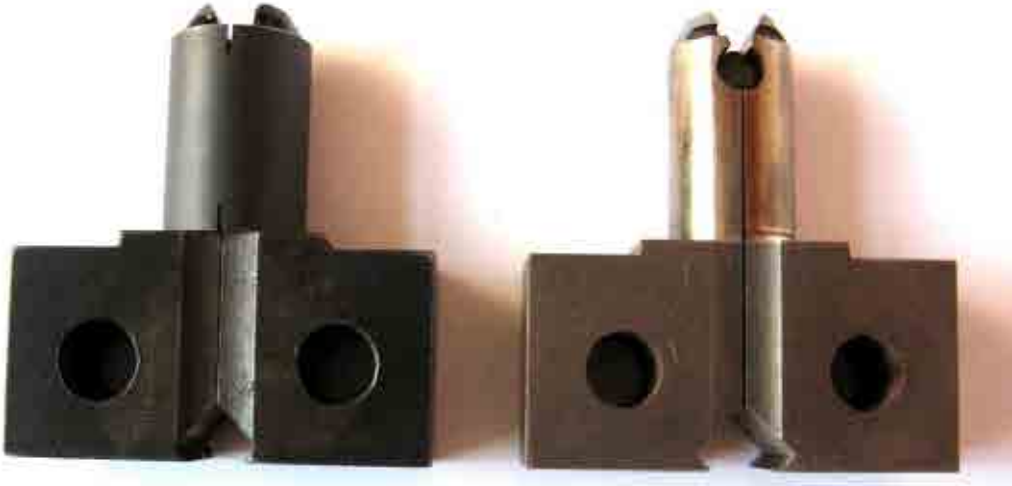
FIG. 12. The PLT fixture; a specimen is in place on the left side.

One laboratory used a cladding specimen with a single notch at one end and was tested in tension (Switzerland). The test setup used to apply a load on the sample is depicted on Fig. 13. The sample, a Zircaloy tube about 12 mm long was inserted on two half mandrels. This ensemble was then placed in a sample holder, on which a tensile force was applied by a universal tensile testing machine. The overall extension of the sample was monitored using an extensometer placed so that the rods of the extensometer measured the variation in external diameter of the sample. When first mounted in the sample holder, the Zircaloy tube contained a notch, about 1 mm long and 0.2 mm wide, machined at one end. This notch was extended by fatigue by cycling under tensile force at low load and room temperature. The total length of the notch and fatigue crack, prior to DHC test, was usually between 1.5 and 2.5 mm.
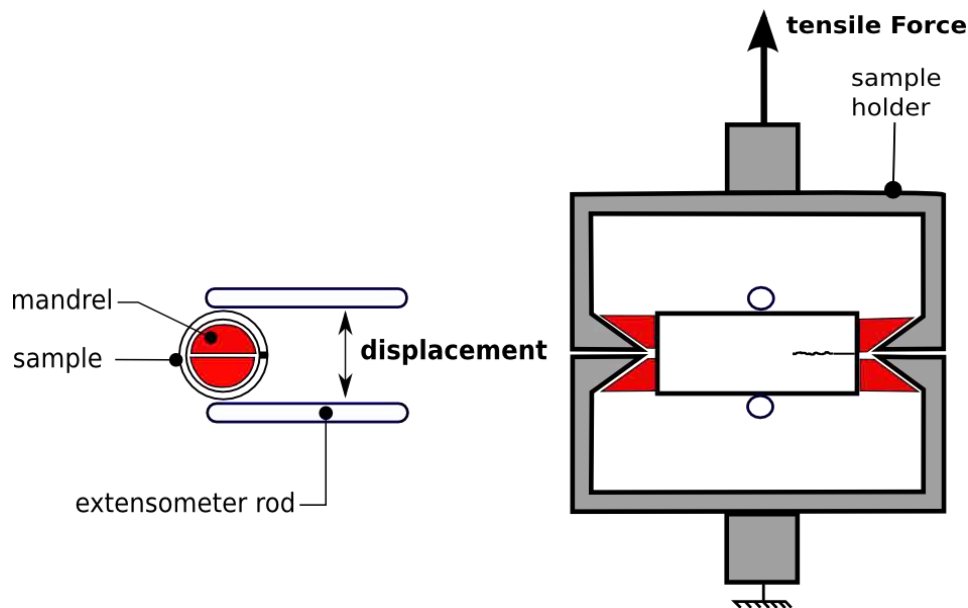
FIG. 13. Tensile loading of cladding with single axial flaw at one end.

2.4.   DHC TESTING

To start a DHC test, the specimen was heated to between 360 to 385°C for 60 minutes to dissolve all the hydrides then cooled slowly with no undercooling to the test temperature, Fig. 14. (In Brazil the peak temperature was 315°C.) This temperature history encouraged cracking and minimised variation; this sequence represented T_4 to below T_6 in Fig. 2, rather than T_1 to T_3 in Fig. 2, where cracking can be difficult.
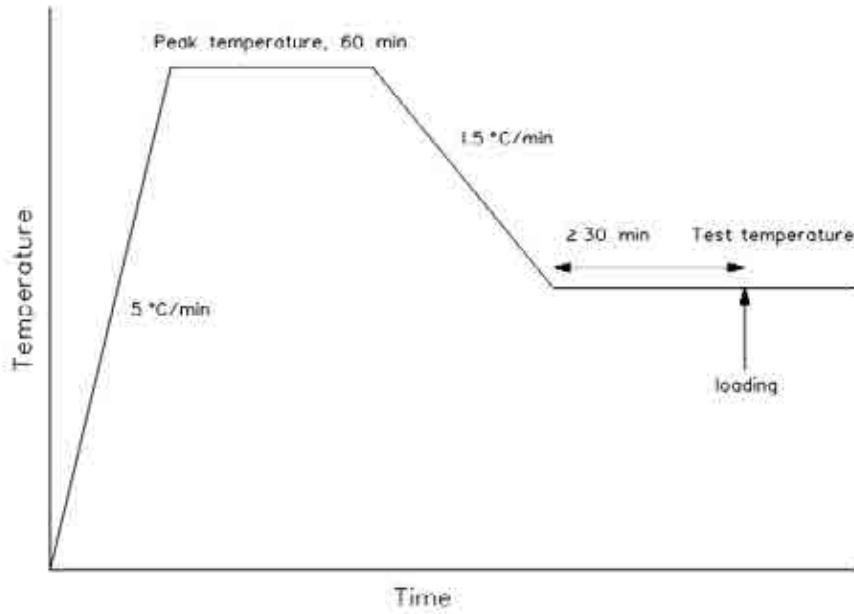
FIG. 14. Schematic diagram of temperature cycle used for DHC tests.

After a short period at constant temperature, at least 30 minutes, the specimen was loaded to a starting value of K_I calculated from Equation (2):

$$K_I = [P/(2t\sqrt{W})]f(a/W) \tag{2}$$

where
P is the load (N);
t is the wall thickness of the cladding (m);
W is the effective width of specimen (m), being distance from the load line to the axis of rotation; see Fig. 11;
A is the effective crack length (m), being distance from load line to the crack tip; see Fig. 11.
$f(a/W)$ is the geometry correction factor.

The value of $f(a/W)$ was determined experimentally from compliance measurements, resulting in:

$$f(a/W) = 92.203 - 468.73(a/W) + 787.15(a/W)^2 - 360.99(a/W)^3 \tag{3}$$

for PWR cladding [28] and

$$f(a/W) = -0.4759 + 13.185(a/W) + 39.533(a/W)^2 - 23.65(a/W)^3 + 12.135(a/W)^4 - 2.9162(a/W)^5 \tag{4}$$

for CANDU cladding [15]

Cracking was detected by several methods:
- Detecting the change in crack length from the change in voltage across the crack tip; called Direct Current Potential Drop (PD).

- Measuring the displacement of each side of the crack or specimen holder, which is equivalent to crack opening.

-   Observing the crack directly on the specimen surface.

    The threshold for DHC was evaluated by four methods:
-   *Multiple specimen method*: measuring crack growth rate, V_c, using the methods established in the previous CRP [15], on several specimens subjected to different values of K_I and finding the value at which $V_c = 0$. An example of what might be expected is provided in Fig. 15, showing the reduction in crack growth with initial K_I in tests on Zr-2.5Nb pressure tubes [29].
-   *Constant displacement method*: starting at a moderate value of K_I and fixing the displacement. When the crack grew, the load decayed until it reached a constant value; K_{IH} was reached when the load did not change for 24 h. A typical load history is depicted in Fig. 16. Previously the reduction in crack growth rate with declining K_I was demonstrated with double cantilever beam specimens of Zr-2.5Nb cracking in hydrogen gas, Fig. 17 [30].
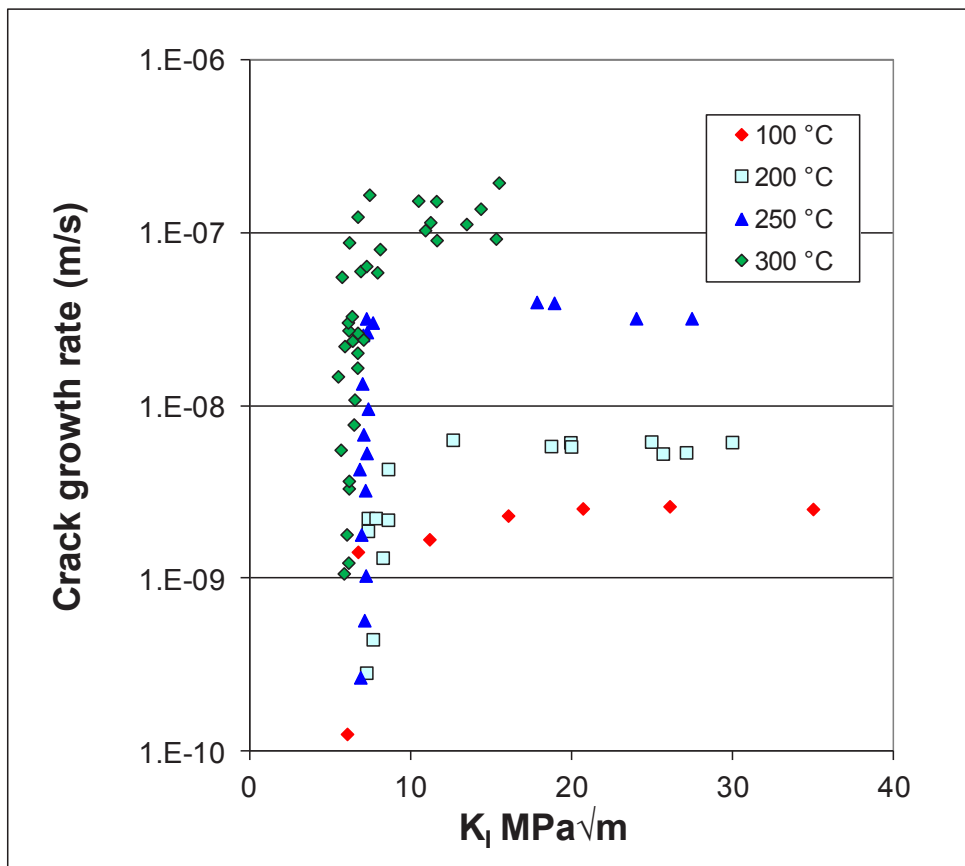
FIG. 15. Crack growth rate in Zr-2.5Nb showing decline at low values of K_I; based on values in [29].
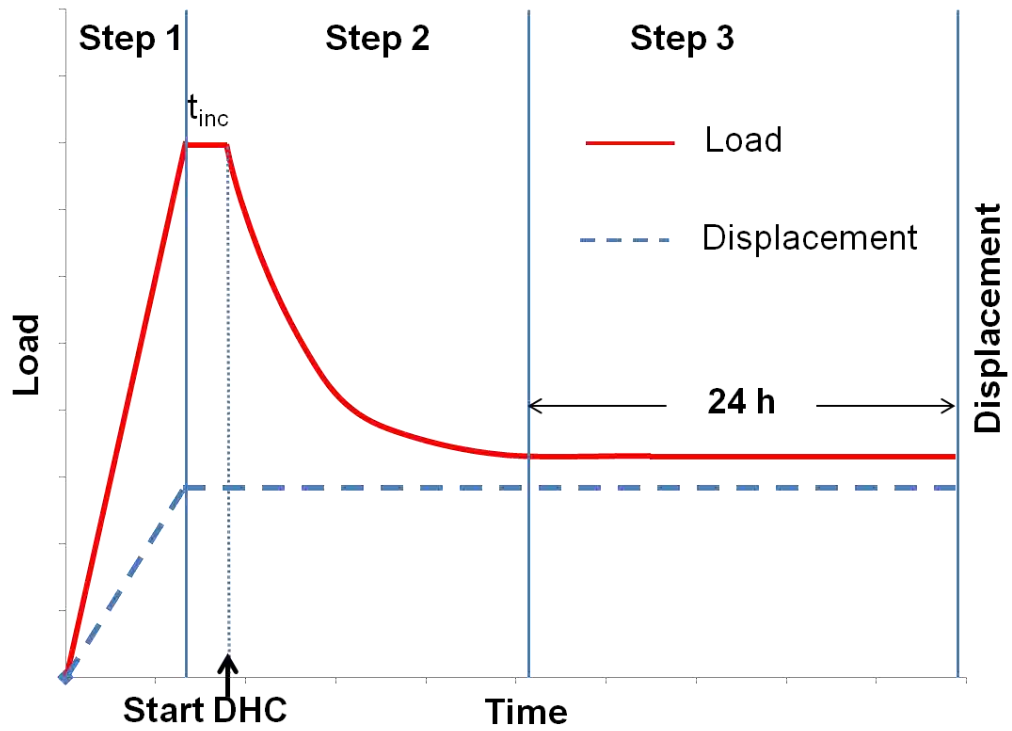
FIG. 16. Schematic diagram of determination of K_{IH} by following the reduction in loading at fixed constant displacement.
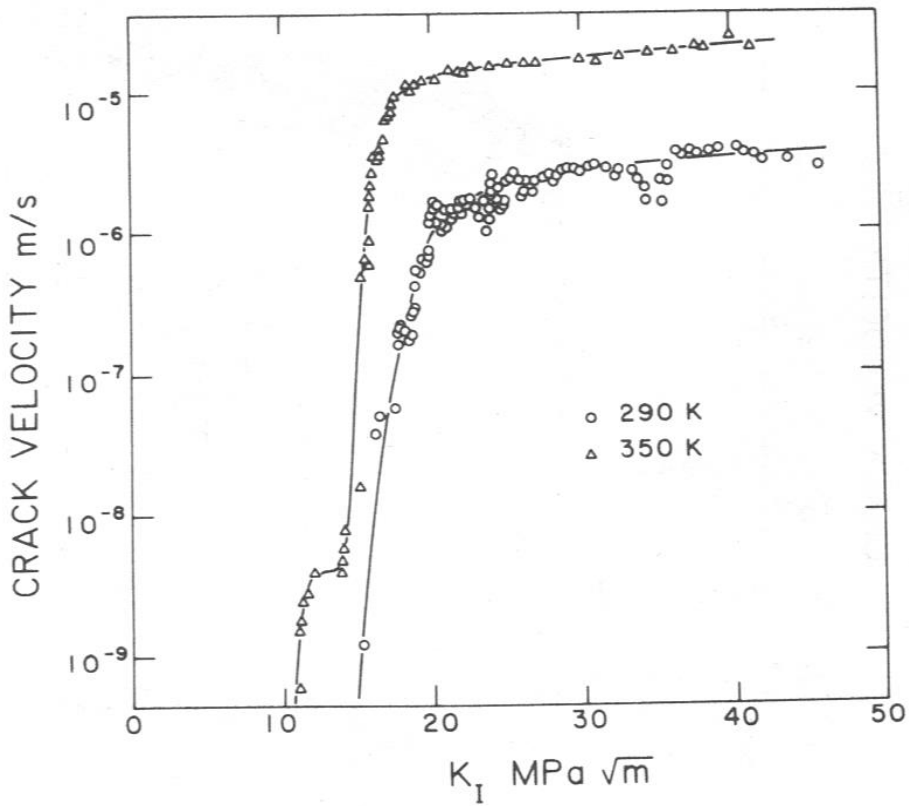
FIG. 17. Cracking of Zr-2.5Nb in hydrogen gas. Double cantilever beam loaded at constant displacement [30].

These two methods are based on ASTM E1681 [31].

- *Uploading method*: starting at a low value of K_I and raising the load 3 to 5% after 24 h if no cracking was observed or until cracking started. K_{IH} was calculated from the load immediately before cracking was detected;
- *Unloading method*: starting at a moderate value of K_I and lowering the load in small steps until cracking has stopped for up to 24 h. This value of K_I represented K_{IH}. The principle is shown with Zr-2.5Nb pressure tube material in Fig. 18, where the increase in incubation time with reduction in K_I approaches a limiting low value [32], indicating K_{IH}.

In some tests, partial unloading was followed by the constant displacement method.
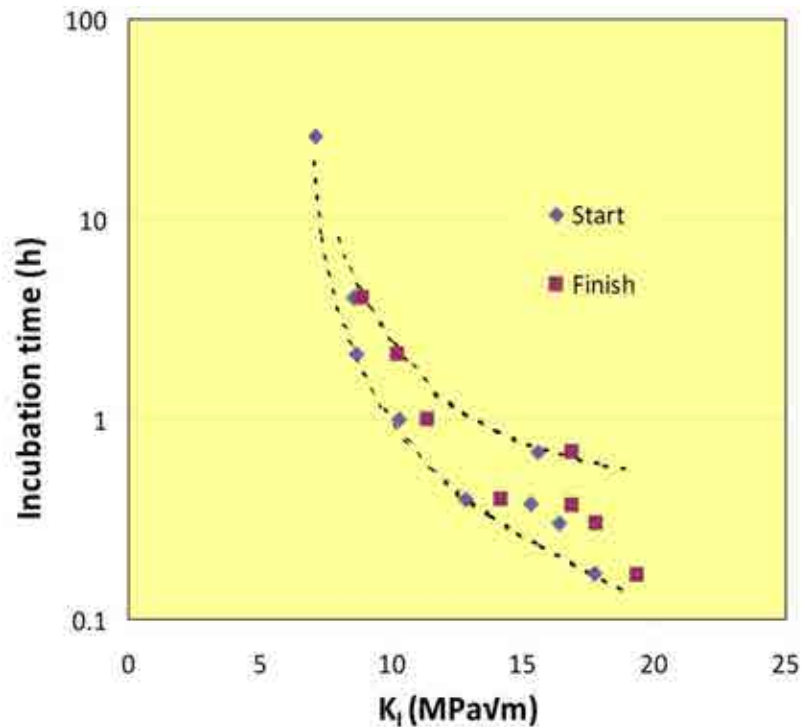
FIG. 18. Reduction in incubation time as K_I is decreased on cantilever beams of Zr-2.5Nb loaded at 230°C; based on values in [32].

Once K_{IH} had been established, the load was removed and the specimen cooled to room temperature. The crack surfaces were lightly heat-tinted from oxidation and the ends of the crack could usually be discerned on the fracture surface. An alternative was to briefly fatigue the specimen at room temperature to mark the end of the DHC. Subsequently, the specimen was broken open and the fracture surface examined. A typical pair of fracture surfaces is shown in Fig. 19.

26
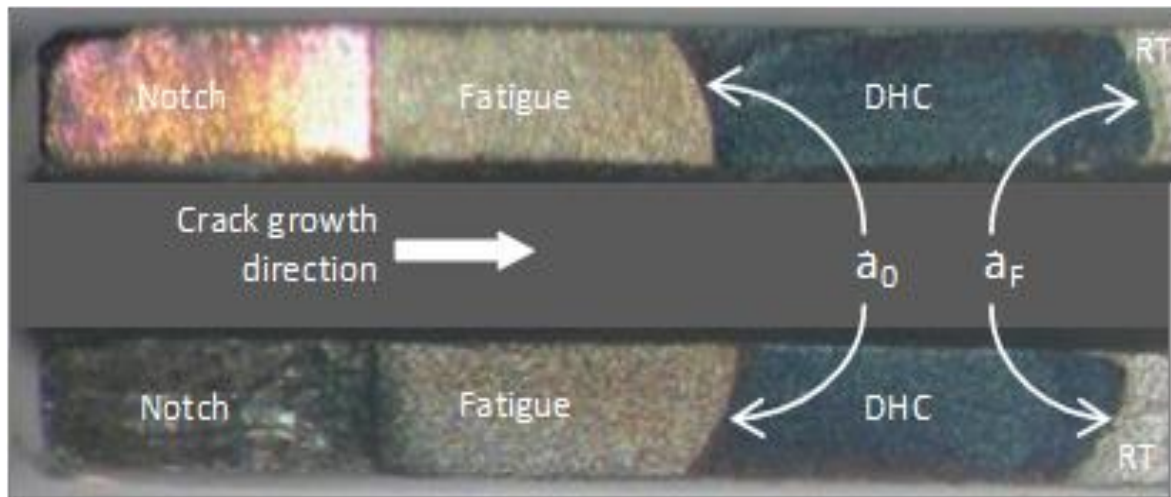
FIG. 19. View of the fracture surfaces of CWSR Zircaloy-4 specimen. The top and bottom edges are the outside surfaces of the cladding. The initial (a_0) and the final (a_F) length of the DHC crack are indicated as well as the areas of notch, fatigue pre-cracking, DHC crack propagation and room temperature fracture after the DHC test (RT).

In this example the delayed hydride crack is about 1.6 mm long. Crack growth by DHC, a_0 to a_F (Fig. 19), was estimated on each crack from the average of nine, PWR, or five, CANDU, equally spaced measurements; the value for the specimen, a_S, was the average of the values of the two cracks. The difference in the two crack lengths provided a measure of uniformity of loading and represented an acceptance criterion; a difference of <20% was set as a provisional acceptance criterion. Other acceptance criteria were based on crack shape; these methods are used during testing of CANDU pressure tubes. Fig. 20 was used to evaluate crack tunnelling by comparing the size of the uncracked ligaments with the crack area. The acceptance criteria were: (area dfg)/(area abhgd) and (area emk)/(area bcekh) < 0.1. The uniformity of crack length was measured by comparing the crack length at three locations, ℓ_n, with the mean length, ℓ_a, Fig. 21. The crack length includes the notch and fatigue crack. The acceptance criteria were: $(\ell_n - \ell_a)/\ell_a < 0.1$.
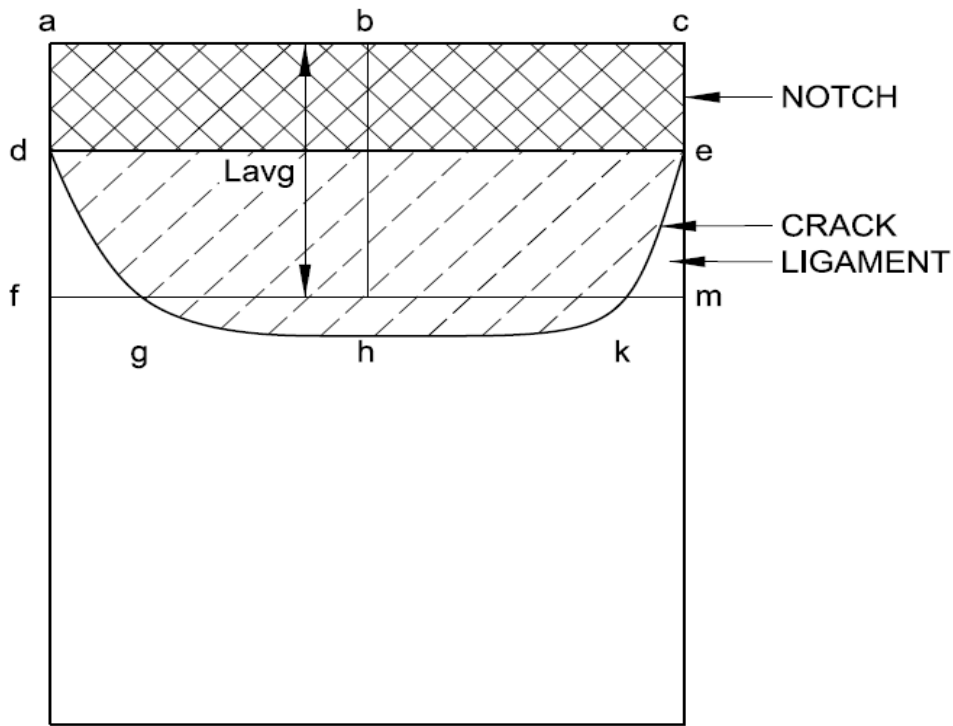
FIG. 20. Geometry of features on crack surface used to define critical dimensions of ligaments. The acceptance criteria were: (area dfg)/(area abhgd) and (area emk)/(area bcekh) < 0.1.
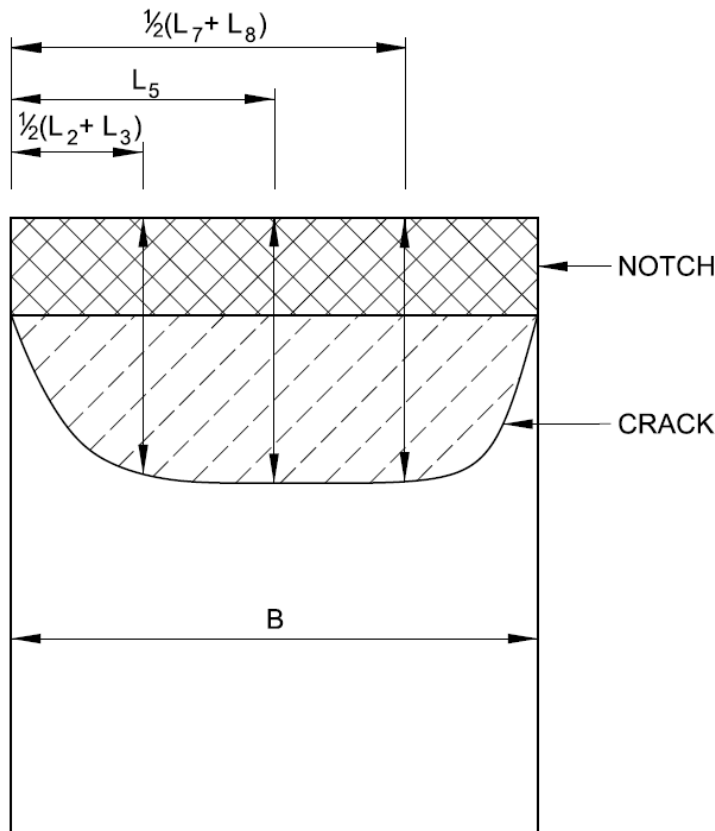
FIG. 21. Geometry of features on a crack surface used to define uniformity of crack growth. L_2, L_3, L_5, L_7 and L_8 are the lengths at each position across the crack face out of nine measurements. The uniformity of crack length was measured by comparing the crack length at three locations, ℓ_n, with the mean length, ℓ_a [20]. The crack length included the notch and fatigue crack. The acceptance criteria were: $(\ell_n - \ell_a)/\ell_a < 0.1$.

Often an incubation period, t_i, was required before DHC started and during tests in which the load was reduced. Crack growth rate, V, in the axial direction was often estimated during the tests; the value obtained before K_I was reduced close to K_{IH} was compared with previous values. The estimate of V was based on the estimate of crack growth divided by the cracking time, that is, time at the specific load minus incubation time.

The techniques used by each laboratory are summarised in Table 6.

The fracture surfaces of all specimens were examined by light microscopy and some were examined by scanning electron microscopy (SEM) to provide details of the fracture mechanism.

TABLE 6. METHODS USED BY EACH PARTICIPATING LABORATORY

Country	Hydrogen addition	Hydrogen measurement	Crack preparation	Crack detection and measurement	Load history for K_{IH}
Argentina	Anneal hydride layer Annealed at 385°C	Inert gas fusion.	Machined notch, fatigued in four reducing load steps; 5 Hz; final maximum load 100 N	Crack opening displacement	Load reduction in steps; some tests unloaded overnight
Brazil	Anneal hydride layer Annealed at 350°C	LECO hot gas extraction, thermal conductivity	Cut at tip of 0.16 mm wide notch	Surface by macroscope; markers 0.2 mm apart	Load reduction in steps; some tests unloaded overnight
Canada	Gaseous 340°C	Differential scanning calorimetry (DSC); Calibrated by hot vacuum extraction mass spectrometry (HVEMS)	Machined notch, fatigued in four reducing load steps; 5 Hz; final maximum load 100 N	Crack opening displacement	Several specimens at various K_I; load reduction in steps; load increase in steps
India	Gaseous 363°C	Volume added, inert gas fusion	Machined notch, fatigued in four reducing load steps; frequency 40 Hz; Final K_I = 8 MPa√m	DC potential drop	Load reduction in steps; Fixed load line displacement
Japan	Anneal hydride layer Annealed at 350°C	LECO hot gas extraction, thermal conductivity	Machined notch, fatigued in four reducing load steps; 5 Hz; final maximum load 150 N	Crack opening displacement	Load reduction in steps
Lithuania	Anneal hydride layer Annealed at 350°C	Estimated from hydride thickness	Machined, fatigued at either 1.6 Hz or 5 Hz; gradual reduction to final maximum load 100 N	Crack opening displacement	Load reduction in steps
Pakistan	Anneal hydride layer Anneal at 365°C	STROLEIN hot gas extraction, thermal conductivity	DHC at 200°C; final K_I = 9 to 17 MPa√m	Crack opening displacement	Load reduction in steps
Romania	Anneal hydride layer Annealed at 365°C	ELTRA hot gas extraction, thermal conductivity	Notch machind by spark erosion; fatigued in three (Final maximum load 100 N) or four steps (Final maximum load 90 N); 5 Hz	DC potential drop	Load reduction in steps
Russia	Gaseous 380°C	LECO hot gas extraction, thermal conductivity	Machined notch, fatigued in reducing load steps 1 to 4 Hz, final maximum load 100 N	Crack opening displacement; Camera outside furnace	Load reduction in steps; Fixed load line displacement

	Anneal hydride layer				
Sweden	Annealed at 350 and 375°C	ELTRA-OH 800 hot gas extraction, thermal conductivity	Machined notch, fatigued in reducing load steps 5 to 10 Hz, final maximum load 120 N	DC potential drop	Load reduction in steps
Switzerland	Gaseous, 380°C Homogenise, 4 cycles to 400°C	Volume of gas; hot gas extraction	Single machined notch, 1 mm; fatigued 0.5 mm	Extensometer on diameter; camera and microscope	Continuous with holds
Ukraine	Gaseous, 380°C	Weighing; volume absorbed; light metallography	Spark machined notch; fatigued at 0.01 Hz	Crack opening displacement	Not done

3. RESULTS

3.1. INITIAL TEST DATA

The preliminary information from which K_{IH} is derived from each test method is illustrated in this section. Both the incubation times between cracking stages and the progress of crack growth may be inferred from the instrumentation during a test. Crack growth is observed directly from the fracture surfaces after test completion.

3.1.1. Fracture surfaces

A set of typical fracture surfaces of CWSR Zircaloy-4 cladding tested at four temperatures is depicted in Figure 22. The variation in colour is produced by the differences in oxide thickness on the fracture surface caused by the cracking times at the four test temperatures. The amount of cracking by fatigue and DHC is summarised for these four specimens in Table 7; the total crack length includes the notch.

TABLE 7. SUMMARY OF CRACK EXTENSION ON BOTH CRACKS BY FATIGUE AND DHC BASED ON THE FRACTURE SURFACES DEPICTED IN FIG. 22

Specimen	Temperature, C°	Crack	Fatigue, mm	DHC, mm	Total, mm	Difference in crack length, %
In5	250	Upper	1.92	2.75	6.28	13.7
		Lower	1.41	2.56	5.46	
In13	267	Upper	1.33	3.28	6.16	6.1
		Lower	1.66	3.38	6.55	
In17	282	Upper	1.1	2.6	5.21	0.2
		Lower	0.86	2.74	5.22	
Inmag25	295	Upper	1.06	3.05	5.72	5.9
		Lower	1.56	2.98	6.07	

250 °C (Specimen In-5)
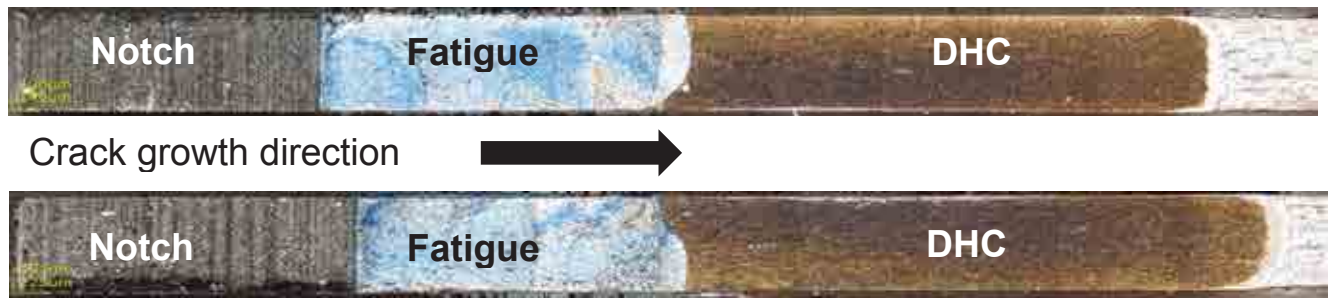
267 °C (Specimen In-13)
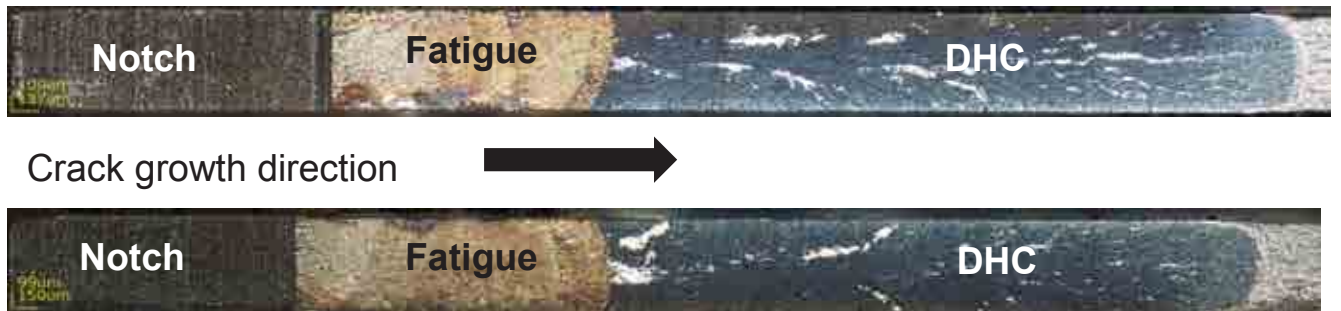
282°C(Specimen In-17)
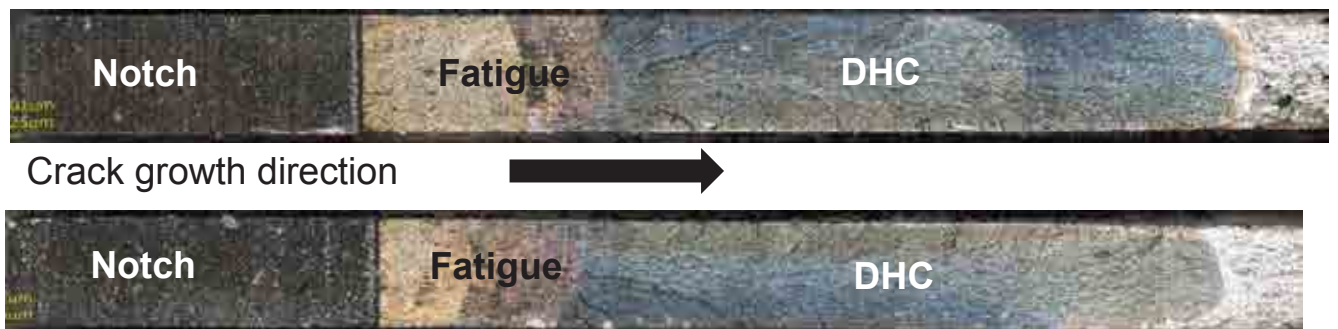
295°C (Specimen Inmag-25)
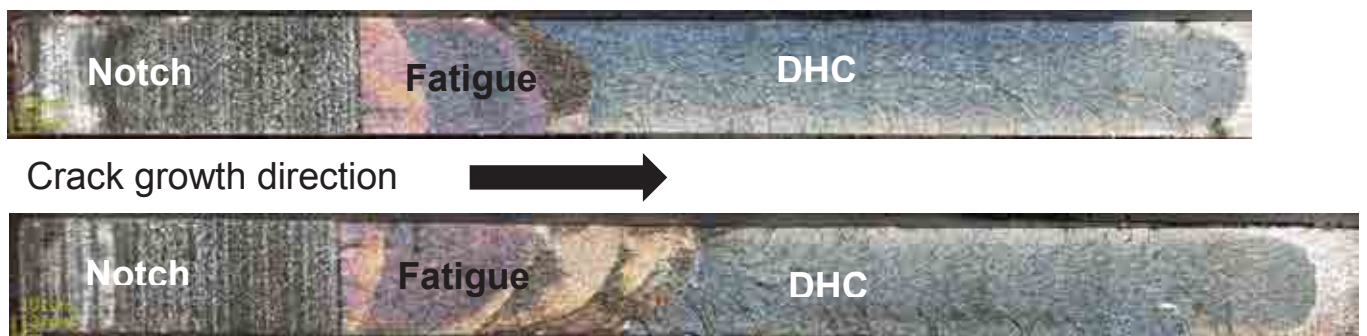
FIG. 22. Fracture surfaces of each crack in specimens of CWSR Zircaloy-4 fuel cladding tested for DHC at 250, 267, 282 and 295°C (Russian Specimens In-5, In-13, In-17, Inmag-25).

In 110 cracks in CWSR Zircaloy-4 LWR cladding the mean amount of fatigue cracking was 1.43 mm with a standard deviation of 0.40 mm and range of 0.56 to 2.67 mm. The amount of DHC was much more variable having a mean of 2.14 mm with standard deviation of 1.10 mm and range of 0 to 5.6 mm. The total crack length (including the notch) reflected

these variations having a mean value of 5.2 mm with a standard deviation of 1.3 mm and a range of 2.8 to 9.0 mm. The difference between the two cracks on each specimen indicated the variation of the initial notches and how well the specimen was aligned during loading, as well as the inherent variation in the fatigue and DHC processes. The total variation is shown in Fig. 23. In 62% of the specimens, the difference between the two cracks was <20%. The remainder had a greater variation and three specimens had a difference of 75%.
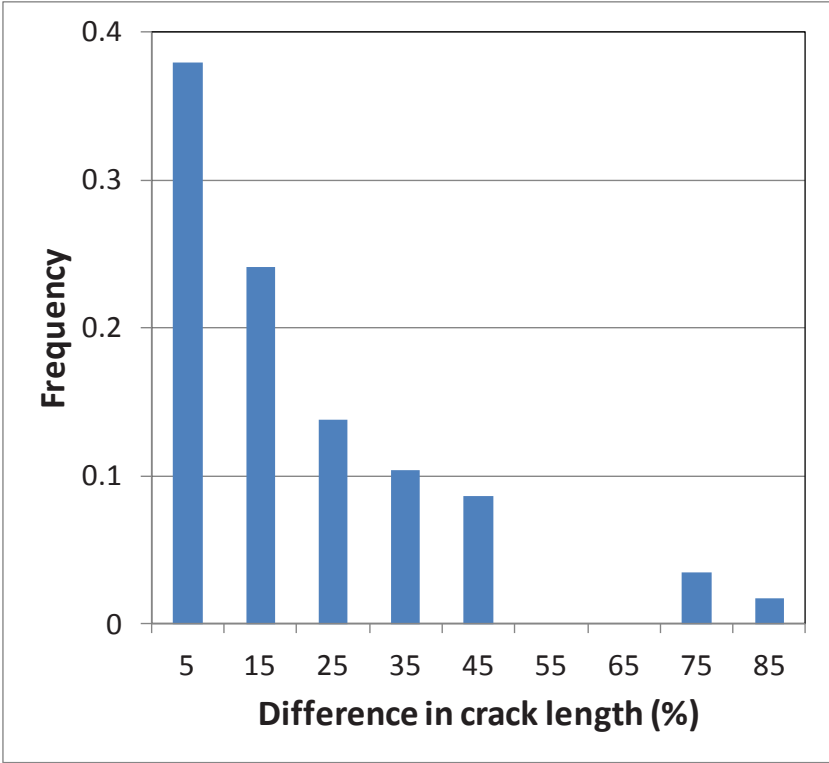
FIG. 23. Frequency distribution of the difference in the two crack lengths in PLT specimens of CWSR Zircaloy-4 at all test temperatures.

The information used to evaluate K_{IH} by each method is illustrated in the following examples.

3.1.2. Multiple specimen method

The dependence on K_I of crack growth rate, V, in CANDU cladding at 250°C for nine individual specimens is shown in Fig. 24.
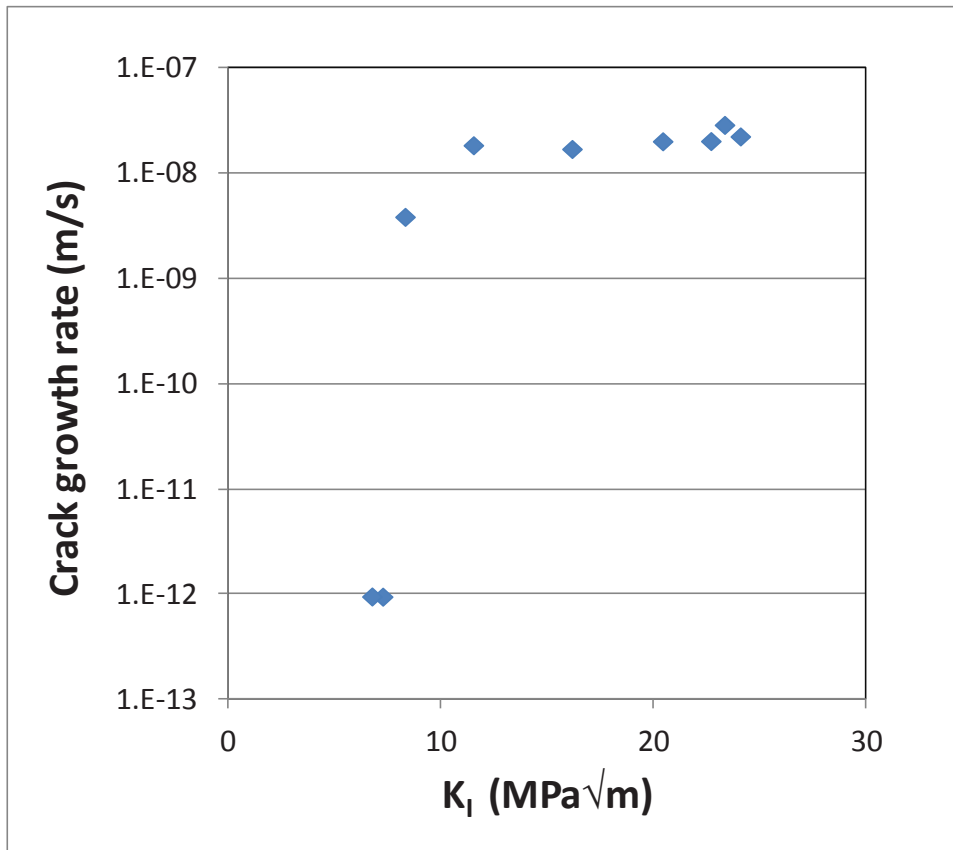
FIG. 24. K_I-dependence of crack growth rate in CANDU cladding at 250°C showing drop at K_{IH} around 7.0 MPa√m (Canadian results).

The crack growth rate is independent of K_I above about 10 MPa√m then declines suddenly with little cracking below 8 MPa√m indicating a value of K_{IH} of 7.0 MPa√m. This behaviour is identical to that in cold-worked Zr-2.5Nb, as shown in Fig. 15. The value of V in the plateau region was about 2.2×10^{-8} m/s, nearly four times larger than the previous mean value of 5.9×10^{-9} m/s [15]. This difference may be attributed to differences in the Zircaloy-4 batches and peak temperature before loading.

3.1.3. Constant displacement method

Two typical results are shown in Fig. 25. As the cracks grew the loads declined until a constant value was withstood, indicating a halt in cracking and representing K_{IH}. The average crack growth rate over small time intervals remained almost constant with increase in crack length and reduction in load but decreased sharply over a narrow range in K_I as K_{IH} was approached. Fig. 26 is an example for a test on CWSR Zircaloy-4 at 282°C indicating a constant crack growth rate of about 1.0×10^{-7} m/s between K_I values from 20 down to 7.5 MPa√m followed by an abrupt drop and no cracking below 6.73 MPa√m. This behaviour is similar to that reported for cracking of Zr-2.5Nb in hydrogen gas, Fig. 17.
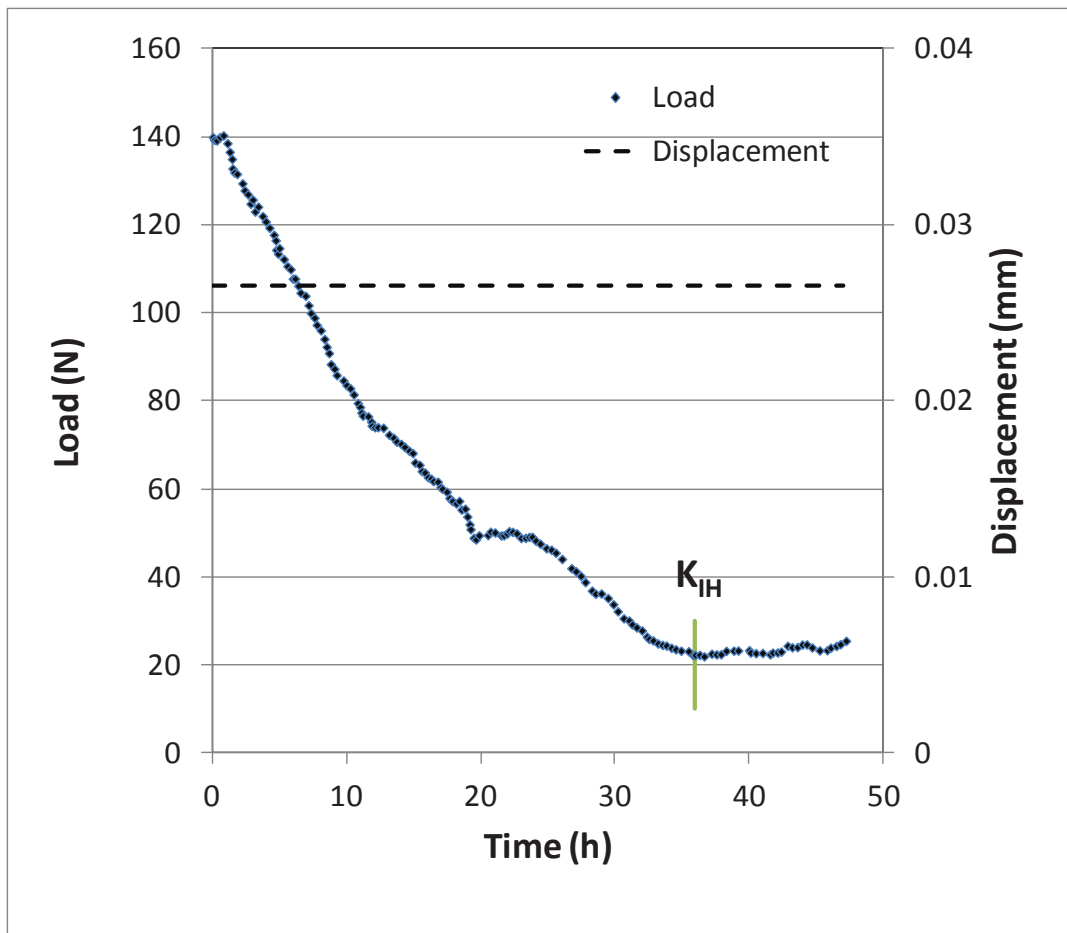
(a)
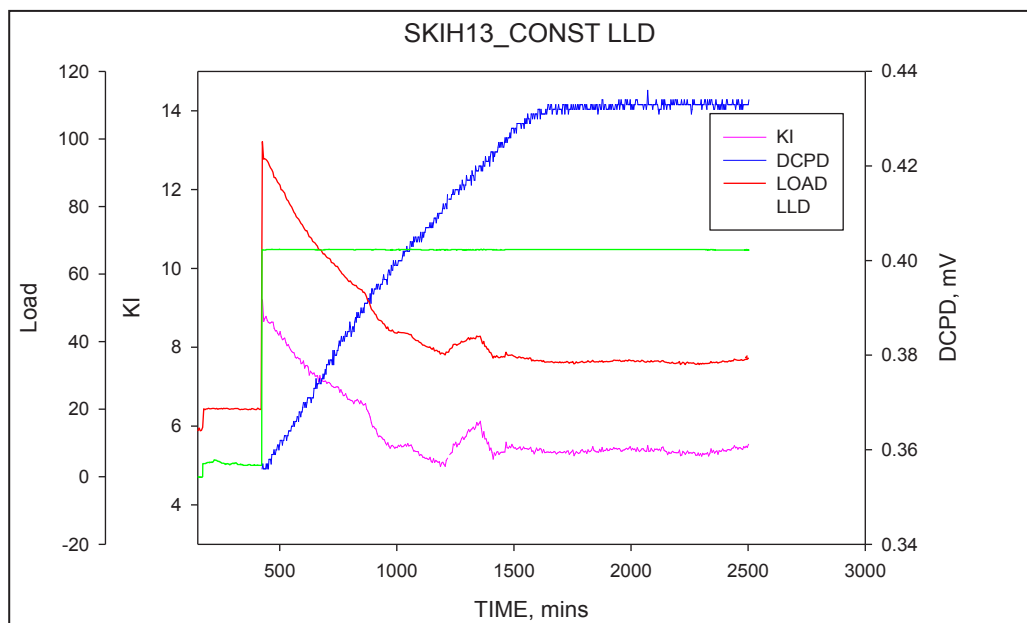
(b)

FIG. 25. Basic test data on CWSR Zircaloy-4 cladding at 250°C showing decline in load as the crack extends under constant displacement; (a) Russian Specimen In-7 providing K_{IH} of 5.5 MPa√m, (b) Indian Specimen SKIH 13 providing K_{IH} of 5.2 MPa√m.
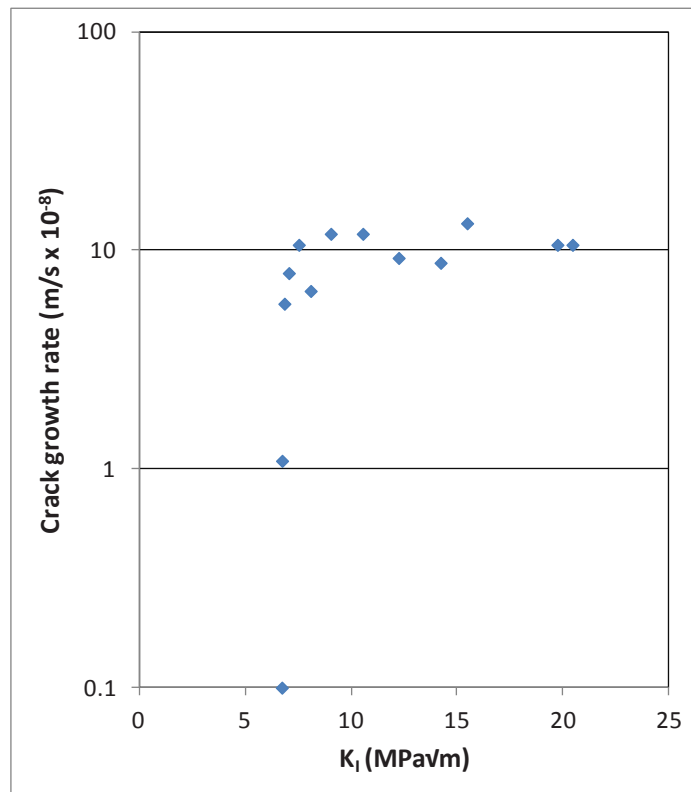
FIG. 26. Crack growth rates as a function of K_I derived from Russian constant displacement test Inmag-23 at 282°C on CWSR Zircaloy-4 cladding indicating K_{IH} of 6.73 MPa√m.

A specimen containing a fatigue sharpened notch but no extra hydrogen was loaded to 200 N at 300°C. The conditions for DHC were absent. The load remained constant for over 8 h, Fig. 27, showing that the load drop in Fig. 25 was caused by cracking rather than stress relaxation from plastic deformation.
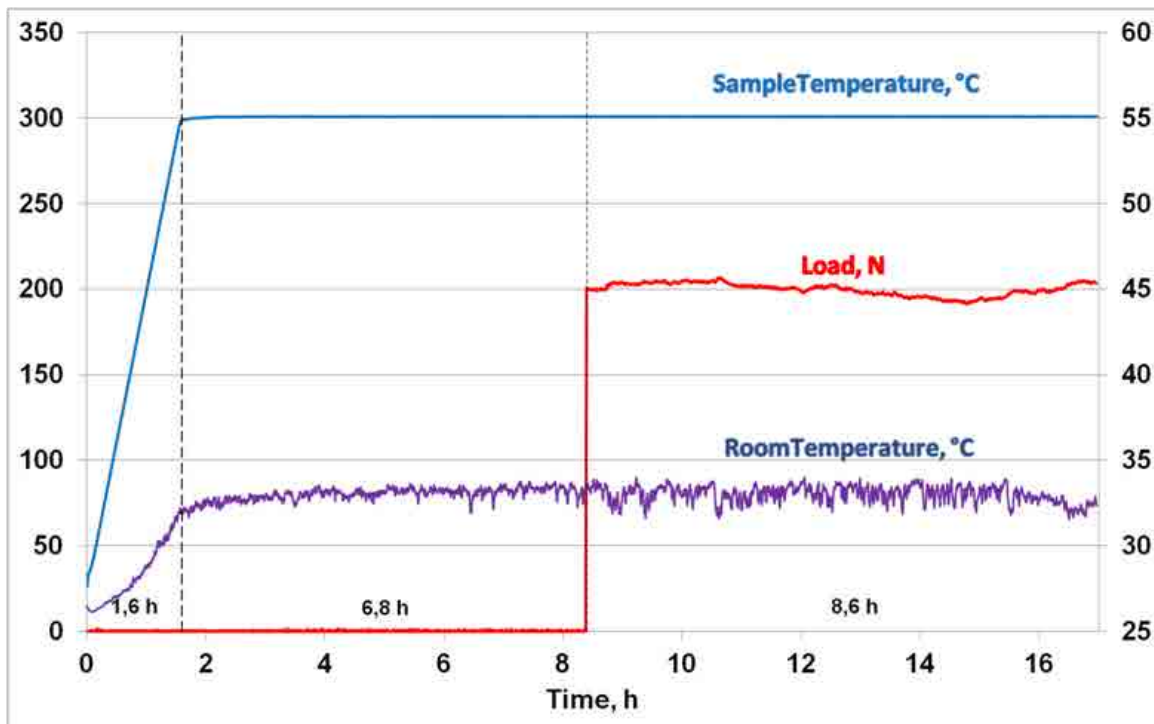
FIG. 27. Russian specimen of Zircaloy-4 cladding containing a notch and fatigue crack but no extra hydrogen loaded to 200 N at 300°C showing no drop in load indicating no stress relaxation in over 8 h.

The load values in Fig. 25 fluctuated because small variations in room temperature caused the tension rod in the testing machine to expand and contract thus affecting the applied load. The effect is illustrated in Fig. 28 with loading at room temperature (a) and at 282°C close to K_{IH} (b).
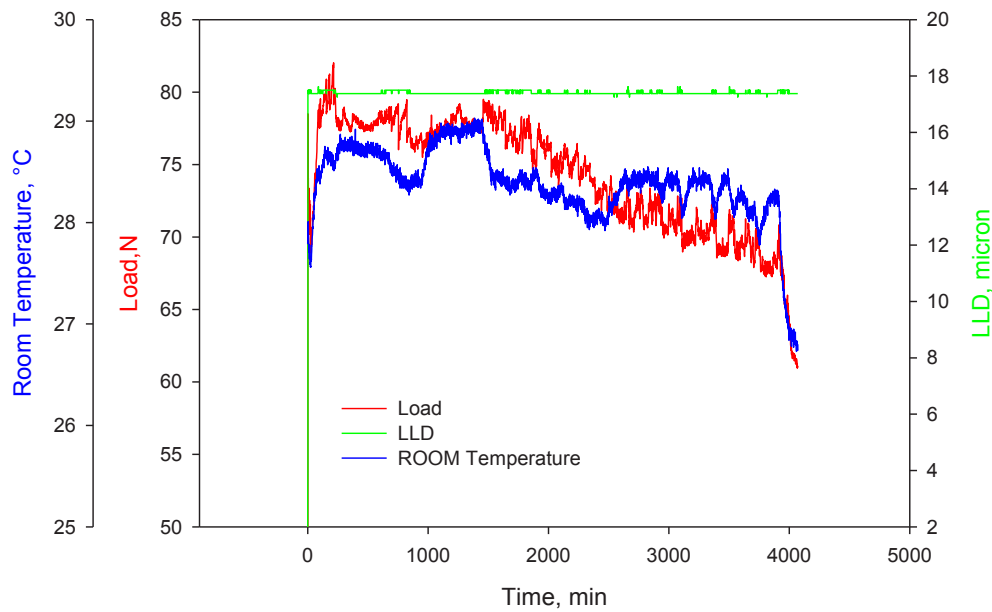
(a)
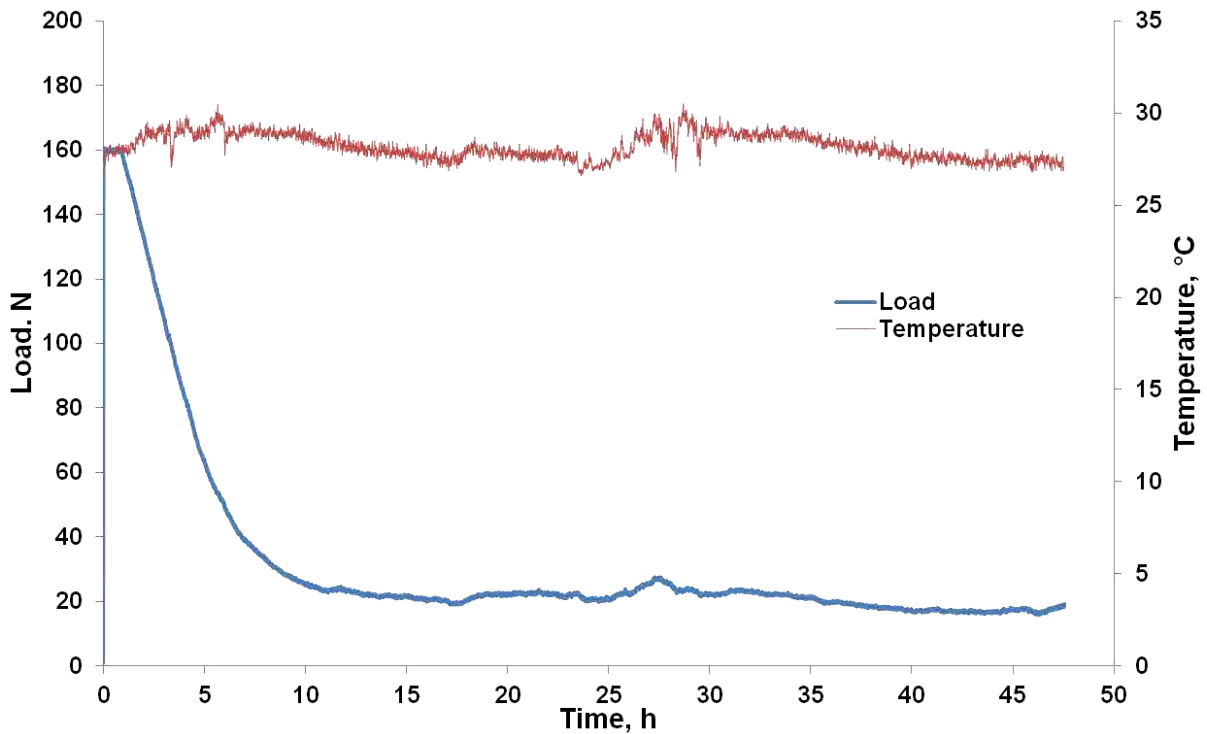
(b)

FIG. 28. Variation of load with change in room temperature: a)the Indian specimen was loaded at room temperature with a force of 80 N and then allowed to relax at room temperature; b) fluctuation in load corresponding with change in room temperature at end of constant displacement test (Russian Specimen In 16) at 282°C.

3.1.4. Uploading method

The load is low at the start of a test using the uploading method and it is increased in steps after 24 h of no cracking until a load is reached where cracking is detected. A typical sequence at 292°C for CANDU cladding was 113, 118, 124, 130, 137, 144 and 151 N, where cracking started. This load corresponded to a K_I of 11.6 MPa√m. K_{IH} was taken from the highest load without cracking, that is, 144 N corresponding to 11.1 MPa√m. The amount of DHC in this type of test is very small, usually in the range 0.2 to 0.5 mm.

3.1.5. Unloading method

Typical histories for tests at 250 and 284°C on LWR Zircaloy-4 are provided in Fig. 29. After loading, a short period with no cracking was observed representing an incubation time. Once cracking started, the load was gradually reduced in 35 to 37 steps of 3 to 4.5% after crack increments of 0.03 mm until cracking stopped. No cracking was detected after 24 h with the load corresponding to K_{IH} of 5.2 MPa√m at 250°C and 18 hours at 7.2 MPa√m at 284°C.
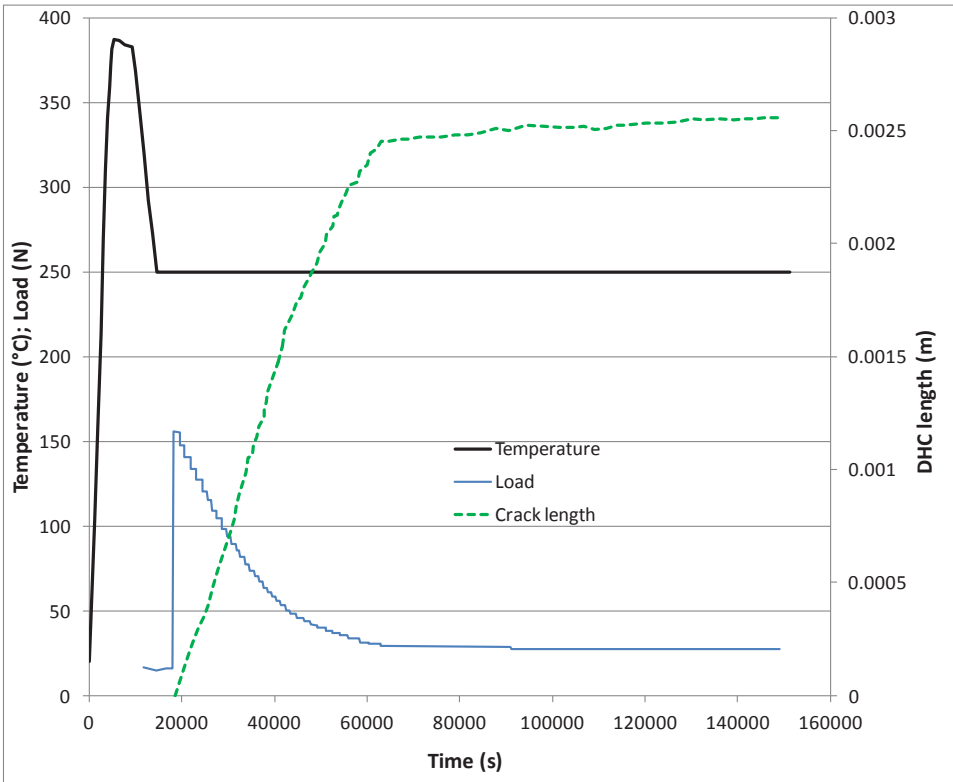
a)
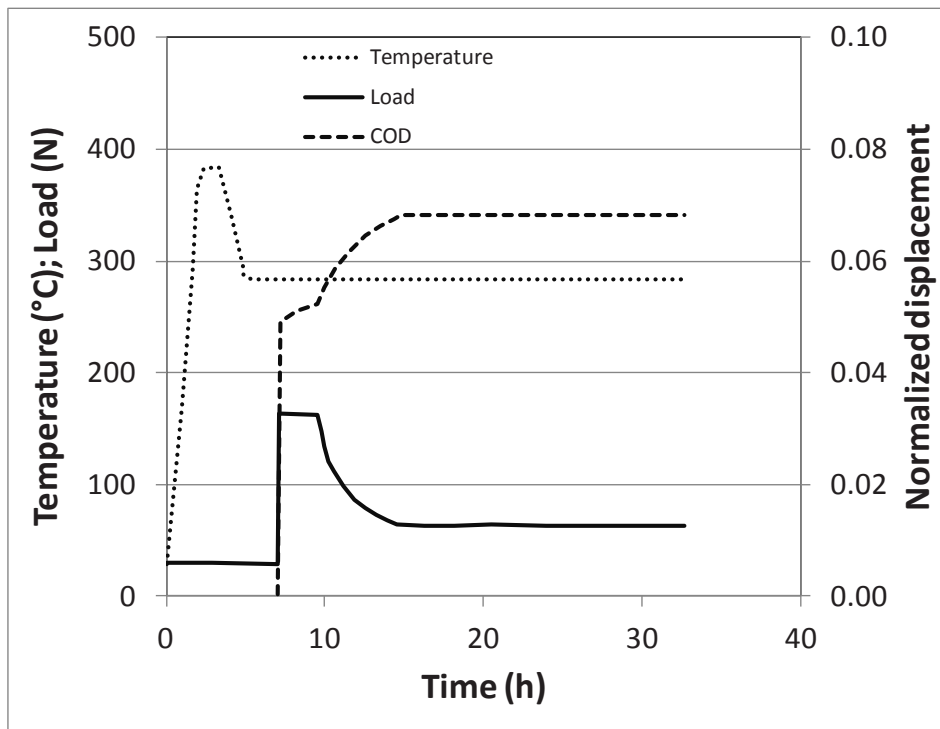
b)

FIG. 29. Test history for DHC test on LWR Zircaloy-4 (a) Romanian specimen S2-4, b) Pakistani specimen SIF3) showing decline in crack growth and unloading to constant value when the crack stops to represent a K_{IH} of a) 5.2 MPa√m at 250°C and b) 7.2 MPa√m at 284°C.

The form of the crack growth rate vs. K_I curve, Fig. 15, was derived from test data. Typical examples for CWSR Zircaloy-4 are illustrated in Fig. 30 for two tests at 250°C; the crack growth rate has a low dependence on K_I above 6 MPa√m but drops suddenly as K_{IH} is approached between 5 and 6 MPa√m. Crack growth rate in the K_I independent region was in the range 7 to 10 × 10^{-8} m/s, about two to three times faster than in the previous study [15]. Again this difference may be attributed to differences in the Zircaloy-4 batches and peak temperature before loading.

Another way to represent the approach to K_{IH} is to plot the incubation time after each load decrement. Close to K_{IH} the time to reinitiate cracking increases markedly, as illustrated in Fig. 31 for a sample of CWSR Zircaloy-4 tested at 250°C, indicating a value of K_{IH} of 4.2 MPa√m. This behaviour is as expected from Fig. 18.
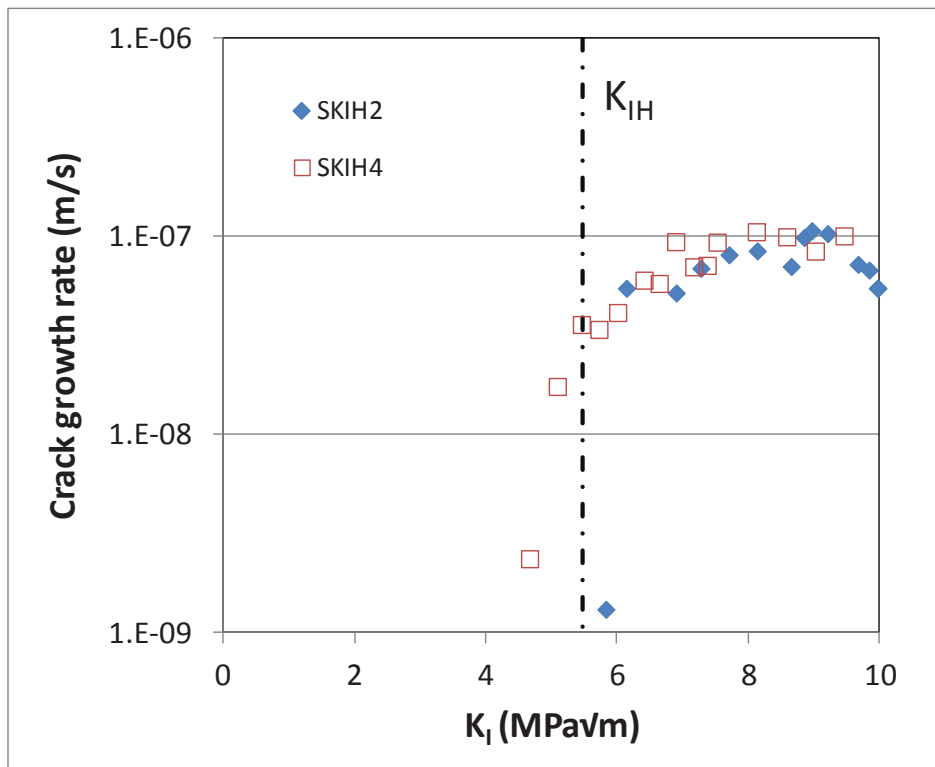
FIG. 30. Dependence of crack growth rate at 250°C derived from unloading tests on CWSR cladding (Indian specimens SKIH2 and SKIH4). Values of K_{IH} straddle the mean value of the whole population of 5.5 MPa√m.
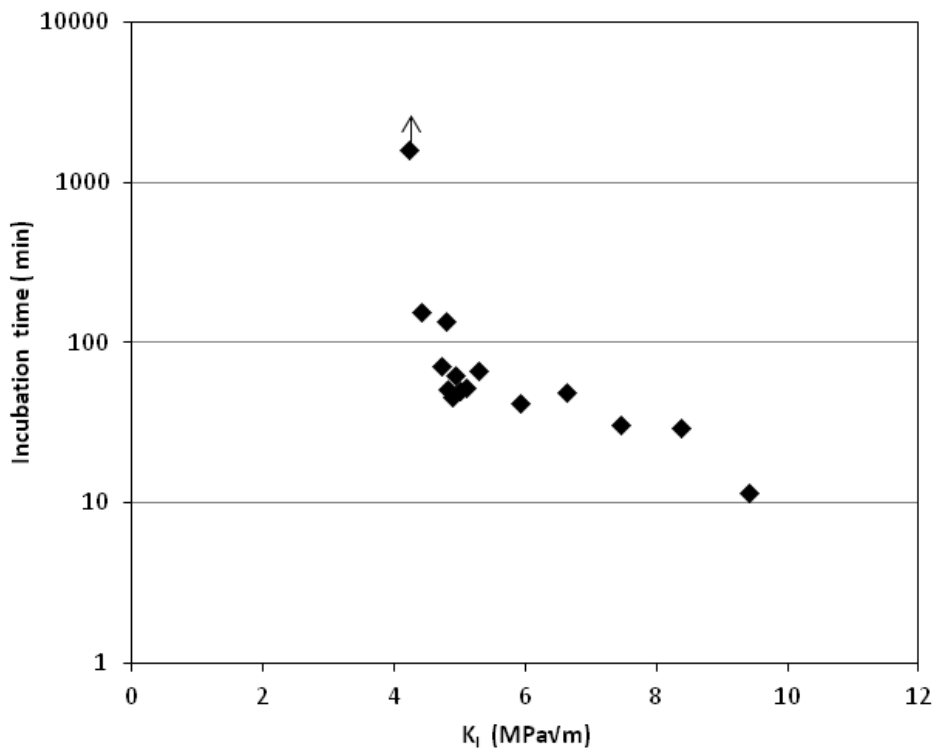
FIG. 31. Increase in incubation time as K_I is decreased in CWSR Zircaloy-4 tested at 250°C (Lithuanian specimen S8-9). K_{IH} is 4.2 MPa√m.

3.1.6. Specimens with a single crack

The method used was equivalent to the unloading method on the PLT specimens and the experimental problems were similar. When a high force was applied for a long time, crack initiation was difficult and this behaviour was attributed to blunting of the crack tip that prevented attaining a high enough stress concentration at the crack tip to initiate DHC. Three successful tests were reported at 250°C.

3.2. VALUES OF K_{IH}

3.2.1. PWR Zircaloy-4

3.2.1.1. Tests at 250°C

The values of K_{IH} from tests at 250°C are summarised in Table 8.

TABLE 8. VALUES OF K_{IH} FOR PWR ZIRCALOY-4 AT 250°C (HIGHLIGHTED VALUES MAY BE UNRELIABLE AND NOT INCLUDED IN MEAN AND STANDARD DEVIATION OF ACCEPTABLE VALUES)

	Brazil	Canada	India	Lithuania	Pakistan	Romania	Russia	Sweden	Switzerland
	2.3	7	5.8	5.48	5.11	3.7	5.69	3.47	5.72
	9.6	7.1	6.7	4.2	5.26	5.2	7.14	2.87	6.577
	7.3		4.7	4.64	5.18	5.3	7.91	3.74	5.25
	6.1		6.7	4.95	7.25	3.4	4.99		
	9.6		5.1	2.91	9.6	4.1	5.42		
	12.4		5.2	6.43	8.81	4.8	8.07		
	12.7		4.4	2.55	7.13	1.23	10.06		
				3.7	6.92		10.63		
					7.27		10.81		
					7.67		5.97		
							5.1		
Number of specimens	Total number of tests: 58; Number of acceptable tests: 35								
Mean value MPa√m	Based on total: 5.88; Based on acceptable tests: 5.20								
Standard. deviation MPa√m	Based on total: 2.20; Based on acceptable tests: 1.31								
Maximum value MPa√m	Total tests: 12.7; Acceptable tests: 7.91								
Minimum value MPa√m	Total tests: 1.23; Acceptable tests: 2.55								

They are very scattered, partly because of experimental vagaries and partly because the cracking process is variable. About 60% of the tests were judged by the individual experimenters to be acceptable. The sources of concern for high values of K_{IH} were cracks that started to propagate then suddenly stopped or could not be restarted after an over-night shut-down; if the starting load was too high the crack could be blunted by plastic deformation; if equipment malfunctioned in the middle of a test the value of K_{IH} was suspect. Similarly,

low values were obtained with very long cracks, especially when the limit of unloading was reached. Despite this perceived effect, using the pooled data it was difficult to definitively show that low values were caused by long cracks, Fig. 32.
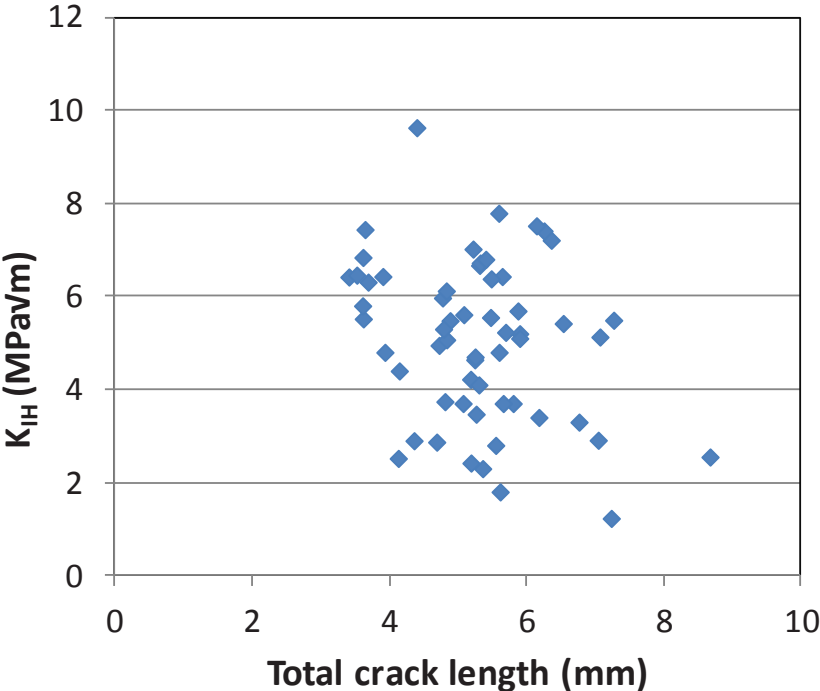
FIG. 32. Lack of dependence of K_{IH} on the total crack length in specimens of CWSR Zircaloy-4 fuel cladding tested at 250°C.

Similarly, one might expect that asymmetric cracking may contribute to the wide dispersion of the results but the data do not support such a conclusion, Fig. 33.
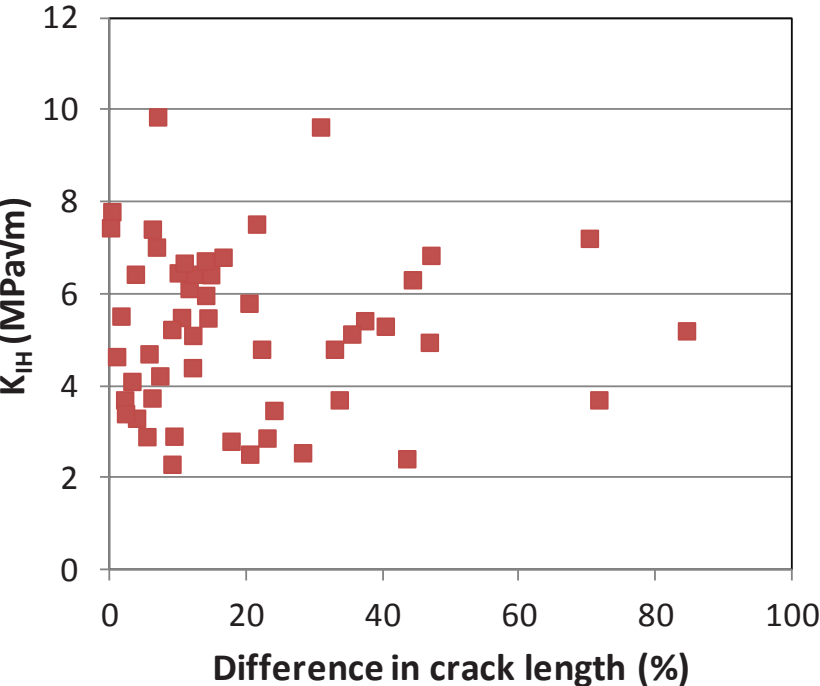
FIG. 33. Lack of dependence of K_{IH} on the difference in the lengths of the two cracks on each specimen in tests on CWSR Zircaloy-4 fuel cladding at 250°C.

44

The other acceptance criteria based on crack shape, Figs. 20 and 21, were derived from testing cantilever beams of Zr-2.5Nb pressure tubes. Here the cracks are through the tube wall of thickness 4 mm and the specimen width is 3.8 mm. The relative uncracked ligaments and the variation of crack length induce more stringent criteria in specimens of pressure tubes than with the PLT loading arrangement in fuel cladding because the ratio of crack length to wall thickness is small: about 0.5 in pressure tubes and 10 in fuel cladding. Although clear uncracked ligaments are developed during DHC testing of fuel cladding, Fig. 22, their contribution to the cracking process is small, usually about 1% with a maximum value of 2.5%, considerably smaller than the 10% rejection criterion for a test on a pressure tube. Similarly, the criterion based on variability of crack length is smaller than the 10% rejection criterion, being usually about 2 %, with a maximum value of 5%.

The dispersion of the total population is presented in Fig. 34. The mean value is 5.88 MPa√m with a standard deviation of 2.20 MPa√m. When the results considered unacceptable were eliminated, the dispersion (Fig. 35), mean (5.20 MPa√m) and standard deviation (1.31 MPa√m), Table 8, were all smaller than with the whole population.
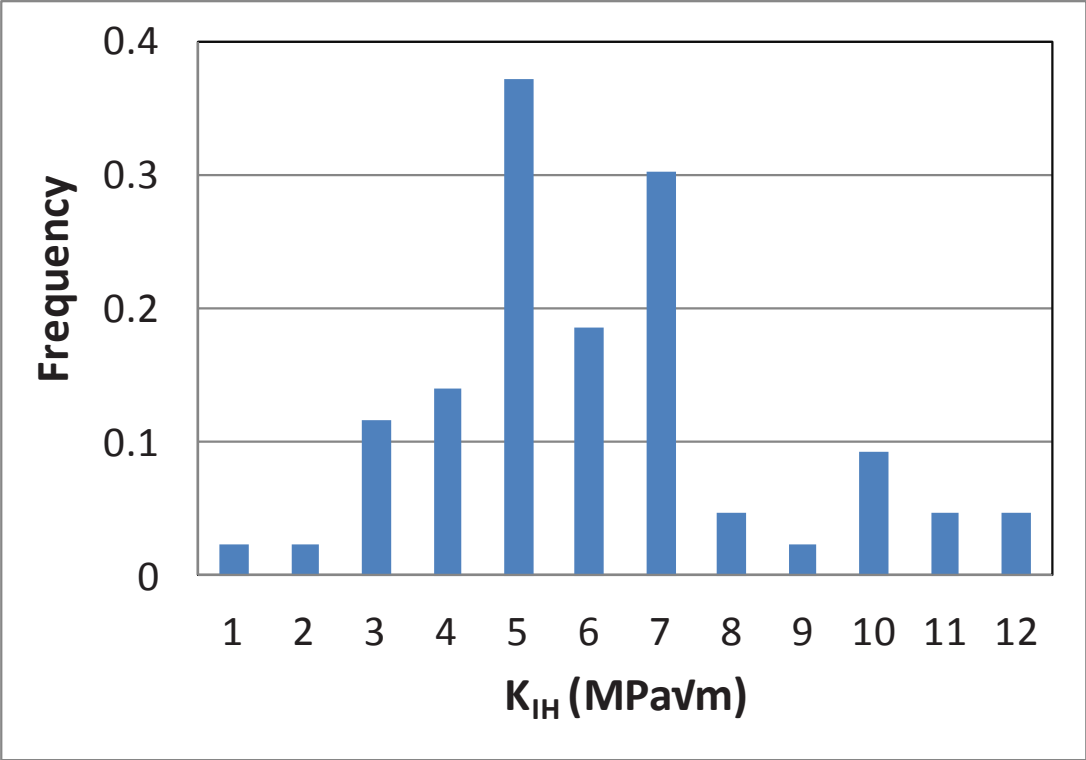
FIG. 34. Distribution of the whole population of values of K_{IH} of PWR Zircaloy-4 tested at 250°C.
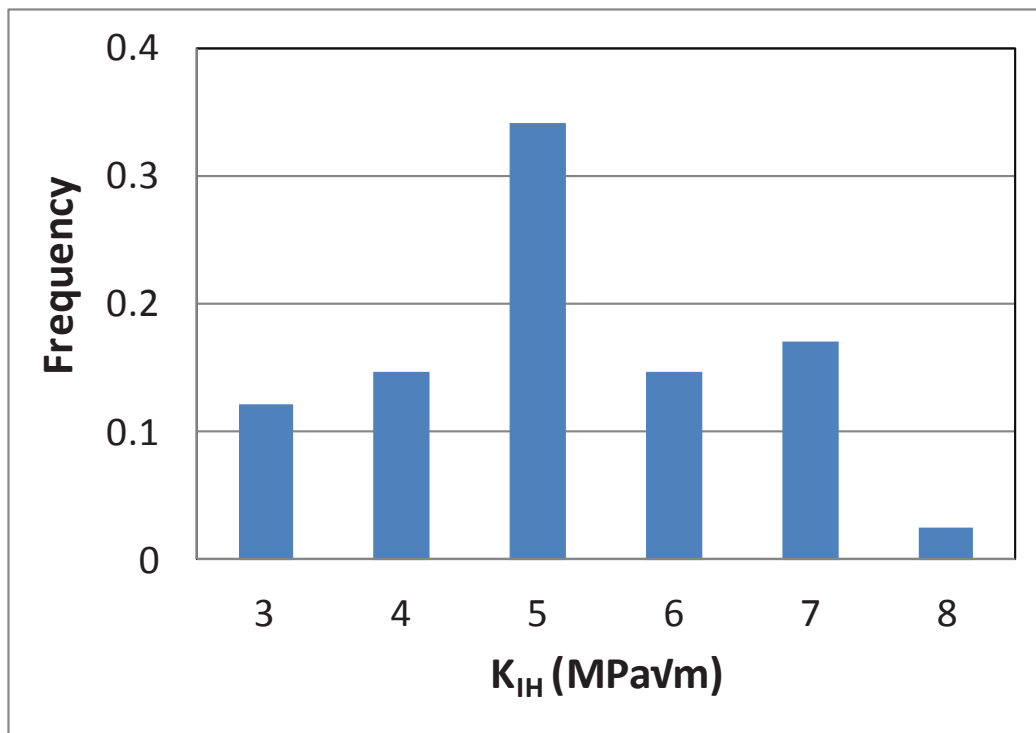
FIG. 35. Distribution of acceptable values of K_{IH} of PWR Zircaloy-4 tested at 250°C.

3.2.1.2. Tests at other temperatures

Tables 9 to 12 list the values of K_{IH} obtained at other temperatures in the range 227 to 313°C.

TABLE 9. VALUES OF K_{IH} FOR PWR ZIRCALOY-4 AT 227°C (HIGHLIGHTED VALUES MAY BE UNRELIABLE AND NOT INCLUDED IN MEAN AND STANDARD DEVIATION OF ACCEPTABLE VALUES)

	Brazil	Russia	Sweden
	20.3	6	2.9
	16.2	6.12	2.42
	0	5.13	2.52
	8.5	3.3	
	12.9		
Number of acceptable specimens		6	
Mean value MPa√m		4.74	
Standard deviation MPa√m		2.50	

TABLE 10. VALUES OF K_{IH} FOR PWR ZIRCALOY-4 AT 267°C (HIGHLIGHTED VALUES MAY BE UNRELIABLE AND NOT INCLUDED IN MEAN AND STANDARD DEVIATION OF ACCEPTABLE VALUES)

	Lithuania	Russia
	5.07	6.88
	5.55	7.21
	5.61	10.15
	6.43	12.95
	6.38	7.07
		8.27
Number of acceptable specimens	6	
Mean value MPa√m	6.46	
Standard deviation MPa√m	1.24	

TABLE 11. VALUES OF K_{IH} FOR PWR ZIRCALOY-4 AT 282 AND 288°C (HIGHLIGHTED VALUES MAY BE UNRELIABLE AND NOT INCLUDED IN MEAN AND STANDARD DEVIATION OF ACCEPTABLE VALUES)

Canada	India	Pakistan	Romania	Russia	Sweden (288 °C)
8.8	6.8	7.21	3.7	6.73	4.8
9.2	6.84	6.81	2.8	10.81	6.46
			1.8	7.41	5.52
			2.3	5.49	
				7.02	

Number of acceptable specimens	282°C:12; 288°C: 3
Mean value MPa√m	282°C: 5.37; 288°C: 5.59
Standard deviation MPa√m	282°C: 2.11; 288°C: 0.83

TABLE 12. VALUES OF K_{IH} FOR PWR ZIRCALOY-4 AT 295 AND >300°C (HIGHLIGHTED VALUE MAY BE UNRELIABLE AND NOT INCLUDED IN MEAN AND STANDARD DEVIATION OF ACCEPTABLE VALUES)

	Russia	Sweden
	7.66	7.44
	7.52	9.85 (315°C)
	7.79	
	13.75 [296.5 °C]	
	18.4 [303 °C]	
	18.9 [302 °C]	
Number of acceptable specimens	4 (295 to 296.5°C)	3 (302 to 313°C)
Mean value MPa√m	9.125	15.72
Standard deviation MPa√m	3.09	5.1

Fig. 36 shows the temperature dependence of the whole population of tests while Fig. 37 depicts the mean and standard deviation of the values considered acceptable. The few measurements of crack growth rate and those from the previous study [15] exhibit a maximum value around 290°C followed by a sudden drop in rate; this drop coincides with the rapid increase in K_{IH}, Fig. 38, and is in agreement with the behaviour of Zr-2.5Nb, Fig. 3.

FIG. 36. Temperature dependence of K_{IH} of PWR Zircaloy-4 showing whole population.
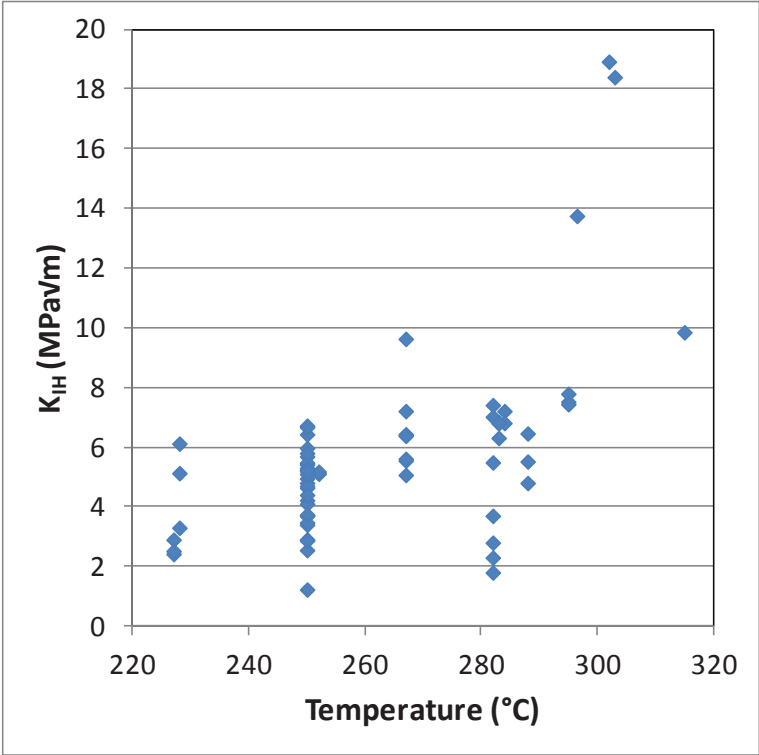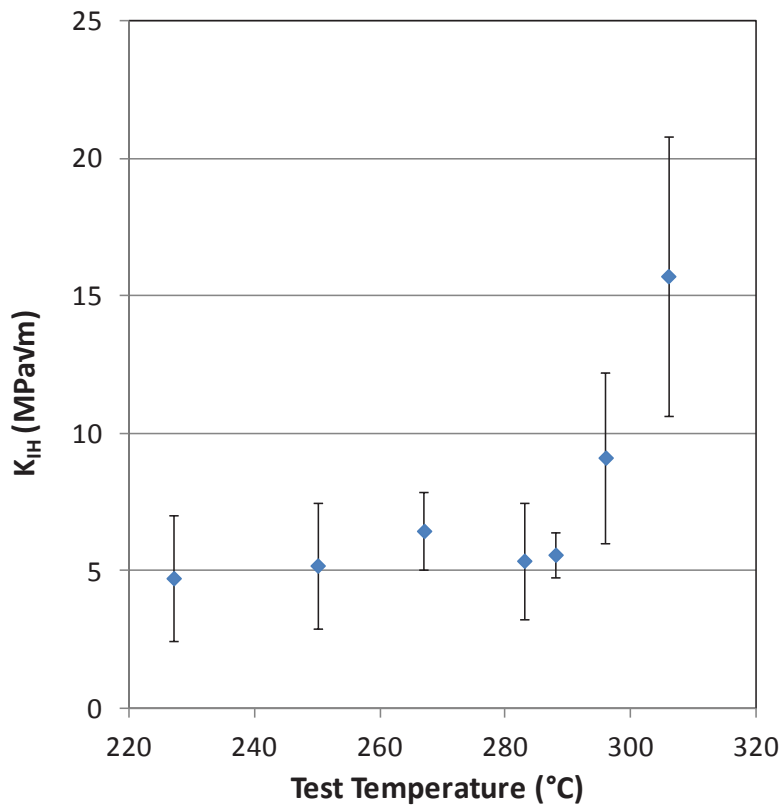
FIG. 37. Temperature dependence of K_{IH} of PWR Zircaloy-4 based on values deemed acceptable showing mean values and a single standard deviation.
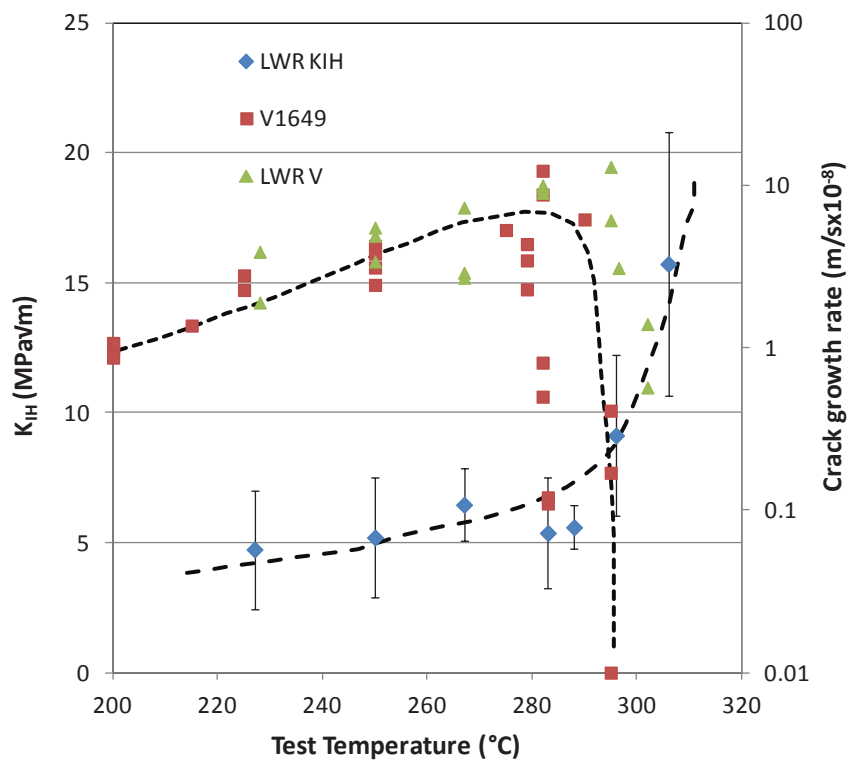
FIG. 38. Temperature dependence of K_{IH} and crack growth rate of PWR Zircaloy-4 (data from TECDOC-1649) showing the temperature for the rise in K_{IH} coinciding with that for the drop in crack growth rate, V.

3.2.2. CANDU Zircaloy-4

Tables 13 to 16 list the small number of values of K_{IH} in CANDU Zircaloy-4 obtained at temperatures in the range 250 to 296°C.

TABLE 13. K_{IH} DATA OF CANDU ZIRCALOY-4 CLADDING AT 250 °C (HIGHLIGHTED VALUES MAY BE UNRELIABLE AND NOT INCLUDED IN MEAN AND STANDARD DEVIATION OF ACCEPTABLE VALUES)

Brazil	Canada	India	Lithuania	Romania
41.7	8.2	28.4	20.5	8.2
73.3	7.4	26.88	18.5	7.8
61.6	8.1		23.2	14.6[*]
61.6	7.3			13.8[#]
	7.3			
Number of acceptable specimens		7		
Mean value MPa√m		7.76		
Standard deviation MPa√m		0.42		

K_{IH} = 14.6* - crack did not start
K_{IH} = 13.8# - crack stopped after 3 steps

TABLE 14. K_{IH} DATA OF CANDU ZIRCALOY-4 CLADDING AT 282 °C

	Canada	Romania
	9.3	12.8
	9.3	5.2
	9.8	7.9
	10.4	7.5
		6.7
		17.3[*]
Number of acceptable specimens	9	
Mean value MPa√m	8.8	
Standard deviation MPa√m	2.2	

K_{IH} = 17.3* - crack did not re-start after overnight unloading

TABLE 15. K_{IH} DATA OF CANDU ZIRCALOY-4 CLADDING AT 292 °C (HIGHLIGHTED VALUE MAY BE UNRELIABLE AND NOT INCLUDED IN MEAN AND STANDARD DEVIATION OF ACCEPTABLE VALUES)

	Canada
	11.6
	10.8
	9.5
Number of acceptable specimens	2
Mean value MPa√m	11.2
Standard deviation MPa√m	0.4

TABLE 16. K$_{IH}$ DATA OF CANDU ZIRCALOY-4 CLADDING AT 296 °C

	Canada
	17.2
	15.7
	18.9
Number of acceptable specimens	3
Mean value MPa√m	17.2
Standard deviation MPa√m	1.6

As with the LWR cladding, the temperature dependence is low below 280°C then increases rapidly above 290°C, Fig. 39, and coincides with a drop in crack growth rate in the same temperature range, Fig. 40. K$_{IH}$ appears larger and approaches the high value at a lower temperature in CANDU cladding compared with LWR cladding, Fig. 41.
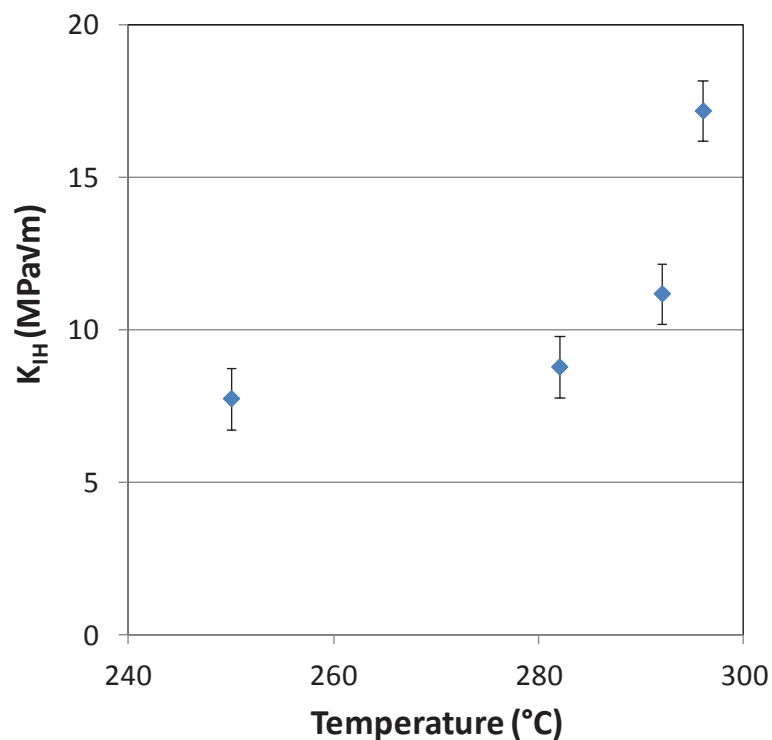
FIG. 39. Temperature dependence of K$_{IH}$ of CANDU Zircaloy-4 based on values deemed acceptable, showing mean values and a single standard deviation.
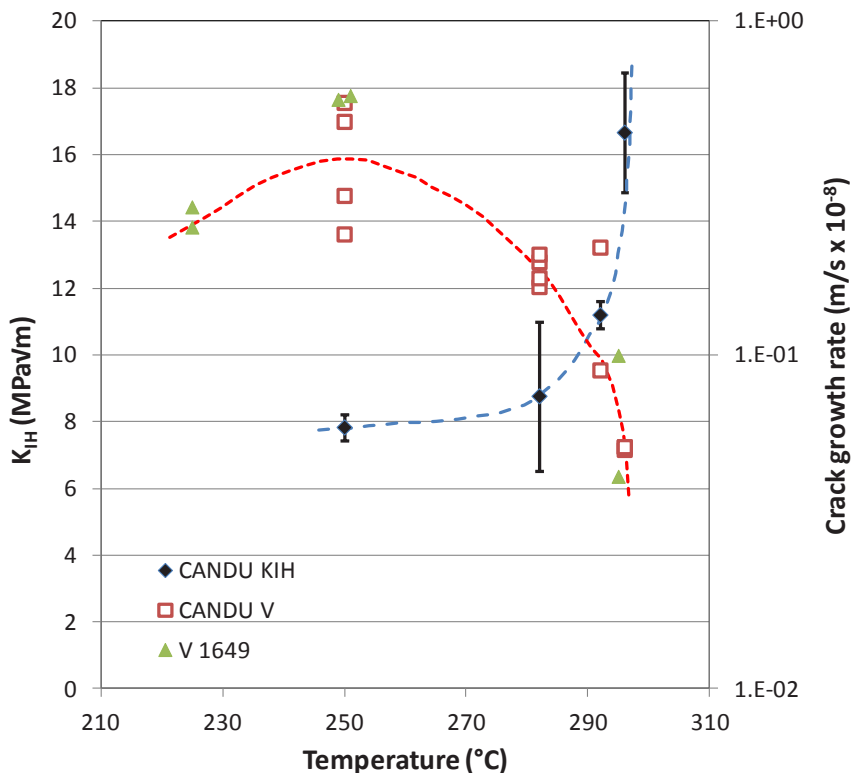
*FIG. 40. Temperature dependence of K_{IH} and crack growth rate of CANDU Zircaloy-4 and data from TECDOC-1649) showing the temperature for the rise in K_{IH} coinciding with that for the drop in crack growth rate, V.*
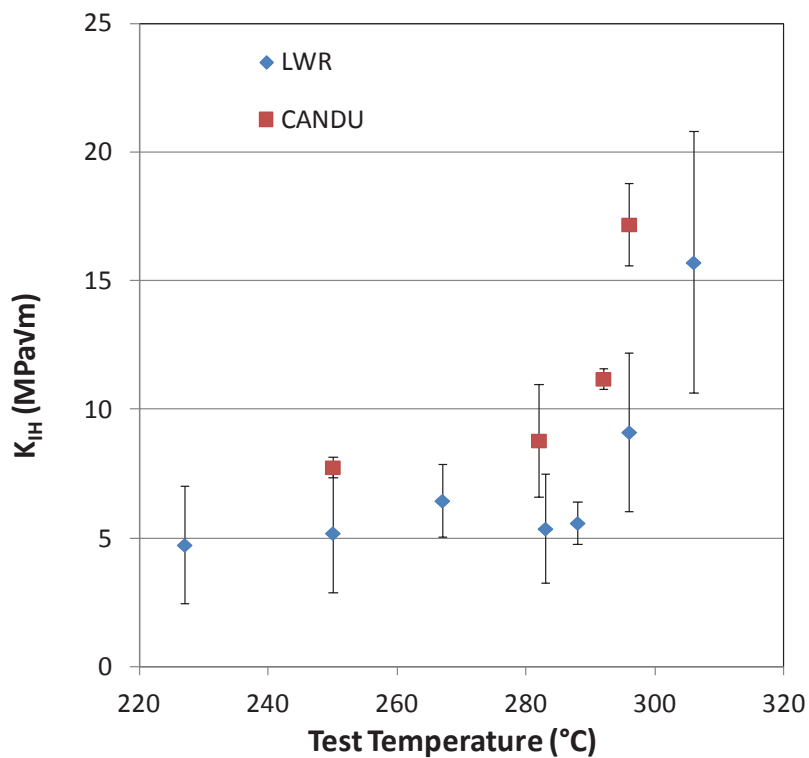
FIG. 41. Comparison of values of K_{IH} measured on CANDU and LWR Zircaloy-4 fuel cladding.

3.2.3. VVER alloy E635M

Three tests were performed at 250°C on this alloy using the constant displacement method. The values had a mean of 7.59 MPa√m in the range 7.07 to 7.91 MPa√m, being about 40% greater than in CWSR Zircaloy-4.

3.3.   FRACTOGRAPHY

During testing of (α+β) alloys, a common feature on the fracture surface after DHC is a series of striations, observed by light microscopy, corresponding with cracking of a line of hydrides being halted by ductile fracture. This feature is seldom observed after DHC in Zircaloy. In this study only one specimen exhibited striations, Fig. 42(a) but no others have been reported. Striations were highly visible after DHC of E635M, Fig. 42(b).

(a)

(b)

FIG. 42. (a) A rare sighting of striations on a fracture surface caused by DHC at 267°C in Zircaloy-4 – Russian specimen Inmag-31; (b) Clear striations on E635M after DHC at 250°C.

When examined in a scanning electron microscope, the main features are patches of cleaved hydride and small ductile regions between the broken hydrides, Fig. 43.
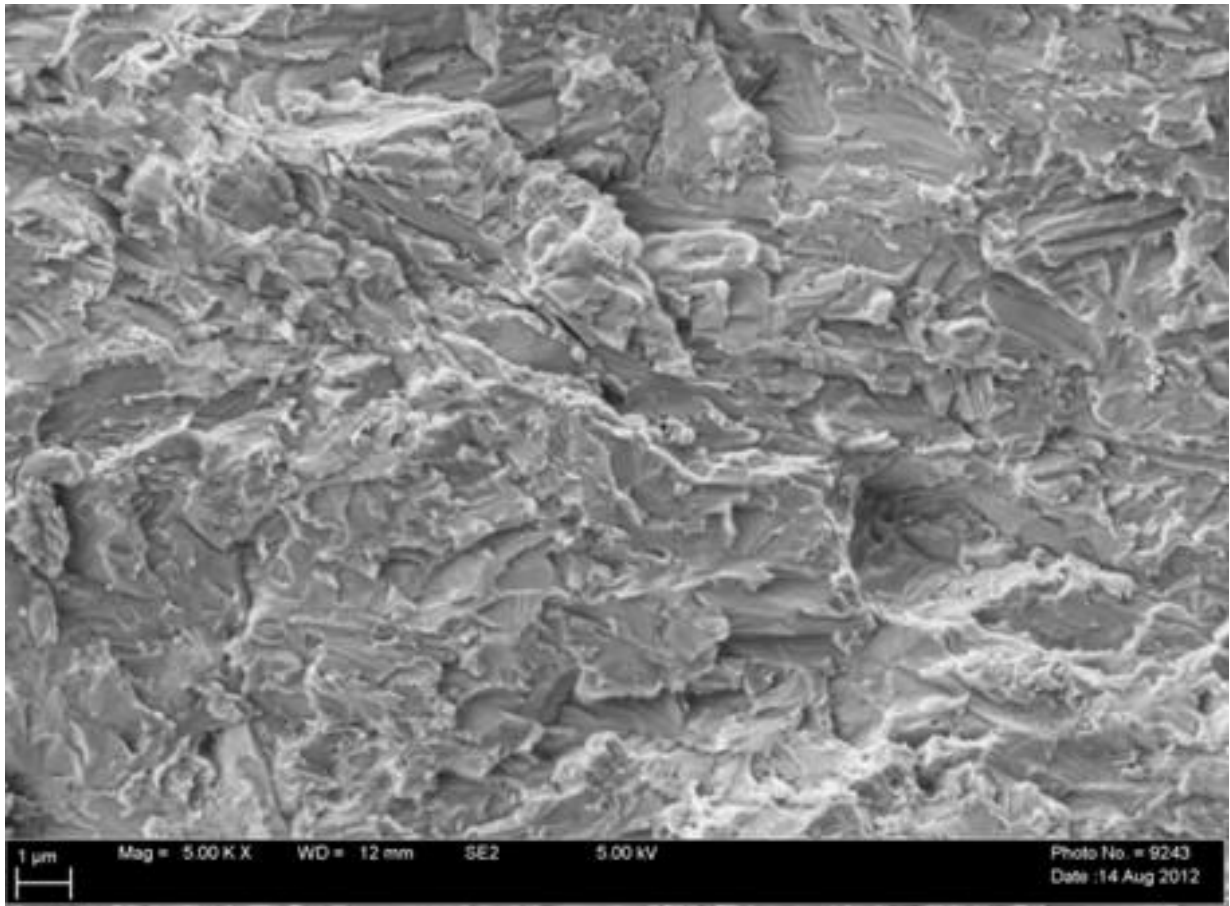
FIG. 43. Cleaved hydride on the fracture surface of CANDU Zircaloy-4 after DHC testing at 250°C.

4. DISCUSSION

The results summarised in Section 3 demonstrate that each of the four test methods can be applied to the Pin-Loading Tensile (PLT) test configuration to measure K_{IH} in fuel cladding made from zirconium alloys. Each method has advantages and disadvantages:

Multiple specimen method. This method is the simplest. It can be implemented with no instrumentation. Rupture time is measured in several specimens loaded to a range of K_I. K_{IH} is approached when the rupture time is very large. More useful information, for example, crack growth rate, requires the ability to detect the start of cracking so the duration of DHC can be obtained. Now K_{IH} is estimated from the graph of crack growth rate as a function of K_I, as in Figs. 15 and 24. The main drawback of the method is the need for much material for each test temperature, although several values of crack growth rate are gained.

Constant displacement method. The load automatically declines as K_{IH} is approached, requiring no attention from an operator or need for computer feedback control. K_{IH} is calculated from the crack length and the final load. A full crack history may be obtained if the specimen is instrumented or the crack is directly observable. The ambient conditions need careful control so the expansion or contraction of the tension rods do not interfere with the load applied to the specimen.

Uploading method. Although in principle one could perform this test without instrumentation by using rupture as an indication of cracking, at low temperatures, where the crack growth rate is low, the loads to start cracking could be missed during some steps of increasing load and the resulting value of K_{IH} would be optimistic. Preferably, some method for detecting cracking is required to indicate that K_{IH} has been exceeded. Once detected, only a small amount of cracking is needed to confirm that K_{IH} has been exceeded, thus avoiding any problems with long cracks.

Unloading method. This method is the most complicated although it has been very successful with specimens of CANDU Zr-2.5Nb pressure tube. Acoustic emission, direct current potential drop (DCPD) and crack opening are used to indicate cracking and provide clear feedback for software to control unloading. Unfortunately, acoustic emission does not provide a clear signal in Zircaloy (for unknown reasons) but the other two techniques work well. Computer control minimises operator involvement and avoids the need for unloading the specimen over-night and during weekends. Choosing the size of the load drops and the extent of cracking between steps are important for an acceptable test. Since many of the tests in this project were done using this method, the problems with implementing adequate feedback for load control led to several unacceptable tests. The instrumentation can provide good information on crack growth rates and incubation times. Tests on Zr-2.5Nb using the uploading and unloading methods on the same materials indicated that each technique produced similar values of K_{IH} at 130 and 250°C, Fig. 44 [33], in agreement with the current study.
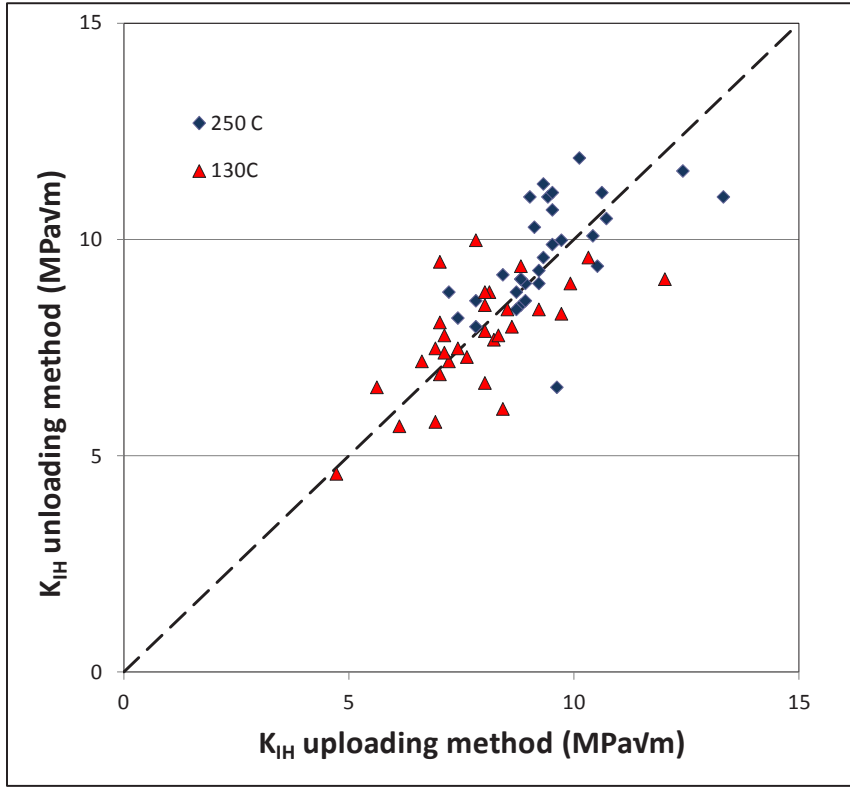
FIG. 44. Comparison of uploading and unloading methods to determine K_{IH} in cold-worked Zr-2.5Nb pressure tube material [33].

In several analyses of K_{IH} a hydride fracture stress is invoked [34-38]. If cracking is confined to breaking hydride, a lower bound, K_{IH}^∞, is estimated from:

$$(K_{IH}^\infty)^2 = E^2 \varepsilon_\perp t/8\pi(1-v^2)^2.((1/1-2v)-\sigma_f/\sigma_y) \tag{5}$$

where

E is the Young's modulus of the Zr alloy;

$\varepsilon_\perp$ is the transformation strain normal to hydride platelet;

t is the thickness of hydride;

v is the Poisson's ratio of hydride;

σ_y is the yield strength of the Zr alloy;

σ_f is the fracture strength of hydride.

K_{IH}^∞ increases as $t^{1/2}$; some of the variation in measured values may be the result of different hydride configurations at the crack tip. K_{IH}^∞ decreases with increase in strength; LWR cladding is stronger and K_{IH} is lower than in CANDU cladding, Fig. 41. The temperature dependence of K_{IH}^∞ is mainly controlled by the temperature dependence of the elastic properties and strength of the zirconium alloy, and the fracture strength of the hydride precipitate. The crack tip described by Equation (5) is assumed to be completely covered by hydride and low values of the threshold are predicted. With a variation of hydride configuration at the crack tip, a contribution to the cracking resistance will be because of the presence of some zirconium alloy between hydrides. This material has higher toughness, K_{IC},

than the hydride so it will contribute to raising the threshold for cracking. If f represents the fraction of the crack front covered by hydride, using a rule-of-mixtures, a practical evaluation of the threshold would be:

$$K_{IH} = f K_{IH}^{\infty} + (1-f)K_{IC}. \tag{6}$$

Evaluation of Equations 5 and 6 are provided as a function of temperature, T (°C), in Fig. 45 for both versions of Zircaloy-4 with a crack front containing 0.5% zirconium alloy.
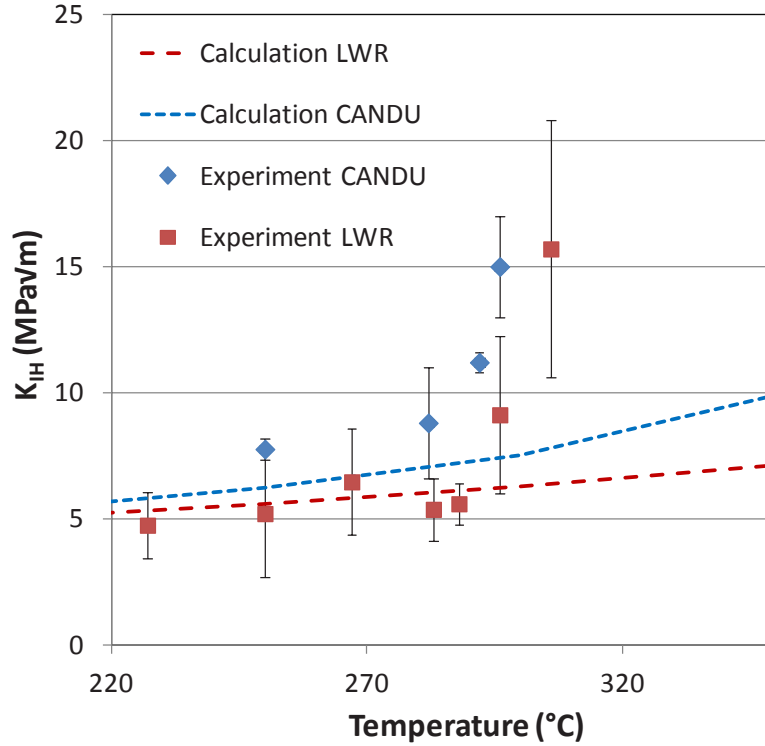
FIG. 45. The temperature dependence of K_{IH} for LWR and CANDU CWSR Zircaloy-4 fuel cladding with a crack front with 0.5% zirconium alloy present: comparison of calculation with experiment.

The values of the variables are t of 2 µm, $\sigma_f = 650 - 0.091T$ [39], the strength of the cladding is from Table 5 and $K_{IC} = 76.8-0.035T+0.0002T^2$ [40]. The values of K_{IH} at low temperature are predicted to be small and have weak temperature dependence as found in the experiments, Fig. 41. The value of K_{IH} for CANDU cladding is predicted to be slightly higher than that for LWR cladding. With both materials the experimental values deviate upwards from the prediction close to 290°C, and, along with the measurements of crack growth rate, indicate that DHC is diminishing towards zero at some high temperature, T_0. The cladding then becomes immune from DHC above about 320°C.

Critical temperatures above which DHC declines to zero can result from:

(a) Lack of hydride. If the hydrogen concentration is insufficient to produce hydrides at the crack tip, DHC will be absent.

(b) Heating to the loading temperature. Above a certain temperature, DHC will not occur if the temperature is attained by heating, even if hydrides are present; above T_2 in Fig. 2. This effect is caused by the stress gradient at the crack tip being insufficient to increase the hydrogen concentration above the solubility limit and precipitate hydrides.

(c)   Inability to fracture the hydride. This effect results when the tensile stress normal to the hydride plate is insufficient to fracture a hydride formed at the crack tip, even when hydrides are present at the crack and the temperature is reached by cooling from above the solubility limit where all the hydrogen is in solution. This effect results from a combination of:

> (i) the temperature dependence of the yield strength being much lower than that of the fracture strength of the hydride, and
>
> (ii) at temperatures about 300ºC, the high stresses at the crack tip can relax by high stress creep leading to the stress concentrating effect of the crack being much diminished and the crack being blunted.

In the current experiments, the hydrogen concentration was sufficient for hydrides to be present at the test temperatures and the test temperatures were attained by cooling from above the solubility limit. Reason c) is a partial explanation for the observed behaviour. The temperature dependence of the fracture strength of the hydride is smaller than that of the flow strength of a zirconium alloy. Fig. 46 schematically shows the temperature where the metal strength, σ_y, and hydride fracture strength, σ_f, intersect at T_0, a temperature above which DHC should be absent. Based on the tensile properties of several materials – Zr-1Nb, Zr-2.5Nb, E635M and Zircaloy-4 fuel cladding [25], and unirradiated and irradiated Zr-2.5Nb pressure tubes [20] – T_0 is expected to have a range from about 150 to 540°C, Fig. 47. The experimental values of T_0 only agree with this analysis around 300°C. With CANDU cladding the experimental value of T_0 – 296°C - is much higher than the calculated value of 150°C, whereas in irradiated Zr-2.5Nb pressure tubing the measurement of T_0 - 365°C - is much lower than the calculated value, 540°C. Further work is required to explain T_0.
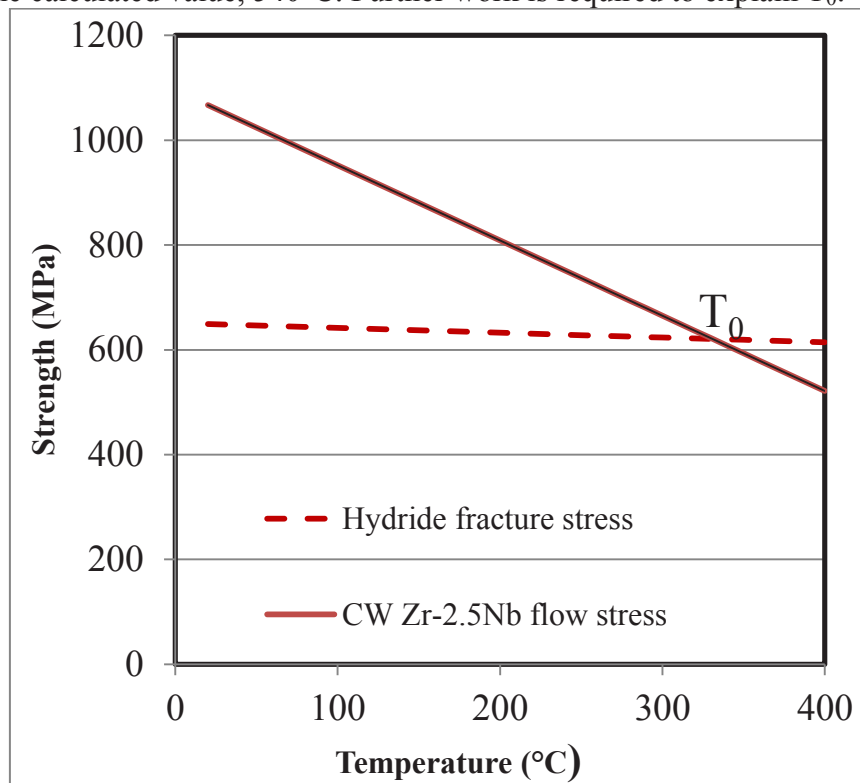
FIG. 46. Schematic representation of temperature T_0 where the hydride fracture strength and flow strength intersect; above T_0 DHC is absent.
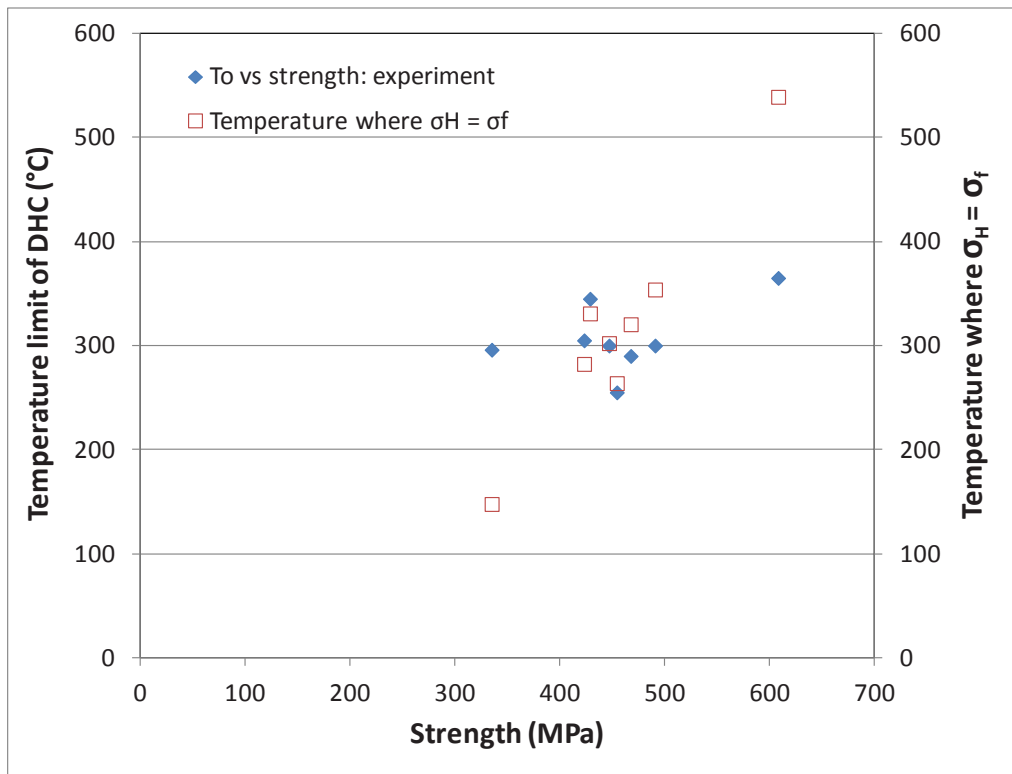
FIG. 47. Comparison of strength dependence of T_0, the temperature limit for DHC, with the temperature where the flow stress of the zirconium alloy, σ_H, equals the fracture stress of zirconium hydride, σ_f.

The recommended highest temperature for dry storage of spent nuclear fuel is 400°C [41]. About 275 ppm hydrogen are required to exceed TSSP at 400ºC and such high hydrogen concentrations have been observed in LWR cladding, for example, after a fuel burn-up of about 57 MWd/kg U, low-tin Zircaloy-4 contained between 600 and 820 ppm hydrogen [42]. Thus DHC would not be limited by lack of hydrogen during dry fuel storage.

Even with favourable stressing conditions, a maximum temperature, T_0, exists above which DHC cannot start. This temperature is around 300ºC in unirradiated cladding material but may be as high as 360ºC in irradiated material. This phenomenon suggests that spent fuel that starts storage at the NRC-stipulated maximum temperature of 400ºC will be immune from DHC until the temperature reaches the critical temperature. This period of immunity is about three years, using the expected cooling rates [43]. If T_0 depends on irradiation damage, its value may be reduced if the damage is annealed out during early storage. Thus the period of immunity may be much longer than estimated; if T_0 returns to 300ºC, the period of immunity increases to about 12 years [43]. The hoop stress will be simultaneously lowered, providing further protection. Once the period of absolute immunity is over, one then has to examine the stress conditions.

Since the wall thickness, w, of fuel cladding is small, normally that would disqualify the application of Linear Elastic Fracture Mechanics (LEFM). With cladding of strength σ_S, for validity:

$$K_I < \sigma_S \sqrt{(w/2.5)} \qquad\qquad (7)$$

A value of $K_I < 7.7$ MPa√m meets this criterion for LEFM so the current mean value below 290°C of 5.4 MPa√m can be used directly to evaluate fuel cladding. For a crack to be initiated, the combination of tensile stress and flaw size must exceed K_{IH}. Assuming the

current value of K_{IH} applies to a radial crack, the maximum depth of sharp surface flaw, a, that can be tolerated without crack growth can be estimated from [44]:

$$a = (K_{IH}/\sigma)^2 . \; Q/1.2 \; \pi \qquad\qquad\qquad (8)$$

where

σ is the applied stress

Q is the shape factor.

For elliptical flaws Q is about 1.5 while for long flaws, for example, a scratch, Q is about 1.0. During dry storage of spent PWR fuel, the hoop stress imposed by the internal pressure is limited by the US NRC to 90 MPa [41]. Applying Equation (8) with the mean value of K_{IH} suggests that the critical flaw size is between 1.7 to 2.5 times the cladding wall thickness, that is, a through-wall crack. Neutron irradiation reduces K_{IH} by about 30%, as measured in Zircaloy-2 fuel cladding [10] and Zr-2.5Nb pressure tubes [45]. Consequently, if the irradiation damage is not annealed out during the high temperature part of fuel storage, the critical flaw size is reduced to between 0.82 to 1.23 times the cladding wall thickness. A through-wall crack would stop growing because the internal pressure disappears. Also, such a crack would be detected before the fuel is placed in storage or should have been detected during surveillance of spent fuel that had been stored for several years. Similarly, a crack mostly through the wall should extend easily during the first stages of storage leading to leakage of filler gas and gasses from fission products. No cracks have been observed in spent fuel after 15 years [46] and 20 years [47] of dry storage suggesting that the combination of flaws and the internal pressure were insufficient to cause DHC.

Safety issues associated with spent fuel storage is the main topic of a long term research programme at EC JRC-ITU aiming for a better understanding of mechanisms affecting the properties of spent fuel and the mechanical integrity of the cladding. Strongly connected to the present CRP scope is the investigation being carried out at the hot cells of this Institution, which is focusing on the assessment of the hydride distribution, defect evolution and cracking processes.

Similar calculations to [43] suggest that at the start of dry storage for a fuel after a burn up of 55 MWd/kg and after about 6 years pool storage, 10 years of dry storage will decrease the temperature from 350-360ºC to 230-240ºC with corresponding hoop stresses starting from an initial value of 60-80 MPa declining to 45-60 MPa [48]. Immediately after removal from pool storage, the conditions in the cladding are at their most severe: the temperature increases several hundred degrees and the pressure of the filler and fission gas mixture increases accordingly. An additional long term contribution to the stress arises from fuel lattice swelling from α-decay, especially when Pu isotopes are present. Some estimations of the contribution are 0.3 to 0.8% swelling in the first 100 years. Therefore, researchers at EC JRC-ITU are attempting to verify the safe behaviour of irradiated cladding under realistic storage conditions.

Pressurization tests will be carried out on cladding specimens containing radial hydrides from LWR irradiated fuel rods with medium and high burn up. The objective of this study is to determine the threshold pressure for crack initiation and follow its growth with time under constant temperature and load. The experiments will be performed at 140°C approaching the temperature range of spent fuel rods after a few decades. After preheating to 240°C, the specimens will be cooled to the desired temperature, the pressure will be increased stepwise

until a defect is detected and then it will be kept constant to follow the development of the crack.

The defect evolution and growth will be monitored by means of a high resolution eddy current device. The hot extraction technique will be employed to determine the hydrogen concentration in the cladding, whereas the morphology of the hydrides and defects and their population will be characterised by metallographic analysis before (at a nearby position) and after the experiment. The results of these experiments will be reported later.

5. CONCLUSIONS AND RECOMMENDATIONS

5.1. CONCLUSIONS

1. Four methods have been demonstrated and evaluated for measuring K_{IH}, the limiting stress intensity factor for delayed hydride cracking (DHC) in Zircaloy-4 fuel cladding.

2. The value of K_{IH} of CWSR LWR Zircaloy-4 cladding has little temperature dependence between 227°C and 285°C rising from 5 MPa√m to 8 MPa√m but increasing rapidly at higher temperature reaching 13 MPa√m at 300°C. In the same temperature range, K_{IH} in CANDU cladding is a little higher than in LWR cladding and increases to a high value at a slightly lower temperature.

3. At 310°C values of both K_{IH} and crack growth rate suggest that only a small increase in temperature would be needed for Zircaloy-4 to be immune from DHC.

4. Theory based on exceeding the fracture strength of the hydride provides a description of the results for the low temperatures, <285°C, but is less successful at high temperatures.

5. In the first part of dry storage of spent nuclear fuel, the temperature can be up to 400°C and DHC is an improbable cause of failure because of immunity. After several years' storage when the temperature of spent fuel has declined sufficiently for DHC, cracking requires the initiating flaw to be greater than the wall thickness. If such a flaw exists it should be detectable and lead to the gas pressure responsible for the stress being dissipated.

5.2. RECOMMENDATIONS

1. For further evaluation of the influence of DHC on storage of spent fuel, it is recommended to implement respective program of testing at EC JRC-ITU.
2. To support recommendation 1, it is needed to measure the effect of neutron irradiation on K_{IH} of Zircaloy-4 fuel cladding.
3. The analysis and application of the results to dry storage of spent fuel assumes that K_{IH} in the radial and axial directions were similar but this assumption needs to be demonstrated.
4. It is recommended to evaluate the effect of Widmanstätten microstructure on DHC properties of Zircaloy-4 since CANDU fuel elements contain heat-affected zones from brazing.

REFERENCES

[1] COLEMAN, C.E., Cracking of hydride-forming metals and alloys, Comprehensive Structural Integrity, I. Milne, R.O. Ritchie and B. Karihaloo, Eds., Elsevier, Chapter 6.03, (2003) 103-161.

[2] SIMPSON, C.J., ELLS, C.E., Delayed hydrogen embrittlement of Zr-2.5wt%Nb, J. Nucl. Mater., **52**, (1974) 289-295.

[3] PERRYMAN, E.C.W., Pickering pressure tube cracking experience, Nucl. Energy, **17**, (1978) 95-105.

[4] PLATONOV, P.A., ET AL., The study of cause of cracking in zirconium alloy channel tubes, Poster Paper at ASTM Zirconium in the Nuclear Industry – Eighth International Symposium, available as AECL Report RC-87 (1988).

[5] FIELD, G.J., DUNN, J.T., CHEADLE, B.A., Analysis of the pressure tube failure at Pickering NGS "A" Unit 2, Can. Met. Quart., 24, (1985) 181-188.

[6] JONSSON, A., HALLSTADIUS, L., GRAPENGIESSER, B., LYSELL, G., Failure of a barrier rod in Oskarshamn, in Fuel in the '90's, International Topical Meeting on LWR Fuel Performance, Avignon, France, ANS and ENS, (1991) 371-377.

[7] SCHRIRE, D., GRAPENGIESSER, B., HALLSTADIUS, L., LUNDHOLM, I., LYSELL, G., FRENNING, G., RONNBERG, G., JONSSON, A., Secondary defect behaviour in ABB BWR fuel, International Topical Meeting on LWR Fuel Performance, West Palm Beach, ANS, (1994) 398-409.

[8] ARMIJO, J.S., Performance of failed BWR fuel, International Topical Meeting on LWR Fuel Performance, West Palm Beach, ANS, (1994) 410-422.

[9] LYSELL, G., GRIGORIEV, V., Characteristics of axial splits in failed BWR fuel rods, Ninth International Symposium on Environment Degradation of Materials in Nuclear Power Systems – Water Reactors, AIME-TMS, (1999) 1.169-1.175.

[10] EFSING, P., PETTERSSON, K., Delayed hydride cracking in irradiated Zircaloy cladding, Zirconium in the Nuclear Industry – 12th International Symposium, ASTM STP 1354, G.P. Sabol and G.D. Moan, Eds., ASTM, West Conshohocken, PA., (2000) 340-355.

[11] EDSINGER, K., DAVIES, J.H., ADAMSON, R.B., Degraded fuel cladding fractography and fracture behavior, Zirconium in the Nuclear Industry – 12th International Symposium, ASTM STP 1354, G.P. Sabol and G.D. Moan, Eds., ASTM, West Conshohocken, PA., (2000) 316-339.

[12] EDSINGER, K., A review of fuel degradation in BWRs, Int. Topical Meeting on Light Water Reactor Fuel Performance, Park City, ANS, (2000) 162-179.

[13] SHIMADA, S., ETOH, E., HAYASHI, H., TUKUTA, Y., A metallographic and fractographic study of outside-in cracking caused by power ramp tests, J. Nucl. Mater., **327**, (2004) 97-113.

[14] CHEADLE, B.A., COLEMAN, C.E., AMBLER, J.F.R., Prevention of delayed hydride cracking in zirconium alloys, ASTM STP 939, Zirconium in the Nuclear Industry – Seventh International Symposium", R.B. Adamson and L.F.P. Van Swam, Eds., American Society for Testing and Materials, Philadelphia, PA., (1987), 224-240.

[15] INTERNATIONAL ATOMIC ENERGY AGENCY, Delayed Hydride Cracking of Zirconium Alloy Fuel Cladding, IAEA-TECDOC-1649, IAEA, Vienna (2010).

[16] SMITH, R.R., EADIE, R.L., High temperature limit for delayed hydride cracking, Scripa Met., 22, (1988) 833-836.

[17] INTERNATIONAL ATOMIC ENERGY AGENCY, Delayed Hydride Cracking in Zirconium Alloys in Pressure Tube Nuclear Reactors, IAEA-TECDOC-1410, IAEA, Vienna (2004).

[18]   COLEMANC, C.E., INOZEMTSEV, V.V., Measurement of rates of delayed hydride cracking (DHC) in Zr-2.5 Nb alloys – an IAEA Coordinated Research Project, J. ASTM International, 5, (2008) Paper JAI101091.

[19]   COLEMAN, C.E., GRIGORIEV, V., INOZEMTSEV, V.V., MARKELOV, V., ROTH, M., MAKAREVICIUS, V., KIM, Y.S., ALI, K.L., CHAKRAVARRTY, J.K., MIZRAHI, R., LALGUDI, R., The effect of microstructure on delayed hydride cracking behavior of Zircaloy-4 fuel cladding– an IAEA Coordinated Research Programme, J. ASTM International, 7, (2011) Paper JAI103008.

[20]   RESTA LEVI, M., PULS, M.P., DHC behaviour of irradiated Zr-2.5Nb pressure tubes up to 365ºC, 18th Inter. Conf. Structural Mechanics in Reactor Technology, (2005) Paper G10-3.

[21]   GRIGORIEV, V., JAKOBSSON, R., Delayed hydride cracking velocity and J-integral measurements on irradiated BWR cladding, J.ASTM International, 2, (2005), Paper JAI 12434 (Also see ASTM STP 1467, (2006) 711-728).

[22]   GRIGORIEV, V., JOSEFSSON, B., LIND, A., ROSBORG, B., A pin-loading tension test for evaluation of thin-walled tubular materials, Scripta Metallurgica et Materialia, **33**, No. 1, (1995) 109-114.

[23]   GRIGORIEV, V., JOSEFSSON, B., ROSBORG, B., Fracture toughness of Zircaloy cladding tubes, Zirconium in the Nuclear Industry – Eleventh International Symposium, ASTM STP 1295, E.R. Bradley and G.P. Sabol, Eds., American Society for Testing and Materials, Philadelphia, PA., (1996) 431-447.

[24]   YAGNIK, S.K., ET AL., Round-robin testing of fracture toughness characteristics of thin-walled tubing, J. ASTM International, **5**, (2008), Paper JAI101140.

[25]   MARKELOV, V., GUSEV, A., KOTOV, P., NOVIKOV, V., Temperature dependence of delayed hydride cracking velocity in fuel claddings made from zirconium alloys of different compositions, TopFuel Reactor Fuel Performance 2012, Manchester, United Kingdom, 2-6 September 2012.

[26]   MARKELOV, V., SABUROV, N., BEKRENEV, S., NOVIKOV, V., Determination of threshold stress intensity factor, K_{IH}, in DHC tests of fuel cladding by method of constant displacement, TopFuel Reactor Fuel Performance 2015, Zurich, Switzerland, September 2015.

[27]   GRIGORIEV, V., JAKOBSSON, R., Application of the pin-loading tension test to measurements of delayed hydride cracking velocity in Zircaloy cladding, SKI Report 0057, Studsvik Nuclear AB, November (2000).

[28]   GRIGORIEV, V., JAKOBSSON, R., DHC axial crack velocity measurements in zirconium alloy fuel cladding, STUDSVIK/N-05/281, Studsvik Nuclear AB, (December 2005), ISBN 91-7010-377-1.

[29]   SIMPSON, L.A., PULS, M.P., The effects of stress, temperature and hydrogen content on hydride-induced crack growth in Zr-2.5 pct. Nb, Met. Trans., **10A**, (1979) 1093-1105.

[30]   COLEMAN, C.E., COX, B., Cracking zirconium alloys in hydrogen, Zirconium in the Nuclear Industry: Sixth International Symposium, ASTM STP 824, FRANKLIN, D.G., ADAMSON, R.B., EDS., American Society for Testing and Materials, Philadelphia, PA., (1984), 675-690.

[31]   AMERICAN SOCIETY FOR TESTING AND MATERIALS, Standard Test Method for Determining Threshold Stress Intensity Factor for Environment-Assisted Cracking of Metallic Materials, E1681-03 (Reapproved 2013).

[32]   AMBLER, J.F. R., COLEMAN, C.E., Acoustic emission during delayed hydrogen cracking in Zr-2.5 wt% Nb alloy, Proc. Second International Congress on Hydrogen in Metals, Pergamon Press, Oxford, (1977), Paper 3C10.

[33]   RESTA-LEVI, M., Private communication (2015).

[34] SHI, S.-Q., PULS, M.P., Criteria for fracture initiation at hydrides in zirconium alloys I. Sharp crack tip, J. Nucl. Mat., **208**, (1994), 232.

[35] SHI, S.-Q., PULS, M.P., Dependence of the threshold stress intensity factor on hydrogen concentration during delayed hydride cracking in zirconium alloys, J. Nucl. Mat., 218, (1994), 30-36.

[36] SMITH, E., The fracture of hydride material during delayed hydride cracking (DHC) crack growth, Int. J. Pres. Ves. Piping, **61**, (1995), 1-7.

[37] WÄPPLING, D., MASSIH, A.R., STÅHLE, P., A model for hydride-induced embrittlement in zirconium-based alloys, J. Nucl. Mater., **249**, (1997), 231-238.

[38] KIM, Y.S., MATVIENKO, Y.G., CHEONG, Y.M., KIM, S.S., KWON, S.C., A model of the threshold stress intensity factor, K_{IH}, for delayed hydride cracking of Zr-2.5Nb alloy, J. Nucl. Mater., **278**, (2000), 251-257.

[39] SHI, S.-Q., PULS, M.P., Fracture strength of hydride precipitates in Zr-2.5 Nb alloys, J. Nucl., Mats., 276, (1999), 312-317.

[40] COLEMAN, C.E, ET AL., Minimizing hydride cracking in zirconium alloys, Can. Met. Quart., **24**, (1985), 245-250.

[41] BRACH, E.W., Cladding consideration for the transportation and storage of spent fuel, USNRC Interim Staff Guidance – 11, Revision 3, Spent Fuel Project Office, (2003).

[42] TSUKUDA, Y., ET AL., Performance of advanced fuel materials for high burnup, ENS TopFuel, Nuclear Fuel for Today and Tomorrow: Experience and Outlook, Würzburg, Germany, (2003).

[43] RASHID, J., MACHIELS, A., Threat of hydride re-orientation to spent fuel integrity during transportation accidents: myth or reality? Proc. Inter. LWR Fuel Performance Meeting, San Francisco, CA., (2007), paper 1039.

[44] TIFFANY, C.F., MASTERS, J.N., Applied Fracture Mechanics, Fracture Toughness Testing and its Applications, J.R. LOW AND W.F. BROWN, Symposium Chairmen, ASTM STP 381, American Society for Testing and Materials, (1965), 249-277.

[45] RODGERS, D.K., COLEMAN, C.E., GRIFFITHS, M., BICKEL, G.A., THEAKER, J.R., MUIR, I., BAHURMUZ, A.A., ST.LAWRENCE, S., RESTA LEVI, M., In-reactor performance of pressure tubes in CANDU reactors, J. Nucl. Mater., **383**, (2008), 22-27.

[46] EINZIGER, R.E., TSAI, H., BILLONE, M.C., HILTON, B.A., Examination of spent Pressurized Water Reactor fuel rods after 15 years in dry storage, Nucl. Tech., **144**, (2003), 186-200.

[47] A. SASAHARA, A., MATSUMURA, T., Post-Irradiation Examinations Focused on fuel integrity of spent BWR-MOX and PWR-UO$_2$ fuels stored for 20 years, Nucl. Eng. Design, **238**, (2008), 1250-1259.

[48] SPILKER, H., PEEHS, M., DYCK, H-P., KASPAR, G., NISSAN, K., Spent LWR fuel dry storage in large transport and storage casks after extended burnup, J. Nucl. Mater., **250**, (1997), 63-74.

ABBREVIATIONS

ASTM	American Society for Testing and Materials
BARC	Bhabha Atomic Research Centre (India)
BWR	boiling water reactor
CANDU	Canadian type pressurised heavy water reactor (Canadian Deuterium Uranium)
CNL	Canada Nuclear Laboratories
CRP	coordinated research project
CW	cold-worked
CWSR	cold-worked stress-relieved
DCPD	direct current potential drop
DHC	delayed hydride cracking
(EC) JRC-ITU	(European Commission) Joint Research Centre - Institute for Transuranium Elements (Germany)
LEFM	linear elastic fracture mechanism
LLD	load line displacement
LWR	light water reactor
NNFD	Nippon Nuclear Fuel Development (Japan)
PD	potential drop
PHWR	pressurised heavy water reactor
PLT	pin loading tension (technique)
PSI	Paul Scherrer Institute (Switzerland)
PWR	pressurised water reactor
RBMK	high power channel type reactor (Russian graphite moderated light water cooled reactor)
RCM	research coordination meeting
VNIINM	A.A. Bochvar High-Technology Research Institute of Inorganic Materials (Russian Federation)
VVER	water cooled water moderated power reactor (Voda Voda Energo Reactor, Russian pressurized light water cooled reactor)

CONTRIBUTORS TO DRAFTING AND REVIEW

Aioanei, L.	Regia Autonoma Tehnologii pentru Energia Nucleara, Romania
Ali, K.L.	Pakistan Institute of Nuclear Science and Technology, Pakistan
Alvarez-Holston, A.M.	Studsvik Nuclear, Sweden
Astrakhantsev, M.	A.A. Bochvar High-Technology Research Institute of Inorganic Materials, Russian Federation
Bekrenev, S.	A.A. Bochvar High-Technology Research Institute of Inorganic Materials, Russian Federation
Buyers, A.	Canadian Nuclear Laboratories, Canada
Castagnet, M.	Instituto de Pesquisas Energéticas e Nucleares, Brazil
Chakravartty, J.	Bhabha Atomic Research Centre, India
Chernyayeva, T.	Kharkov Institute of Physics and Technology, Ukraine
Coleman, C.E.	Canadian Nuclear Laboratories, Canada
Correa, O.	Instituto de Pesquisas Energéticas e Nucleares, Brazil
Grigoriev, V.	Studsvik Nuclear, Sweden
Grybenas, A.	Lithuanian Energy Institute, Lithuania
He, Z.	Canadian Nuclear Laboratories, Canada
Inozemtsev, V.	International Atomic Energy Agency
Johansson, B.	Studsvik Nuclear, Sweden
Kim. Y.S.	KAERI, Republic of Korea
Kotov, P.	A.A. Bochvar High-Technology Research Institute of Inorganic Materials, Russian Federation
Kriukiene, R.	Lithuanian Energy Institute, Lithuania
Makarevicius, V.	Lithuanian Energy Institute, Lithuania
Markelov, V.	A.A. Bochvar High-Technology Research Institute of Inorganic Materials, Russian Federation
McDonald, D.	Canadian Nuclear Laboratories, Canada
Mizrahi, R.	Comisión Nacional de Energia Atómica, Argentina
Nitu, A.	Regia Autonoma Tehnologii pentru Energia Nucleara, Romania
Novikov, V.	A.A. Bochvar High-Technology Research Institute of Inorganic Materials, Russian Federation
Ostapov, A.	Kharkov Institute of Physics and Technology, Ukraine
Papaioannou, D.	Joint Research Centre – Institute for Transuranium Elements, European Union

Ramanathan, L.	Instituto de Pesquisas Energéticas e Nucleares, Brazil
Roth, M.	Regia Autonoma Tehnologii pentru Energia Nucleara, Romania
Sakamoto, K.	Nippon Nuclear Fuel Development, Japan
Saburov, N.	A.A. Bochvar High-Technology Research Institute of Inorganic Materials, Russian Federation
Singh, R.N.	Bhabha Atomic Research Centre, India
Sunil, S.	Bhabha Atomic Research Centre, India
Stjärnsäter, J.	Studsvik Nuclear, Sweden
Vallence, S.	Paul Scherrer Institute, Switzerland

Research Coordinated Meetings

Vienna, Austria, 24-28 October 2011

Villigen, Switzerland, 10-14 December 2012

Mito, Japan, 8-12 September 2014

Consultants Meetings

Chalk River, Canada, 14-16 January 2014

Vienna, Austria, 3-5 March 2015

IAEA
International Atomic Energy Agency

ORDERING LOCALLY

In the following countries, IAEA priced publications may be purchased from the sources listed below or from major local booksellers.

Orders for unpriced publications should be made directly to the IAEA. The contact details are given at the end of this list.

AUSTRALIA
DA Information Services
648 Whitehorse Road, Mitcham, VIC 3132, AUSTRALIA
Telephone: +61 3 9210 7777 • Fax: +61 3 9210 7788
Email: books@dadirect.com.au • Web site: http://www.dadirect.com.au

BELGIUM
Jean de Lannoy
Avenue du Roi 202, 1190 Brussels, BELGIUM
Telephone: +32 2 5384 308 • Fax: +32 2 5380 841
Email: jean.de.lannoy@euronet.be • Web site: http://www.jean-de-lannoy.be

CANADA
Renouf Publishing Co. Ltd.
5369 Canotek Road, Ottawa, ON K1J 9J3, CANADA
Telephone: +1 613 745 2665 • Fax: +1 643 745 7660
Email: order@renoufbooks.com • Web site: http://www.renoufbooks.com

Bernan Associates
4501 Forbes Blvd., Suite 200, Lanham, MD 20706-4391, USA
Telephone: +1 800 865 3457 • Fax: +1 800 865 3450
Email: orders@bernan.com • Web site: http://www.bernan.com

CZECH REPUBLIC
Suweco CZ, spol. S.r.o.
Klecakova 347, 180 21 Prague 9, CZECH REPUBLIC
Telephone: +420 242 459 202 • Fax: +420 242 459 203
Email: nakup@suweco.cz • Web site: http://www.suweco.cz

FINLAND
Akateeminen Kirjakauppa
PO Box 128 (Keskuskatu 1), 00101 Helsinki, FINLAND
Telephone: +358 9 121 41 • Fax: +358 9 121 4450
Email: akatilaus@akateeminen.com • Web site: http://www.akateeminen.com

FRANCE
Form-Edit
5 rue Janssen, PO Box 25, 75921 Paris CEDEX, FRANCE
Telephone: +33 1 42 01 49 49 • Fax: +33 1 42 01 90 90
Email: fabien.boucard@formedit.fr • Web site: http://www.formedit.fr

Lavoisier SAS
14 rue de Provigny, 94236 Cachan CEDEX, FRANCE
Telephone: +33 1 47 40 67 00 • Fax: +33 1 47 40 67 02
Email: livres@lavoisier.fr • Web site: http://www.lavoisier.fr

L'Appel du livre
99 rue de Charonne, 75011 Paris, FRANCE
Telephone: +33 1 43 07 50 80 • Fax: +33 1 43 07 50 80
Email: livres@appeldulivre.fr • Web site: http://www.appeldulivre.fr

GERMANY
Goethe Buchhandlung Teubig GmbH
Schweitzer Fachinformationen
Willstätterstrasse 15, 40549 Düsseldorf, GERMANY
Telephone: +49 (0) 211 49 8740 • Fax: +49 (0) 211 49 87428
Email: s.dehaan@schweitzer-online.de • Web site: http://www.goethebuch.de

HUNGARY
Librotade Ltd., Book Import
PF 126, 1656 Budapest, HUNGARY
Telephone: +36 1 257 7777 • Fax: +36 1 257 7472
Email: books@librotade.hu • Web site: http://www.librotade.hu

INDIA

Allied Publishers
1st Floor, Dubash House, 15, J.N. Heredi Marg, Ballard Estate, Mumbai 400001, INDIA
Telephone: +91 22 2261 7926/27 • Fax: +91 22 2261 7928
Email: alliedpl@vsnl.com • Web site: http://www.alliedpublishers.com

Bookwell
3/79 Nirankari, Delhi 110009, INDIA
Telephone: +91 11 2760 1283/4536
Email: bkwell@nde.vsnl.net.in • Web site: http://www.bookwellindia.com

ITALY

Libreria Scientifica "AEIOU"
Via Vincenzo Maria Coronelli 6, 20146 Milan, ITALY
Telephone: +39 02 48 95 45 52 • Fax: +39 02 48 95 45 48
Email: info@libreriaaeiou.eu • Web site: http://www.libreriaaeiou.eu

JAPAN

Maruzen Co., Ltd.
1-9-18 Kaigan, Minato-ku, Tokyo 105-0022, JAPAN
Telephone: +81 3 6367 6047 • Fax: +81 3 6367 6160
Email: journal@maruzen.co.jp • Web site: http://maruzen.co.jp

NETHERLANDS

Martinus Nijhoff International
Koraalrood 50, Postbus 1853, 2700 CZ Zoetermeer, NETHERLANDS
Telephone: +31 793 684 400 • Fax: +31 793 615 698
Email: info@nijhoff.nl • Web site: http://www.nijhoff.nl

Swets Information Services Ltd.
PO Box 26, 2300 AA Leiden
Dellaertweg 9b, 2316 WZ Leiden, NETHERLANDS
Telephone: +31 88 4679 387 • Fax: +31 88 4679 388
Email: tbeysens@nl.swets.com • Web site: http://www.swets.com

SLOVENIA

Cankarjeva Zalozba dd
Kopitarjeva 2, 1515 Ljubljana, SLOVENIA
Telephone: +386 1 432 31 44 • Fax: +386 1 230 14 35
Email: import.books@cankarjeva-z.si • Web site: http://www.mladinska.com/cankarjeva_zalozba

SPAIN

Diaz de Santos, S.A.
Librerias Bookshop • Departamento de pedidos
Calle Albasanz 2, esquina Hermanos Garcia Noblejas 21, 28037 Madrid, SPAIN
Telephone: +34 917 43 48 90 • Fax: +34 917 43 4023
Email: compras@diazdesantos.es • Web site: http://www.diazdesantos.es

UNITED KINGDOM

The Stationery Office Ltd. (TSO)
PO Box 29, Norwich, Norfolk, NR3 1PD, UNITED KINGDOM
Telephone: +44 870 600 5552
Email (orders): books.orders@tso.co.uk • (enquiries): book.enquiries@tso.co.uk • Web site: http://www.tso.co.uk

UNITED STATES OF AMERICA

Bernan Associates
4501 Forbes Blvd., Suite 200, Lanham, MD 20706-4391, USA
Telephone: +1 800 865 3457 • Fax: +1 800 865 3450
Email: orders@bernan.com • Web site: http://www.bernan.com

Renouf Publishing Co. Ltd.
812 Proctor Avenue, Ogdensburg, NY 13669, USA
Telephone: +1 888 551 7470 • Fax: +1 888 551 7471
Email: orders@renoufbooks.com • Web site: http://www.renoufbooks.com

United Nations
300 East 42nd Street, IN-919J, New York, NY 1001, USA
Telephone: +1 212 963 8302 • Fax: 1 212 963 3489
Email: publications@un.org • Web site: http://www.unp.un.org

Orders for both priced and unpriced publications may be addressed directly to:

IAEA Publishing Section, Marketing and Sales Unit, International Atomic Energy Agency
Vienna International Centre, PO Box 100, 1400 Vienna, Austria
Telephone: +43 1 2600 22529 or 22488 • Fax: +43 1 2600 29302
Email: sales.publications@iaea.org • Web site: http://www.iaea.org/books